

Rock Mass Classification System: Transition from RMR to GSI



Teruhisa Masada & Xiao Han
ORITE, Ohio University

for the
Ohio Department of Transportation
Office of Statewide Planning & Research

and the
United States Department of Transportation
Federal Highway Administration

State Job Number 134693

November 2013



OHIO
UNIVERSITY

Ohio Research Institute for Transportation and the Environment (ORITE)



1. Report No. FHWA/OH-2013/11	2. Government Accession No.	3. Recipient's Catalog No.	
4. Title and Subtitle Rock Mass Classification System: Transition from RMR to GSI		5. Report Date November 2013	
		6. Performing Organization Code	
7. Author(s) Dr. Teruhisa Masada; Xiao Han		8. Performing Organization Report	
9. Performing Organization Name and Address Ohio Research Institute for Transportation and the Environment 141 Stocker Center, Ohio University Athens , OH 45701-2979		10. Work Unit No. (TRAIS)	
12. Sponsoring Agency Name and Address Ohio Department of Transportation 1980 West Broad St. Columbus OH 43223		11. Contract or Grant No. SJN 134693	
		13. Type of Report and Period Covered Final Report	
		14. Sponsoring Agency Code	
15. Supplementary Notes Prepared in cooperation with the Ohio Department of Transportation (ODOT) and the U.S. Department of Transportation, Federal Highway Administration			
16. Abstract The AASHTO LRFD Bridge Design Specifications is expected to replace the rock mass rating (RMR) system with the Geological Strength Index (GSI) system for classifying and estimating engineering properties of rock masses. This transition is motivated by the fact that some difficulties were experienced with RMR in many highway bridge projects. A study was carried out to determine if GSI is applicable to rock materials found in Ohio. To meet this primary objective, a literature review was conducted, many rock samples were tested in the lab, an extensive rock property data set was assembled, and statistical/computation analysis of the data set was performed. The outcome showed that GSI is applicable to rock materials in Ohio.			
17. Key Words Rock, RMR, GSI, strength, unconfined compression, triaxial compression, Hoek cell, statistical analysis, Ohio, bridge foundation design		18. Distribution Statement No Restrictions. This document is available to the public through the National Technical Information Service, Springfield, Virginia 22161	
19. Security Classif. (of this report) Unclassified	20. Security Classif. (of this page) Unclassified	21. No. of Pages 130	22. Price
Form DOT F 1700.7 (8-72)		Reproduction of completed pages authorized	

SI* (MODERN METRIC) CONVERSION FACTORS

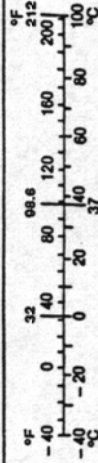
APPROXIMATE CONVERSIONS TO SI UNITS

Symbol	When You Know	Multiply By	To Find	Symbol
LENGTH				
in	inches	25.4	millimetres	mm
ft	square feet	0.305	metres	m
yd	yards	0.914	metres	m
mi	miles	1.61	kilometres	km
AREA				
in ²	square inches	645.2	millimetres squared	mm ²
ft ²	square feet	0.093	metres squared	m ²
yd ²	square yards	0.836	metres squared	m ²
ac	acres	0.405	hectares	ha
mi ²	square miles	2.59	kilometres squared	km ²
VOLUME				
fl oz	fluid ounces	29.57	millilitres	mL
gal	gallons	3.785	litres	L
ft ³	cubic feet	0.028	metres cubed	m ³
yd ³	cubic yards	0.765	metres cubed	m ³
MASS				
oz	ounces	28.35	grams	g
lb	pounds	0.454	kilograms	kg
T	short tons (2000 lb)	0.907	megagrams	Mg
TEMPERATURE (exact)				
°F	Fahrenheit temperature	$5(F-32)/9$	Celsius temperature	°C

NOTE: Volumes greater than 1000 L shall be shown in m³.

APPROXIMATE CONVERSIONS FROM SI UNITS

Symbol	When You Know	Multiply By	To Find	Symbol
LENGTH				
mm	millimetres	0.039	inches	in
m	metres	3.28	feet	ft
m	metres	1.09	yards	yd
km	kilometres	0.621	miles	mi
AREA				
mm ²	millimetres squared	0.0016	square inches	in ²
m ²	metres squared	10.764	square feet	ft ²
ha	hectares	2.47	acres	ac
km ²	kilometres squared	0.386	square miles	mi ²
VOLUME				
mL	millilitres	0.034	fluid ounces	fl oz
L	litres	0.264	gallons	gal
m ³	metres cubed	35.315	cubic feet	ft ³
m ³	metres cubed	1.308	cubic yards	yd ³
MASS				
g	grams	0.035	ounces	oz
kg	kilograms	2.205	pounds	lb
Mg	megagrams	1.102	short tons (2000 lb)	T
TEMPERATURE (exact)				
°C	Celsius temperature	$1.8C + 32$	Fahrenheit temperature	°F



* SI is the symbol for the International System of Measurement

Rock Mass Classification System: Transition from RMR to GSI

A Student Study Project

Final Report

Prepared in cooperation with the
Ohio Department of Transportation
and the
U.S. Department of Transportation, Federal Highway Administration

Prepared by
Teruhisa Masada, Ph.D. (Professor of Civil Engineering)
and
Xiao Han (Doctoral Student)

Civil Engineering Department
Russ College of Engineering and Technology
Ohio University
Athens, Ohio 45701-2979

Disclaimer Statement

The contents of this report reflect the views of the authors who are responsible for the facts and the accuracy of the data presented herein. The contents do not necessarily represent the official views or policies of the Ohio Department of Transportation or the Federal Highway Administration. This report does not constitute a standard, specification, or regulation.

November 2013

Acknowledgement

The authors would like to acknowledge the assistance of the Ohio Department of Transportation technical liaisons (Paul Painter, Steve Taliaferro, Jawdat Siddiqi, Chris Merklin) in setting the clear project objectives, lending a Hoek cell, mining the geotechnical database FALCON GDMS, and securing a variety of rock core samples.

TABLE OF CONTENTS

ACKNOWLEDGEMENT

TABLE OF CONTENTS

LIST OF TABLES

LIST OF FIGURES

CHAPTER 1 : INTRODUCTION	1
1.1 Background	1
1.2 Objectives.....	2
1.3 Potential Benefits	3
CHAPTER 2 : LITERATURE REVIEW	5
2.1 General Information on Geology of Ohio Rock.....	5
2.2 Rock Mass Testing in Midwest and Ohio	8
2.3 Rock Mass Evaluation Methods.....	9
2.3.1 The RMR Method.....	10
2.3.2 The GSI Method	18
2.3.3 RMR-GIS Correlation.....	23
2.4 Rock Slope and Rock Foundation Considerations.....	26
CHAPTER 3 : METHODOLOGY	29
3.1 Rock Specimen Preparation	29
3.2 Unconfined Compression Test.....	31
3.3 Triaxial Compression Test	33
3.3.1 Triaxial Test on Strong Rock Samples	34
3.3.2 Triaxial Test on Weak Rock Samples.....	37
3.4 Calculation of m_i values	41
3.4.1 The Hoek Method	41
3.4.2 The LMA Method.....	42
3.5 Statistical Analysis	43
3.5.1 Confidence Interval of Basic Rock Properties.....	44
3.5.2 t-Test Comparison between Geological Regions.....	44
3.5.3 Correlation between RMR and GSI.....	45
CHAPTER 4 : RESULTS	47
4.1 Literature Review Results	47
4.2 Ohio Rock Property Data Assembled	47
4.3 Basic Rock Properties	47
4.3.1 Statewide Ranges of Basic Rock Properties	47
4.3.2 Regional Comparisons of Basic Rock Properties	55

4.4	Calculations of GSI Parameters	75
4.5	Regression Correlation between RMR and GSI	77
4.6	Critical Design Parameter Calculations	92
4.6.1	Example 1 – Limestone in Southwest Region	93
4.6.2	Example 2 – Sandstone in Northeast Region.....	96
4.6.3	Example 3 – Unweathered Shale in Southeast Region.....	99
4.6.4	Comments on Computation Examples.....	103
CHAPTER 5 : SUMMARY AND CONCLUSIONS		105
5.1	Summary	105
5.2	Findings and Conclusions	107
5.2.1	Literature Review.....	107
5.2.2	Gathering of Ohio Rock Property Data	108
5.2.3	Ranges of Basic Ohio Rock Properties.....	108
5.2.4	Regional Variations of Basic Ohio Rock Properties.....	109
5.2.5	Ranges of GSI Parameter m_i	110
5.2.6	RMR-GSI Correlation.....	111
5.3	Recommendations	112
CHAPTER 6 : IMPLEMENTATIONS		114
REFERENCES.....		115

LIST OF TABLES

Table 2.1: Properties of Typical Rock Types in Ohio	7
Table 2.2: Rock Masses Classification Rating Systems	11
Table 2.3: Joint Orientation Rating Modifications	12
Table 2.4: Rock Classification Based on Final RMR Rating	12
Table 2.5: Intact Rock Elastic Modulus.....	15
Table 2.6: Relationship between Reduction Factor and RQD Value	15
Table 2.7: Intact Rock Poisson’s Ratio.....	16
Table 2.8: Approximate value of Rock Mass Constant m and s	16
Table 2.9: Typical Ranges of Friction Angles for Smooth Joints in Some Rock Types ..	17
Table 2.10: Typical Values of Material Constant m_i (Hoek 2006).....	20
Table 2.11: Determination of Disturbance Factor D	21
Table 2.12: Determination of GSI Value.....	22
Table 2.13: GSI vs. RMR for Very Weak Rock Masses	24
Table 2.14: Values of Joint Discontinuity Parameters.....	25
Table 4.1: Total Number of Ohio Rock Unit Weight Values Assembled	48
Table 4.2: Total Number of Ohio Rock Unconfined Compression Strength Values Assembled.....	48
Table 4.3: Number of Unconfined Compression Strength Tests Performed by OU	49
Table 4.4: Number of Triaxial Compression Tests Performed by OU	49
Table 4.5: Basic Rock Properties of Ohio Rocks Provided by ODOT	50
Table 4.6: Basic Properties of Limestone in Ohio.....	50
Table 4.7: Basic Properties of Sandstone in Ohio	51
Table 4.8: Basic Properties of Unweathered Shale in Ohio.....	51
Table 4.9: Basic Properties of Weathered Shale in Ohio.....	52
Table 4.10: Basic Properties of Claystone in Southeast Region.....	52
Table 4.11: Comparison of Basic Rock Properties between ODOT Report and Current Study	54
Table 4.12: Limestone in Northwest Region	55
Table 4.13: Basic Properties of Limestone in Northeast Region.....	56
Table 4.14: Basic Properties of Limestone in Central Region.....	56
Table 4.15: Basic Properties of Limestone in Southeast Region.....	57
Table 4.16: Basic Properties of Limestone in Southwest Region.....	57
Table 4.17: Basic Properties of Sandstone in Northeast Region	58
Table 4.18: Basic Properties of Sandstone in Eastern Region.....	59
Table 4.19: Basic Properties of Sandstone in Southeast Region	59
Table 4.20: Basic Properties of Unweathered Shale in Northeast Region	61
Table 4.21: Basic Properties of Unweathered Shale in Central Region	61
Table 4.22: Basic Properties of Unweathered Shale in Eastern Region	62
Table 4.23: Basic Properties of Unweathered Shale in Southeast Region	62
Table 4.24: Basic Properties of Unweathered Shale in Southwest Region	63

Table 4.25: Basic Properties of Weathered Shale in Northeast Region	64
Table 4.26: Basic Properties of Weathered Shale in Central Region	64
Table 4.27: Basic Properties of Weathered Shale in Eastern Region	65
Table 4.28: Basic Properties of Weathered Shale in Southeast Region	65
Table 4.29: Basic Properties of Weathered Shale in Southwest Region	66
Table 4.30: T-Test Results for Unit Weight of Limestone in Ohio Regions.....	67
Table 4.31: Ranges of Unit Weight of Limestone in Ohio Regions.....	68
Table 4.32: T-Test Results for Unconfined Compression Strength of Limestone among Ohio Regions	69
Table 4.33: Ranges of Unconfined Compression Strength of Limestone in Ohio Regions	69
Table 4.34: T-Test Results for Unit Weight of Sandstone among Ohio Regions.....	69
Table 4.35: Ranges of Unit Weight of Sandstone in Ohio Regions	70
Table 4.36: T-Test Results for Unconfined Compression Strength of Sandstone among Ohio Regions	70
Table 4.37: Ranges of Unconfined Compression Strength of Sandstone among Ohio Regions	70
Table 4.38: T-Test Results for Unit Weight of Unweathered Shale among Ohio Regions	71
Table 4.39: Ranges of Unit Weight of Unweathered Shale among Ohio Regions.....	71
Table 4.40: T-Test Results for Unconfined Compression Strength of Unweathered Shale among Ohio Regions.....	72
Table 4.41: Ranges of Unconfined Compression Strength of Unweathered Shale among Ohio Regions	73
Table 4.42: T-Test Results for Unit Weight of Weathered Shale among Ohio Regions..	73
Table 4.43: Ranges of Unit Weight of Weathered Shale among Ohio Regions.....	73
Table 4.44: T-Test Results for Unconfined Compression Strength of Weathered Shale among Ohio Regions.....	74
Table 4.45: Ranges of Unconfined Compression Strength of Weathered Shale among Ohio Regions	74
Table 4.46: Quantity of Data Used in m_i and σ_{ci} Calculations	76
Table 4.47: Calculated m_i Ranges.....	76
Table 4.48: Calculated σ_{ci} Ranges (psi).....	77
Table 4.49: RMR-GSI Correlations for Limestone in Ohio	89
Table 4.50: RMR-GSI Correlations for Sandstone in Ohio.....	90
Table 4.51: RMR-GSI Correlations for Unweathered Shale in Ohio.....	91
Table 4.52: RMR-GSI Correlations for Weathered Shale in Ohio.....	92
Table 4.53: Summary of RMR-GSI Computation Examples	104

LIST OF FIGURES

Figure 2.1: Rock Distribution Map of Ohio	6
Figure 3.1: Rock Specimen Undergoing Unconfined Compression Loading	33
Figure 3.2: Details of Hoek Cell.....	35
Figure 3.3: Strong Rock Specimen Undergoing Hoek Cell Triaxial Compression Test..	37
Figure 3.4: Weak rock Specimen Failing During Soil Triaxial Test	40
Figure 4.1: Plot of Ohio Limestone Properties (OU Data).....	51
Figure 4.2: Plot of Ohio Sandstone Properties (OU Data).....	51
Figure 4.3: Plot of Ohio Unweathered Shale Properties (OU Data).....	52
Figure 4.4: Plot of Weathered Shale Properties in Ohio (OU Data).....	52
Figure 4.5: Plot of Claystone Properties in Ohio (OU Data).....	53
Figure 4.6: Plot of Limestone Properties in Northwest Region (OU Data).....	55
Figure 4.7: Plot of Limestone Properties in Northeast Region (OU Data).....	56
Figure 4.8: Plot of Limestone Properties in Central Region (OU Data).....	56
Figure 4.9: Plot of Limestone Properties in Southeast Region (OU Data).....	57
Figure 4.10: Plot of Limestone Properties in Southwest Region (OU Data).....	57
Figure 4.11: Basic Properties of Ohio Limestone Mapped.....	58
Figure 4.12: Plot of Sandstone Properties in Northeast Region (OU Data)	58
Figure 4.13: Plot of Sandstone Properties in Eastern Region (OU Data).....	59
Figure 4.14: Plot of Sandstone Properties in Southeast Region (OU Data)	59
Figure 4.15: Basic Properties of Sandstone in Ohio Mapped.....	60
Figure 4.16: Plot of Unweathered Shale in Northeast Region (OU Data).....	61
Figure 4.17: Plot of Unweathered Shale Properties in Central Region (OU Data)	61
Figure 4.18: Plot of Unweathered Shale Properties in Eastern Region (OU Data)	62
Figure 4.19: Plot of Unweathered Shale Properties in Southeast Region (OU Data).....	62
Figure 4.20: Plot of Unweathered Shale Properties in Southwest Region (OU Data)	63
Figure 4.21: Basic Properties of Unweathered Shale in Ohio Mapped	63
Figure 4.22: Plot of Weathered Shale Properties in Northwest Region (OU Data)	64
Figure 4.23: Plot of Weathered Shale Properties in Central Region (OU Data)	64
Figure 4.24: Plot of Weathered Shale Properties in Eastern Region (OU Data)	65
Figure 4.25: Plot of Weathered Shale Properties in Southeast Region (OU Data).....	65
Figure 4.26: Plot of Weathered Shale Properties in Southwest Region (OU Data)	66
Figure 4.27: Basic Properties of Weathered Shale in Ohio Mapped	66
Figure 4.28: RMR-GSI Correlation for Limestone in Ohio (Linear)	79
Figure 4.29: RMR-GSI Correlation for Limestone in Ohio (Quadratic).....	79
Figure 4.30: RMR-GSI Correlation for Limestone in Ohio (Exponential)	80
Figure 4.31: RMR-GSI Correlation for Limestone in Ohio (Logarithmic).....	80
Figure 4.32: RMR-GSI Correlation for Limestone in Ohio (Power).....	81
Figure 4.33: RMR-GSI Correlation for Sandstone in Ohio (Linear).....	81
Figure 4.34: RMR-GSI Correlation for Sandstone in Ohio (Quadratic)	82
Figure 4.35: RMR-GSI Correlation for Sandstone in Ohio (Exponential).....	82

Figure 4.36: RMR-GSI Correlation for Sandstone in Ohio (Logarithmic)	83
Figure 4.37: RMR-GSI Correlation for Sandstone in Ohio (Power)	83
Figure 4.38: RMR-GSI Correlation for Unweathered Shale in Ohio (Linear)	84
Figure 4.39: RMR-GSI Correlation for Unweathered Shale in Ohio (Quadratic).....	84
Figure 4.40: RMR-GSI Correlation for Unweathered Shale in Ohio (Exponential)	85
Figure 4.41: RMR-GSI Correlation for Unweathered Shale in Ohio (Logarithmic).....	85
Figure 4.42: RMR-GSI Correlation for Unweathered Shale in Ohio (Power)	86
Figure 4.43: RMR-GSI Correlation for Weathered Shale in Ohio (Linear)	86
Figure 4.44: RMR-GSI Correlation for Weathered Shale in Ohio (Quadratic).....	87
Figure 4.45: RMR-GSI Correlation for Weathered Shale in Ohio (Exponential)	87
Figure 4.46: RMR-GSI Correlation for Weathered Shale in Ohio (Logarithmic).....	88
Figure 4.47: RMR-GSI Correlation for Weathered Shale in Ohio (Power)	88

CHAPTER 1 : INTRODUCTION

1.1 Background

In unglaciated region of Ohio, many highway bridge structures have been commonly supported by drilled pier shafts and spread footing foundations bearing on rock. When designing these bridge foundations, civil engineers have been relying on the Rock Mass Rating (RMR) system described in Section 10 of the AASHTO LRFD Bridge Design Specifications that are presented in the NCHRP 24-31 report. In this system, the general rock mass rating (RMR) is assigned to the bedrock existing at the bridge construction site, through the use of the geomechanics classification system first developed by Bieniawski (1974). The RMR is the sum of ratings based on five universal parameters:

- compressive strength of rock;
- rock core quality designation (RQD);
- groundwater conditions;
- joint/fracture spacing; and
- joint characteristics.

In projects related to foundations, tunneling, and mining, the sixth parameter (orientation of joints) is often applied to adjust the original RMR. The AASHTO LRFD Bridge Design Specifications published in NCHRP 24-31 has been utilizing RMR to estimate the elastic modulus and shear strength of the rock mass, which are critical for both settlement and resistance determinations for the deep foundations specified for highway bridges and rock slope stability analysis.

Recently, a new rock mass classification system is becoming more widely utilized for estimating strength of rock masses. This system, commonly known as GSI (Geological Strength Index) was first developed by Hoek during the 1990's. GSI is believed to be

convenient and applicable to a wider range of rock mass situations. GSI has been evolving due to difficulties experienced with RMR in some case studies. Main problem with RMR arises from the fact that at many bridge construction sites rock masses are badly damaged due to blasting and other activities and it is difficult to obtain high-quality rock core specimens for measuring compressive strength required for the RMR system. RMR is good for stronger good quality rock but is inadequate for weaker jointed formations. Also, RMR requires the knowledge on the rock mass's joint orientations. This information is generally unavailable at most bridge foundation project sites, as the rock mass's vertical facing must be largely exposed to attain the joint orientation information.

The AASHTO LRFD Bridge Specifications is expected to transition from RMR to GSI in the near future. With this planned transition, there is a need for ODOT to support a study that is focused on RMR and GSI so that any doubts and confusions related to the change in the rock mass classification system will be dispelled and geotechnical and bridge engineers in Ohio will be well educated about the differences and correlations between RMR and GSI. The main question related to GSI is concerned with the applicability of its general parameters to Ohio rock masses. The challenge is to address regional differences, as for example limestone found in northern Ohio is not the same as limestone found in the central or southern regions. The current project has provided an ideal vehicle to conduct such a study relatively quickly and inexpensively.

1.2 Objectives

The goal of the current study is to carry out research on the rock mass classification systems for ODOT. The specific objectives of the study are as follows:

- 1) To conduct an extensive literature review to gather information on the geology of Ohio rock, the Rock Mass Rating (RMR) system, the Geological Strength Index

(GSI)system, the AASHTO LRFD highway bridge foundation design specifications, and basic/strength properties of Ohio rock samples;

- 2) To evaluate the values of the parameters included in the Geological Strength Index (GSI) classification using the rock sample strength data gathered in Ohio;
- 3) To address regional characteristics in the Ohio rock's properties;
- 4) To refine the design parameter charts to be used by Design Engineers based on regional differences; and
- 5) To develop the correlation between RMR and GSI systems and present it through a set of easy-to-understand charts and/or tables.

For the second objective, assistance was provided by the ODOT Geology & Exploration Section of the Office of Geotechnical Engineering (OGE) so that the Ohio University team could extract available data from the statewide database and also examine and test rock samples that had been taken from ODOT project sites in Ohio. Once a sufficient volume of strength data was secured, the applicability of the recommended values of the parameters included in GSI system was evaluated in light of the range of rock strength typically found in Ohio.

1.3 Potential Benefits

The current study is expected to yield the following four benefits:

- Typical statewide rock properties reported in ODOT's 2011 report "Rock Slope Design Guide" will be verified;
- Recommendations will be made on what laboratory tests consulting companies and test laboratories should perform under the GSI version of the AASHTO LRFD Specifications;

- Ohio rock strength data established in the study will steer ODOT toward developing region-specific bridge foundation design specifications; and
- Ohio rock strength data gathered in the study will assist ODOT to maintain the same level of conservatism in their highway bridge foundation design specifications during the transition from RMR to GSI.

CHAPTER 2 : LITERATURE REVIEW

The first objective of the current study was to conduct an extensive literature review to gather information on the geology of Ohio rock, the Rock Mass Rating (RMR) system, the Geological Strength Index (GSI) classification, and the AASHTO LRFD highway bridge foundation design specifications.

2.1 General Information on Geology of Ohio Rock

According to the distribution of bedrock formations described in ODOT's Rock Slope Design Guide (2011) and illustrated in Figure 2.1, the geology of Ohio is generally divided into the following six geological regions. By far the most common rock materials in Ohio are limestone, sandstone, and shale.

Northwestern Ohio: The main rock types in this area are limestone and dolomite.

Northeastern Ohio: Clastic rock with silicic compound is common in this area. Friable sandstone randomly appears.

Southwestern Ohio: This area is full of Upper-Ordovician shale and marine limestone.

Central Ohio: The rock interbedded in this area consists of fossiliferous carbonates and Silurian-age shale. Sandstones are found in the east region of this area.

Eastern Ohio: This area is covered by Pennsylvanian aged and Mississippian aged rocks. Pennsylvanian aged rock contains sandstones, shale, coal and limestone. The rock type under the cover is coal mine.

Southeastern Ohio: The shallow layer is composed by Permian and Upper Pennsylvanian aged rocks. The deep layer consists of claystone, shale, siltstone, sandstone, limestone and coal.

Table 2.1, which was extracted from the ODOT report (2011) lists the expected ranges of the engineering properties of the common rock types in Ohio. The ranges need to be verified through additional studies.



Figure 2.1: Rock Distribution Map of Ohio

Ref.: ODOT Rock Slope Design Guide, *Ohio Department of Transportation* (2011).

Table 2.1: Properties of Typical Rock Types in Ohio

Rock Type	Unit Weight (pcf)	Unconfined Compressive Strength (psi)	Slake Durability Index (%)
Claystone	160-165	50-1400	0-60
Shale	160-165	1900-2500	20-90
Siltstone	160-170	3600-8100	65-90
Sandstone	155-160	2000-7800	85-100
Friable Sandstone	125-140	2400-3800	60-85
Limestone	155-165	3500-16400	95-100
Dolomite	165-175	4100-10300	95-100
Coal	80-85	1300-7000	N/A
Underclay	125-135	200-400	0-20

The wide range of unconfined compressive strength values listed for some rock types reflect the influences of two factors – weathering (disintegration, decomposition) and discontinuities. Unconfined compressive strength is determined by the weathering and composition of the strata. The discontinuities will reduce the strength of the rock mass. Disintegration is physical damage made to the rock due to water flow, heating, cooling (or icing), debris moving, and tree roots penetrating. Decomposition is chemical change in the rock, such as oxidation, hydration, and carbonation. Rock discontinuities found in Ohio can encompass:

- a. Bedding Planes: The distinct and constant layer exists between two adjacent rock beds.
- b. Joints: The crack splits the rock into two parts without apparent movement.
- c. Valley Stress Relief Joints: This fracture is caused by rock erosion and vertically located in the valley walls.
- d. Stress Induced Fractures: This high-angle crack is formed by rock's uneven subsidence.
- e. Faults: The crack divides the rock into two parts with obvious movement.
- f. Shears: The interface of this crack is smooth and parallel to the rock surface.

Discontinuity b through f will affect the rock mass, but not the rock strength. Strength is determined by the weathering and composition of the strata. The discontinuities will reduce the strength of the rock mass. For any rock mass with discontinuities, it is important to find out the overall quality of the rock mass, the orientation of the discontinuities, the spacing between discontinuities, roughness of the walls, and the presence/absence of groundwater.

2.2 Rock Mass Testing in Midwest and Ohio

Masada, T. (1986) conducted a series of laboratory strength tests on shale specimens that were collected from a cut slope in Noble County, Ohio and a bridge construction site in Chesapeake, Ohio. The rock specimens were cut down into 4-inch cubes using dry saw cutting technique and then loaded inside a multi-axial cubical test system. This system is more sophisticated than the conventional triaxial test system and is capable of applying various stress paths to the test specimens. For the conventional triaxial compression loading, the ultimate strength ranged from 1.40 to 3.13 ksi (ave. 2.35 ksi) under the lowest confining stress level of 100 psi. Moisture contents of the test specimens were typically between 2 and 3% (ave. 2.6%). Their moist unit weight values varied from 150 to 164 pcf (ave. 158 pcf). The Noble County specimens were drier and slightly stronger than the Chesapeake specimens.

Rusnak and Mark (2000) tested bedrock materials at numerous sites spread throughout Midwest. According to their work, the average and standard deviation of the unconfined compression strength data compiled on siltstone were 5.93 ksi and 1.03 ksi, respectively. For sandstone, the values were 6.77 ksi and 1.60 ksi. For limestone, the values were 18.75 ksi and 6.65 ksi.

Nusairat et al. (2006) measured the unconfined compression strength of rock formations that were encountered at the Pomeroy-Mason Bridge construction site. The average

strength values were 903 psi for shale, 4,861 psi for siltstone, and 28 psi for mudstone. Rock Quality Designation (RQD) values ranged generally from 40 and 60% for the rock masses.

Failmezger et al. (2008) utilized a rock borehole shear test (RBST) device at two sites in Ohio to measure shear strength properties of rock formations. At a site near I-270 in Columbus, they tested shale. At the other site by SR 7 in Marietta, OH, where rock slope problems had been reported, they tested a blocky sandstone overlying shale/siltstone formation. Their test results at these two sites are summarized below:

Shale in Columbus, OH: cohesion = 0 to 319 psi (ave. 218 psi); and friction angle = 21.5° to 33.4° (ave. 26.8°)

Sandstone in Marietta, OH: cohesion = 145 to 319 psi (ave. 232 psi); and friction angle = 14.9° to 26.8° (ave. 19.9°)

2.3 Rock Mass Evaluation Methods

A large heavy structure can be supported by either end-bearing piles on rock or friction piles set in deep soil deposits. Although many rock masses appear to be solid and strong in compression, the determination of their mechanical (or strength) properties is not straightforward. This is because rock weathers and is more discontinuous than soil. With different mineral content in rock layers and non-homogeneous joints existing in various directions, the mechanical properties of a large area of rock mass cannot be evaluated merely through simple laboratory tests. There are two generally accepted methods for Rock Classification in highway engineering. The first method is the Rock Mass Rating (RMR), which was first established by Z.T. Bieniawski in 1976 and then developed further in 1989. The second method is known as the Geological Strength Index (GSI), which was first developed by Hoek in 1980 and has been modified a number of times over the years. In this project, the RMR₇₆, the one that appeared in 1976, is selected

since it is adopted into the AASHTO LRFD Bridge Design Specification 4th edition. For GSI, the latest version published by Hoek in 2006 is accepted in this project.

Since the RMR method came out earlier, this method has been popular among bridge and geotechnical/rock mechanics engineers. It is suitable for the evaluation of rock masses in the field. But this method requires a few laboratory experiments and in-situ tests conducted on rock cores to produce the final results. Thus, its total evaluation process is somewhat time-consuming and costly.

The GSI method is a newer method whose theoretical basis is very different from that of the RMR method. The GSI method is more visually based and takes the confining pressure into consideration, which makes it applicable to the evaluation of very deep foundations, tunnels, and mining excavations. Although Hoek provided a range of the values for several parameters used in his method, the determinations of the parameter values for each design are rather subjective.

2.3.1 The RMR Method

For any rock mass, the original RMR value is a sum of relative ratings of five parameters.

The five parameters are:

- strength of intact rock
- drill core Rock Quality Designation (RQD)
- joint spacing
- joint conditions, and
- groundwater conditions.

The rating systems for these five parameters are listed in Table 2.2. The information presented in the table reflects the Bieniawski's 1976 rock mass rating system. His 1989

rating system differs from the 1976 version in terms of having slightly higher rating scores assigned to the joint spacing and groundwater parameters.

Once the initial RMR value is obtained, it is adjusted using the joint orientation modifier listed in Table 2.3. Then, the rock mass classification can be obtained using the adjusted final RMR value, in accordance with the classification system summarized in Table 2.4.

Table 2.2: Rock Masses Classification Rating Systems

Strength of Intact Rock	Ranges of Values						
Point Load Strength	>8 MPa (>175 ksf)	4–8 MPa (85-175 ksf)	2–4 MPa (45-85 ksf)	1–2 MPa (20-45 ksf)	Uniaxial compressive test is suitable for the lower strength		
Uniaxial Compressive Strength	>200 MPa (>4320 ksf)	100–200 MPa (2160-4320 ksf)	50–100 MPa (1080-2160 ksf)	25–50 MPa (520-1080 ksf)	10–25 MPa (215-520 ksf)	3.5–10 MPa (70-215 ksf)	1.0–3.5 MPa (20-70 ksf)
Relative Rating	15	12	7	4	2	1	0

Drill Core Quality RQD	90%–100%	75%–90%	50%–75%	25%–50%	<25%
Relative Rating	20	17	13	8	3

Spacing of Joints	>3000 mm (>10 ft)	900–3000 mm (3-10 ft)	300–900 mm (1-3 ft)	50–300 mm (2 in-1 ft)	<50 mm (<2 in)
Relative Rating	30	25	20	10	5

Table 2.2 – Cont'd

Condition of Joints	a. Very rough surface b. Not Continuous c. No separation d. Hard joint wall rock	a. Slightly rough surface b. Separation <1.25 mm (0.05 in) c. Hard joint wall rock	a. Slightly rough surface b. Separation <1.25 mm (0.05 in) c. Soft joint wall rock	a. Slickensided surfaces or Gouge <5 mm (0.2 in) thick or Joints open 1.25–5 mm (0.05-0.2 in) b. Continuous joints	a. Soft gouge >5 mm (0.2 in) thick or Joints open >5 mm (0.2 in) b. Continuous joints
Relative Rating	25	20	12	6	0

Groundwater Conditions	Ranges			
Inflow per 10000 mm tunnel length	none	<25 L/min (<400 gal/hr)	25–125 L/min (400-2000 gal/hr)	>125 L/min (>2000 gal/hr)
Ratio = joint water pressure / major principle stress	0	0.0–0.2	0.2–0.5	>0.5
General Conditions	Range			
Completely dry	Moist dry	Water under moderate pressure	Severe water problem	
10	7	4	0	

Table 2.3: Joint Orientation Rating Modifications

Strike and Dip Orientations of Joints	Ratings		
	Tunnels	Foundations	Slopes
Very Favorable	0	0	0
Favorable	-2	-2	-5
Fair	-5	-7	-25
Unfavorable	-10	-15	-50
Very Unfavorable	-12	-25	-60

Table 2.4: Rock Classification Based on Final RMR Rating

RMR Rating	100–81	80–61	60–41	40–21	<20
Class No.	I	II	III	IV	V
Description	Very good	Good	Fair	Poor	Very poor

Physical appearance of rock mass in each RMR rock classification is listed below:

Intact: The rock mass does not have discontinuities and is not weathered. This situation is very rare in nature. However, small rock cores can exhibit this condition in the laboratory.

Very Good (Class I): The rock mass is tightly interlocked and undisturbed. No weathering has occurred in the joints. The space between adjacent joints is 3 to 10 ft.

Good (Class II): The rock mass is disturbed, and the joints are slightly weathered with joint spaced of 3 to 10 ft.

Fair (Class III): There are several sets of joints in the rock mass. The joints are moderately weathered, and the joint space is 1 to 3 ft.

Poor (Class IV): Numerous weathered joints exist in the rock mass, and the space of joints is only 2 to 12 in. The rock mass has some gouges and clean compacted rock waste.

Very Poor (Class V): The rock mass is full of weathered joints spaced at less than 2 in. Many gouges and clean compacted waste rock with fines are spread through the rock mass.

The relative rating of the uniaxial compression strength needs to be determined in the laboratory according to applicable ASTM protocol D-7012. The uniaxial compressive strength q_u (Pa or psf) is defined as:

$$q_u = \frac{F}{A}$$

where F = the applied load at failure (N or lbf); and A = the cross area of the rock specimen (mm^2 or ft^2).

The relative rating of RQD can be obtained either in the field or in the laboratory by examining rock core samples, per ASTM D-6032. The definition of RQD is as follow:

$$RQD = \frac{l_s}{l_t} \cdot 100$$

where l_s = the sum of length of core sticks longer than 100 mm (4 in.), measured along the center line of the core; and l_t = the total length of the core run (mm or in.).

Naturally, the elastic modulus of rock mass should be smaller than that of intact sample of the same rock. Hence, AASHTO offered two equations to estimate the elastic modulus of rock mass E_m . The first equation, Eq. 3, is based on the RMR value. The other equation, Eq. 4, involves the elastic modulus of intact rock and a reduction factor.

$$E_m = 1000 \cdot 10^{(RMR-10)/40}$$

$$E_m = E_i(E_m/E_i)$$

where E_m = elastic modulus of the jointed rock mass (MPa); E_i = elastic modulus of intact rock mass (MPa) (its values are listed in Table 2.5 for typical rock types); and E_m/E_i = a reduction factor of the rock mass (its values are listed in Table 2.6 for typical rock types).

Another elastic constant, Poisson's ratio, is tabulated in Table 2.7.

Table 2.5: Intact Rock Elastic Modulus

Rock Type	No. of Values	No. of Rock Types	Elastic Modulus, E _i (GPa)			Standard Deviation (GPa)
			Max	Min	Mean	
Granite	26	26	100.0	6.410	52.70	24.48
Diorite	3	3	112.0	17.100	51.40	42.68
Gabbro	3	3	84.1	67.600	75.80	6.69
Diabase	7	7	104.0	69.000	88.30	12.27
Basalt	12	12	84.1	29.000	56.10	17.93
Quartzite	7	7	88.3	36.500	66.10	16.00
Marble	14	13	73.8	4.000	42.60	17.17
Gneiss	13	13	82.1	28.500	61.10	15.93
Slate	11	2	26.1	2.410	9.58	6.62
Schist	13	12	69.0	5.930	34.30	21.93
Phyllite	3	3	17.3	8.620	11.80	3.93
Sandstone	27	19	39.2	0.620	14.70	8.20
Siltstone	5	5	32.8	2.620	16.50	11.38
Shale	30	14	38.6	0.007	9.79	10.00
Limestone	30	30	89.6	4.480	39.30	25.72
Dolostone	17	16	78.6	5.720	29.10	23.72

Table 2.6: Relationship between Reduction Factor and RQD Value

RQD (%)	E _m /E _i	
	Closed Joints	Open Joints
100	1.00	0.60
70	0.70	0.10
50	0.15	0.10
20	0.05	0.05

Shear strength is another important property especially for evaluating the rock mass resistance and rock slope stability. Rock mass shear strength is also critical for bridge foundation design. The AASHTO adopted the Hoek and Brown criteria to estimate the shear strength of the rock mass. The equation is:

$$\tau = (\cot\phi'_i - \cos\phi'_i)m \frac{q_u}{8}$$

where τ = the shear strength of the rock mass (MPa); q_u = the average unconfined compressive strength (MPa); m, s = the rock mass constant (their values are listed in Table 2.8); and ϕ'_i = the instantaneous rock friction angle (degree).

Table 2.7: Intact Rock Poisson's Ratio

Rock Type	No. of Values	No. of Rock Types	Poisson's Ratio			Standard Deviation
			Max	Min	Mean	
Granite	22	22	0.39	0.09	0.20	0.08
Gabbro	3	3	0.20	0.16	0.18	0.02
Diabase	6	6	0.38	0.20	0.29	0.06
Basalt	11	11	0.32	0.16	0.23	0.05
Quartzite	6	6	0.22	0.08	0.14	0.05
Marble	5	5	0.40	0.17	0.28	0.08
Gneiss	11	11	0.40	0.09	0.22	0.09
Schist	12	11	0.31	0.02	0.12	0.08
Sandstone	12	9	0.46	0.08	0.20	0.11
Siltstone	3	3	0.23	0.09	0.18	0.06
Shale	3	3	0.18	0.03	0.09	0.06
Limestone	19	19	0.33	0.12	0.23	0.06
Dolostone	5	5	0.35	0.14	0.29	0.08

Table 2.8: Approximate value of Rock Mass Constant m and s

Rock Quality		A	B	C	D	E
Intact RMR = 100	m	7.00	10.00	15.00	17.00	25.00
	s	1.00	1.00	1.00	1.00	1.00
Very Good RMR = 85	m	2.40	3.43	5.14	5.82	8.567
	s	0.082	0.082	0.082	0.082	0.082
Good RMR = 65	m	0.575	0.821	1.231	1.395	2.052
	s	0.00293	0.00293	0.00293	0.00293	0.00293
Fair RMR = 44	m	0.128	0.183	0.275	0.311	0.458
	s	0.0009	0.0009	0.0009	0.0009	0.0009
Poor RMR = 23	m	0.029	0.041	0.061	0.069	0.102
	s	3×10^{-6}				
Very Poor RMR = 3	m	0.007	0.010	0.015	0.017	0.025
	s	1×10^{-7}				

Footnote:

A: Carbonate rocks with well developed crystal cleavage (dolomite, limestone, marble);

B: Lithified argillaceous rocks (mudstone, siltstone, shale, slate);

C: Arenaceous rocks with strong crystal and poorly developed crystal cleavage (sandstone, quartzite);

D: Fine-grained polyminerallic igneous crystalline rocks (andesite, dolerite, diabase, rhyolite);

E: Coarse-grained polyminerallic igneous & metamorphic crystalline rocks (amphibolite, gabbro gneiss, granite, norite, quartz-diorite).

The values of ϕ'_i for typical rock types are listed in Table 2.9. It can also be determined by:

$$\phi'_i = \tan^{-1}\{4h \cos^2[30 + 0.33 \sin^{-1}(h^{-1.5})] - 1\}^{-0.5}$$

where $h = 1 + 16 \left(\frac{m\sigma'_n + sq_u}{3m^2q_u} \right)$; σ'_n = effective normal stress (MPa).

Table 2.9: Typical Ranges of Friction Angles for Smooth Joints in Some Rock Types

Rock Class	Friction Angle Range	Typical Rock Types
Low Friction	20~27°	Schists (high mica content), Shale, Marl
Medium Friction	27~34°	Sandstone, Siltstone, Chalk, Gneiss, Slate
High Friction	34~40°	Basalt, Granite, Limestone, Conglomerate

2.3.2 The GSI Method

In 2002, Hoek developed his GSI theory into its latest version, which is known as the Hoek-Brown Failure Criterion. Its general equation for the jointed rock masses is:

$$\sigma'_1 = \sigma'_3 + \sigma_{ci} \left(m_b \frac{\sigma'_3}{\sigma_{ci}} + s \right)^a$$

where σ'_1, σ'_3 = major, minor effective principal stress; σ_{ci} = the intact rock's uniaxial compressive strength; m_b = the deducted value of m_i , and $m_b = m_i \exp\left(\frac{GSI-100}{28-14D}\right)$; m_i = a material constant of the intact rock (values of m_i for typical rock types are listed in Table 2.10); s = rock mass constant, and $s = \exp\left(\frac{GSI-100}{9-3D}\right)$, ($s = 1$ for intact rock); a = rock mass constant, and $a = \frac{1}{2} + \frac{1}{6} \left[\exp\left(\frac{GSI}{-15}\right) - \exp\left(\frac{20}{-3}\right) \right]$; D = the factor to show the degree of rock mass disturbance caused by blast damage and stress relaxation (its values are listed in Table 2.11); and GSI = the value determined visually by the structure and the surface conditions of the rock mass (its values are listed in Table 2.12).

In the triaxial compression test, the major principle stress (σ'_1) and minor principle stress (σ'_3) are directly measured by the apparatus. Using these two principle stresses, the uniaxial compressive strength (σ_{ci}) and material constant (m_i) of intact rock can be determined for intact rock through the following functions.

Assume $x = \sigma'_3$ and $y = (\sigma'_1 - \sigma'_3)^2$, the parameters can be determined as:

$$\sigma_{ci}^2 = \frac{\sum y}{n} - \frac{\sum x}{n} \cdot \frac{n \sum xy - \sum x \sum y}{n \sum x^2 - (\sum x)^2}$$

$$m_i = \frac{1}{\sigma_{ci}} \cdot \frac{n \sum xy - \sum x \sum y}{n \sum x^2 - (\sum x)^2}$$

The coefficient of determination (r) is calculated as:

$$r = \frac{(n \sum xy - \sum x \sum y)^2}{[n \sum x^2 - (\sum x)^2][n \sum y^2 - (\sum y)^2]}$$

Based on the principal stresses derived from the triaxial test, the normal stress (σ'_n) and the shear stress (τ) can also be estimated through the following equations.

$$\sigma'_n = \frac{\sigma'_1 + \sigma'_3}{2} - \frac{\sigma'_1 - \sigma'_3}{2} \cdot \frac{d\sigma'_1/d\sigma'_3 - 1}{d\sigma'_1/d\sigma'_3 + 1}$$

$$\tau = (\sigma'_1 - \sigma'_3) \frac{\sqrt{1 + d\sigma'_1/d\sigma'_3}}{d\sigma'_1/d\sigma'_3 + 1}$$

$$d\sigma'_1/d\sigma'_3 = 1 + am_b(m_b\sigma'_3/\sigma_{ci} + s)^{a-1}$$

After determining the uniaxial compressive strength (σ_{ci}), the uniaxial compressive strength (σ_c) and tensile strength (σ_t) can be calculated by:

$$\sigma_c = s^a \sigma_{ci} \text{ when } \sigma'_3 = 0$$

$$\sigma_t = -\frac{s\sigma_{ci}}{m_b}$$

Table 2.10: Typical Values of Material Constant m_i (Hoek 2006)

Rock Type	Class	Group	Texture				
			Coarse	Medium	Fine	Very Fine	
Sedimentary	Clastic		Conglomerates 21±3	Sandstones 17±4	Siltstones 7±2	Claystones 4±2	
			Breccias 19±5		Greywackes 18±3	Shales 6±2	
						Marls 7±2	
	Non-Clastic		Crystallines Limestone 12±3	Sparitic Limestone 10±2	Micritic Limestone 9±2	Dolomites 9±3	
			Evaporites	Gypsum 8±2	Anhydrite 12±2		
			Organic			Chalk 7±2	
Metamorphic	Non Foliated		Marble 9±3	Hornfels 19±4	Quartzites 20±3		
				Metasandstone 19±3			
	Slightly Foliated		Migmatite 29±3	Amphibolites 26±6			
	Foliated		Gneiss 28±5	Schists 12±3	Phyllites 7±3	Slates 7±4	
Igneous	Plutonic		Granite 32±3	Diorite 25±5			
			Granodiorite 29±3				
			Dark		Gabbro 27±3	Dolerite 16±5	
	Norite 20±5						
	Hypabyssal		Prophyries 20±5		Diabase 15±5	Peridotite 25±5	
	Volcanic		Lava		Rhyolite 25±5	Dacite 25±3	Obsidian 19±3
					Andesite 25±5	Basalt 25±5	
Pyroclastic		Agglomerate 19±3	Breccia 19±5	Tuff 13±5			

Table 2.11: Determination of Disturbance Factor D

Appearance of rock mass	Description of rock mass	Suggested value of <i>D</i>
	Excellent quality controlled blasting or excavation by Tunnel Boring Machine results in minimal disturbance to the confined rock mass surrounding a tunnel.	<i>D</i> = 0
	Mechanical or hand excavation in poor quality rock masses (no blasting) results in minimal disturbance to the surrounding rock mass. Where squeezing problems result in significant floor heave, disturbance can be severe unless a temporary invert, as shown in the photograph, is placed.	<i>D</i> = 0 <i>D</i> = 0.5 No invert
	Very poor quality blasting in a hard rock tunnel results in severe local damage, extending 2 or 3 m, in the surrounding rock mass.	<i>D</i> = 0.8
	Small scale blasting in civil engineering slopes results in modest rock mass damage, particularly if controlled blasting is used as shown on the left hand side of the photograph. However, stress relief results in some disturbance.	<i>D</i> = 0.7 Good blasting <i>D</i> = 1.0 Poor blasting
	Very large open pit mine slopes suffer significant disturbance due to heavy production blasting and also due to stress relief from overburden removal. In some softer rocks excavation can be carried out by ripping and dozing and the degree of damage to the slopes is less.	<i>D</i> = 1.0 Production blasting <i>D</i> = 0.7 Mechanical excavation

Table 2.12: Determination of GSI Value

<p>GEOLOGICAL STRENGTH INDEX FOR JOINTED ROCKS (Hoek and Marinos, 2000)</p> <p>From the lithology, structure and surface conditions of the discontinuities, estimate the average value of GSI. Do not try to be too precise. Quoting a range from 33 to 37 is more realistic than stating that GSI = 35. Note that the table does not apply to structurally controlled failures. Where weak planar structural planes are present in an unfavourable orientation with respect to the excavation face, these will dominate the rock mass behaviour. The shear strength of surfaces in rocks that are prone to deterioration as a result of changes in moisture content will be reduced if water is present. When working with rocks in the fair to very poor categories, a shift to the right may be made for wet conditions. Water pressure is dealt with by effective stress analysis.</p>		SURFACE CONDITIONS				
		VERY GOOD Very rough, fresh unweathered surfaces	GOOD Rough, slightly weathered, iron stained surfaces	FAIR Smooth, moderately weathered and altered surfaces	POOR Stickensided, highly weathered surfaces with compact coatings or fillings or angular fragments	VERY POOR Stickensided, highly weathered surfaces with soft clay coatings or fillings
STRUCTURE		DECREASING SURFACE QUALITY →				
	INTACT OR MASSIVE - intact rock specimens or massive in situ rock with few widely spaced discontinuities	90			N/A	N/A
	BLOCKY - well interlocked undisturbed rock mass consisting of cubical blocks formed by three intersecting discontinuity sets	80	70			
	VERY BLOCKY- interlocked, partially disturbed mass with multi-faceted angular blocks formed by 4 or more joint sets		60	50		
	BLOCKY/DISTURBED/SEAMY - folded with angular blocks formed by many intersecting discontinuity sets. Persistence of bedding planes or schistosity			40	30	
	DISINTEGRATED - poorly interlocked, heavily broken rock mass with mixture of angular and rounded rock pieces				20	
	LAMINATED/SHEARED - Lack of blockiness due to close spacing of weak schistosity or shear planes	N/A	N/A			10
		↑ DECREASING INTERLOCKING OF ROCK PIECES ↓				

In the GSI system, the elastic modulus of the rock mass can be estimated by:

$$E_m(\text{GPa}) = \left(1 - \frac{D}{2}\right) \sqrt{\frac{\sigma_{ci}}{100}} \cdot 10^{[(\text{GSI}-10)/40]} \quad \text{when } \sigma_{ci} \leq 100 \text{ MPa}$$

$$E_m(\text{GPa}) = \left(1 - \frac{D}{2}\right) \cdot 10^{[(\text{GSI}-10)/40]} \quad \text{when } \sigma_{ci} > 100 \text{ MPa}$$

The GSI criterion can also be transferred to the Mohr-Coulomb criterion for shear strength evaluation. The general relationship between the principle stresses and parameters in Mohr-Coulomb criterion is:

$$\sigma'_1 = \frac{2c' \cos \phi'}{1 - \sin \phi'} + \frac{1 + \sin \phi'}{1 - \sin \phi'} \sigma'_3$$

where c' = the cohesion strength, which is determined by:

$$c' = \frac{\sigma_{ci}[(1 + 2a)s + (1 - a)m_b \sigma'_{3\max}/\sigma_{ci}](s + m_b \sigma'_{3\max}/\sigma_{ci})^{a-1}}{(1 + a)(2 + a)\sqrt{1 + [6am_b(s + m_b \sigma'_{3\max}/\sigma_{ci})^{a-1}]/[(1 + a)(2 + a)]}}$$

ϕ' = the friction angle, which is determined by:

$$\phi' = \sin^{-1} \left[\frac{6am_b(s + m_b \sigma'_{3\max}/\sigma_{ci})^{a-1}}{2(1 + a)(2 + a) + 6am_b(s + m_b \sigma'_{3\max}/\sigma_{ci})^{a-1}} \right]$$

Therefore, the shear strength (τ) can be determined by:

$$\tau = c' + \sigma \tan \phi'$$

Under the Mohr-Coulomb criterion, the uniaxial compressive strength (σ_{cm}) of rock mass can be determined by:

$$\sigma'_{cm} = \frac{2c' \cos \phi'}{1 - \sin \phi'}$$

If $\sigma_t < \sigma'_3 < 0.25\sigma_{ci}$

$$\sigma'_{cm} = \sigma_{ci} \cdot \frac{[m_b + 4s - a(m_b - 8s)](m_b/4 + s)^{a-1}}{2(1 + a)(2 + a)}$$

2.3.3 RMR-GIS Correlation

Hoek (1995) examined the relationship between RMR and GSI briefly. For finding the correlation against RMR_{76} , he assumed that the rock mass is completely dry

(groundwater rating = 10) and joint orientations are very favorable (rating modifier = 0). For linking GSI and RMR₈₉, he set the groundwater rating at 15 (rock completely dry) and the rating adjustment at 0 (very favorable joint orientations). The resulting equations were:

$$\text{GSI} = \text{RMR}_{76} \quad \text{for } \text{RMR}_{76} > 18$$

$$\text{GSI} = \text{RMR}_{89} - 5 \quad \text{for } \text{RMR}_{89} > 23$$

The lower limit is specified for RMR, since for very poor quality rock masses it is difficult to obtain the strength and a reliable RMR. The above equations are obviously only applicable to the specific groundwater and joint orientation conditions.

Coşar (2004) tabulated the relationship between GSI and RMR for weak rock masses (RMR < 40) as shown in Table 2.13.

Table 2.13: GSI vs. RMR for Very Weak Rock Masses

GSI	RMR	GSI	RMR
32	26 to 35	38	36
33	30	40	27 to 40
34	37 to 39	41	30 to 39
36	26 to 40	45	36 to 39
37	35 to 37		

Osgoui and Ünal (2005) examined poor rock masses (in metasiltestone, sandstone, shale, phyllite) surrounding a railroad tunnel in Turkey, where a large amount of deformations had developed. After testing rock core specimens taken from 67 boreholes and estimating their uniaxial compressive strength, they developed the following exponential function to correlate RMR and GSI:

$$\text{GSI} = 6\exp(0.05 \text{ RMR}) \quad \text{for } \text{RMR} < 30$$

The above correlation is compatible with the definition of GSI by Hoek (1994), as the minimum value of GSI at RMR = 0 is 6.

The current AASHTO practice as of 2008 is described in the NCHRP Report 651 (2010). In it, it states that for RMR less than 23 the RMR-GSI correlation can go through the modified Tunneling Quality Index (Q') as:

$$GSI = 9 \log(Q') + 44 = 9 \log\left(\frac{RQD}{J_n} \cdot \frac{J_r}{J_a}\right) + 44$$

where J_n = number of sets of discontinuities; J_r = roughness of discontinuities; and J_a = discontinuity condition and infilling.

The following table is referenced to evaluate the values of the joint discontinuity parameters associated with Q'.

Table 2.14: Values of Joint Discontinuity Parameters

Value of J_n		Value of J_r	
Massive	0.5	Noncontinuous joints	4
One set	2	Rough, wavy	3
Two sets	4	Smooth, wavy	2
Three sets	9	Rough, planar	1.5
Four or more sets	15	Smooth, planar	1
Crushed rock	20	Slick, planar	0.5
		Filled discontinuities	1

Value of J_a		
Unfilled Discontinuities	Healed	0.75
	Stained, no alteration	1
	Silty or sandy coating	3
	Clay coating	4
Filled Discontinuities	Sand or crushed rock infill	4
	Stiff clay infill < 5 mm thick	6
	Soft clay infill < 5 mm thick	8
	Swelling clay < 5 mm thick	12
	Stiff clay infill > 5 mm thick	10
	Soft clay infill > 5 mm thick	15
	Swelling clay > 5 mm thick	20

2.4 Rock Slope and Rock Foundation Considerations

Rock slopes exist along many miles of highways in Ohio. Due to limited right-of-way space, these slopes are made nearly vertical. Rock masses on the cut surfaces have natural as well as construction-induced discontinuities. Thus, a certain amount of rock fall and slide movement is unavoidable. In addition, steep cuts in weak rock such as shale can over time slump or slide down almost like soil slopes as the rock weather progressively. When analyzing the stability of rock slopes, important design parameters are the slope's height and steepness, the orientations of discontinuity planes, rock's unit weight, and cohesion and friction angle of the rock.

For shallow foundations on soil, settlement limit is usually the most controlling factor in design. Compared to soils, most rock masses are much more strong and stiff. Thus, for shallow foundations on rock, the bearing capacity may be more limiting than the settlement. Only if the rock is highly disjointed/weathered, settlement may be again more important than the bearing capacity. Engineering properties of rock that are relevant to these situations include the elastic modulus, Poisson's ratio, and internal friction angle of the rock.

NCHRP Report 651 (2010) has a review of bearing capacity issues for shallow foundations on rock. The key concept is that the bearing capacity failure mechanism for these foundations depends on the nature of joints (spacing, opening, and orientations) in relationship to the loaded area.

The simplest bearing capacity method for spread footings on rock is described by the Canadian Geotechnical Society (2006). The method is supposedly applicable to wide ranges of rock type and rock quality. In this approach that requires the joint spacing to be more than 1 ft (0.3 m), the allowable bearing pressure q_{allow} is expressed as:

$$q_{\text{allow}} = K_{\text{sp}} (q_u)$$

where K_{sp} = an empirical coefficient (ranges from 0.1 to 0.4); and q_u = average unconfined compression strength of rock.

The coefficient includes a factor of safety of 3 and is given by:

$$K_{sp} = \frac{3 + (s/B)}{10\sqrt{1 + 300(\delta/s)}}$$

where s = joint spacing; B = foundation width; and δ = joint opening size.

A few more elaborate bearing capacity theories are also available for foundations on rock. When the joint spacing s is close (i.e., much narrower than the loaded width B ; $s \ll B$), joints are open, and joint orientations are vertical, the ultimate bearing capacity (q_{ult}) will be dictated by the unconfined compression strength (q_u) of rock columns, that is:

$$q_{ult} = q_u$$

When the joint spacing s is small compared to the foundation width ($s \ll B$), joints are closed, and joint orientations are vertical, the rock mass tends to behave as one continuous body (rather than disconnected columns). In this case, the ultimate bearing capacity (q_{ult}) of the rock mass can be given by:

$$q_{ult} = 2c \tan(45^\circ + \phi/2)$$

where c = cohesion of the rock mass; and ϕ = friction angle of the rock mass.

When the joint spacing s is larger than the loaded width B ($s \gg B$) and joints are running vertically, the joints do not play any role. The ultimate bearing capacity will be provided by the cone-shape zone beneath the loaded area in the solid rock block. In this case, the ultimate bearing capacity (q_{ult}) of the rock mass can be given by:

$$q_{ult} \approx JcN_{cr}$$

where J = a correction factor (depends on the foundation width B and the thickness of the rock block); and N_{cr} = bearing capacity factor.

According to Bishoni (1968), the value of J is estimated based on the ratio between the horizontal joint spacing s and the foundation width B .

$$J = 1.0 \quad \text{for } \frac{s}{B} > 5$$

$$J = 0.12 \left(\frac{H}{B} \right) + 0.40 \quad \text{for } \frac{s}{B} \leq 5$$

Goodman (1980) expressed N_{cr} in terms of the classic bearing capacity factor N_ϕ as:

$$N_{cr} = \frac{2N_\phi^2}{1 + N_\phi} \left(1 - \frac{1}{N_\phi} \right) (\cos \phi) \left(\frac{S}{B} \right) - N_\phi (\cos \phi) + 2\sqrt{N_\phi}$$

where $N_\phi = \tan^2(45^\circ + \phi/2)$.

Carter and Kulhawy (1988) incorporated the Mohr-Coulomb failure equation developed by Hoek and Brown into the bearing capacity theory. The resulting equation for strip footings resting on jointed rock mass is:

$$q_{ult} = \left(\sqrt{s} + \sqrt{m\sqrt{s} + s} \right) q_u$$

where s, m = empirical RMR rock mass strength parameters (see Table 2.8 for their values).

The above equation is supposed to give the lower bound of the ultimate bearing pressure.

CHAPTER 3 : METHODOLOGY

This chapter describes methodologies that were employed in the current study to procure rock samples and prepare and test them. The chapter also explains how the test data were analyzed using computer software tools.

3.1 Rock Specimen Preparation

Rock samples cored by geotechnical consultants/test labs at many bridge construction sites in Ohio were provided to the Ohio University research team via ODOT Material Testing Laboratory located in Columbus as part of ODOT design projects. Types of rock supplied included claystone, limestone, sandstone and shale. These rock materials came from a variety of geological regions in Ohio (shown previously in Figure 2.1), but not every geological region supplied all four rock types. Recovered rock cores were protected in commercially produced rock core storage boxes, and basic information (such as site ID, depth range, and rock type) was marked on each box. Most rock cores were covered tightly with plastic wrap and aluminum foil to keep their moisture content intact, while some rock samples were naked when they arrived at the Ohio University lab. After receiving each box full of rock cores, the following steps were taken one by one:

Step 1) All rock core samples in the box are checked for their quality and verifying the information marked on the box. The diameter of the rock samples should be 2 inches, which is required by the Hoek cell and the triaxial compression test devices used in the current study. Since the most desirable length to diameter ratio is 2:1 for strength testing according to ASTM D-7012, the core pieces that were shorter than 4 inches in length were not generally considered for any testing. However, core samples of specific rock types that are rare in some geological regions were retained for further testing even if their lengths were shorter than 4 inches.

Step 2) The shape of the ready-to-test specimen should be a near-perfect cylinder. Vertical sides of most cores met the surface tolerance of 0.02 inches required by ASTM D-4543. Thus, the original irregular ends were cut off perpendicular to the longitudinal axis of the core. This was done by fixing the core sample on the platform normal to the sawing direction and bringing the circular saw slowly to slice the rock without much pressure and vibration to minimize unnecessary cracking/chipping on the core sample. Dry technique was employed during the cutting process, since spraying of water (to cool the saw blade) would change the sample's moisture content significantly. For sensitive materials such as claystone and shale, the use of water might disintegrate the rock completely. After cutting, both ends were grinded to ensure that the tolerance of surface flatness does not exceed 0.001 inches, which is also required by ASTM D-4543.

According to ODOT lab report (2013), the diameter and length of rock specimen are to be each measured three times. The average of three diameter measurements and the average of three length measurements should represent the sample's geometric dimensions. The weight is measured on the electric scale that is accurate to 0.001 pound.

Step 3) A relatively narrow range of the GSI value of the rock specimen is determined visually using Figure 2.11 and recorded.

Step 4) To determine the mechanical properties of the rock samples and calculate their relative RMR and GSI parameters, the rock samples should be compressed to failure in the unconfined compression test and triaxial compression test modes. The detail procedure for each of the two test methods are described in the following sections. When the axial compression load suddenly drops a lot or continuously decreases, it implies that the rock specimen has failed. The loading test can be stopped, and the compression strength can be calculated by:

$$\sigma = CF \cdot \frac{P}{A}$$

where σ = the compressive strength; P = the peak compression load; A = the average cross-sectional area of the test specimen; and CF = correction factor.

Per ODOT (2013), the compression strength should be corrected in cases where the specimen's length-to-diameter (L/D) ratio is less than 2.0. ODOT has developed the following guideline on the correction factor:

Correction Factor = 1.0	for $L/D \geq 2$
Correction Factor = $(L/D) \times 0.08 + 0.84$	for $2 > L/D \geq 1.5$
Correction Factor = $(L/D) \times 0.12 + 0.77996$	for $1.5 > L/D \geq 1.25$
Correction Factor = $(L/D) \times 0.24 + 0.6301$	for $L/D < 1.25$

where L/D = the ratio of the specimen's length to its diameter.

In the current study, none of the test specimens ended up shorter than 3 inches (L/D ratio > 1.5).

Step 5) After completing the rock specimen's load test, the specimen's weight is recorded on an electronic scale before and after oven-drying it for 24 hours. Then, the specimen's moisture content can be calculated.

3.2 Unconfined Compression Test

The unconfined compression strength is a property that directly expresses the rock sample's ability to sustain the axial compression. The unconfined compression test is a simple and efficient method to measure the rock's compressive strength. The loading

machine used for this test was Gilson CM 1000D, whose maximum load is one million pounds and accuracy is 20 pounds. Its loading rate can be adjusted from 1,000 lb/min. to 10,000 lb/min. This is a bottom loading hydraulic machine, with its top loading platen being self-adjusting because it is equipped with a universal joint.

The following steps were taken to perform this test on each rock specimen:

Step 1) The loading machine is turned on by activating the hydraulic pump first and then the electric panel. Once the panel is on, the load reading is initialized by pressing the ZERO button. The “PEAK HOLD” function needs to be activated before loading so that the onboard computer can register the maximum load that is supported by the test specimen. The headroom in the loading area is adjusted by operating the loading lever to either “RETRACT” or “FULL ADVANCE” position. When the space is enough to accommodate the rock sample and two loading platens, the lever can be set in the “HOLD” position. Then, the self-adjusting platen is placed at the center of the bottom loading platform. The rock specimen is positioned on top of the self-adjusting loading platen and also centered. Then, the loading lever is set in the “FULL ADVANCE” to close most of the gap that exists between the top of the rock specimen and top loading surface. Next, the loading lever is pushed into the “METERED ADVANCE” position to move the specimen upward to slowly close the remaining gap.

Step 2) As soon as the display window shows a seating load of about 100 lbs, the test can begin by starting the stop watch. The load reading is recorded every 30 seconds, while maintaining the loading lever in the “METERED ADVANCE” position. According to ASTM D-7012, the rock specimen must be under a steadily-increasing compression load. Based on the experience gained in the current study, the satisfactory loading rate may be close to 2,000 lb/minute for sandstones, 3,000 to 4,000 lb/minute for limestone and unweathered shale, and only 50 lb/minute for weathered shale and claystone.

Step 3) The loading test is stopped when the load reading keeps decreasing after registering a pronounced peak. By this stage, some cracks may appear visibly on the specimen surface (accompanied by audible noises). The time that took to reach the failure point is also recorded.



Figure 3.1: Rock Specimen Undergoing Unconfined Compression Loading

Step 4) After the failure of the rock sample, the test specimen is unloaded completely and studied to document its failure mode. The specimen is quickly put on a scale and then into a laboratory oven to obtain its moisture content. The final step is to take the peak load value to calculate the compressive strength.

3.3 Triaxial Compression Test

In the field, the rock mass lies beneath the ground surface and is confined by its surrounding solid materials. To simulate the in-situ conditions, a confining pressure should be placed on the rock specimen's side and maintained while applying the axial

compression loading. Depending on the rock material type and the confining pressure level, the axial compressive strength of rock may increase substantially with the presence of the confining pressure. This is why the triaxial test method is more realistic and better than the unconfined compression test.

Both pier and abutment foundations designed for highway bridges in Ohio typically extend no more 100 feet into the ground. Hence, the maximum confining pressure should be 50 psi for testing rock materials for highway bridge considerations due to the rule of thumb of ½ psi per foot of depth. This limit is also justified because the confining pressure acting at a 100-ft deep rock mass basement is estimated through the theory of linear elasticity to be:

$$\sigma_c = \frac{\mu}{1 - \mu} \sigma_v = \frac{0.15}{1 - 0.15} \times 165 \times 100 = 2912 \text{ psf} = 20 \text{ psi}$$

where σ_c = the confining pressure; μ = the Poisson's Ratio, which is assumed to be 0.15; and σ_v = the vertical pressure, which is the product of the rock unit weight (assumed to be 165 pcf) and depth (assumed to be 100 ft).

3.3.1 Triaxial Test on Strong Rock Samples

In the current study, limestone, sandstone, and unweathered shale were all classified as strong rock materials. To test these materials in the triaxial compression mode, each rock specimen was loaded axially while being encased in a special chamber called the Hoek Cell. This remarkably simple cell, designed by Hoek in 1968, was necessary for maintaining a constant confining pressure against the side of the specimen. Figure 3.2 illustrates the Hoek Cell construction. The annular space between the membrane jacket and the cell body is filled with hydraulic oil. A hydraulic pump is connected to the cell through the oil inlet port. After inserting a test specimen and before applying the axial load, the oil in the space is pressurized. Two levels of confining pressure (25, 50 psi)

were involved in the triaxial testing program. The axial compression load was provided by the loading machine Gilson CM 1000D, which was previously utilized to run the unconfined compression tests. The following steps were taken to perform the Hoek Cell triaxial compression test on each strong rock specimen:

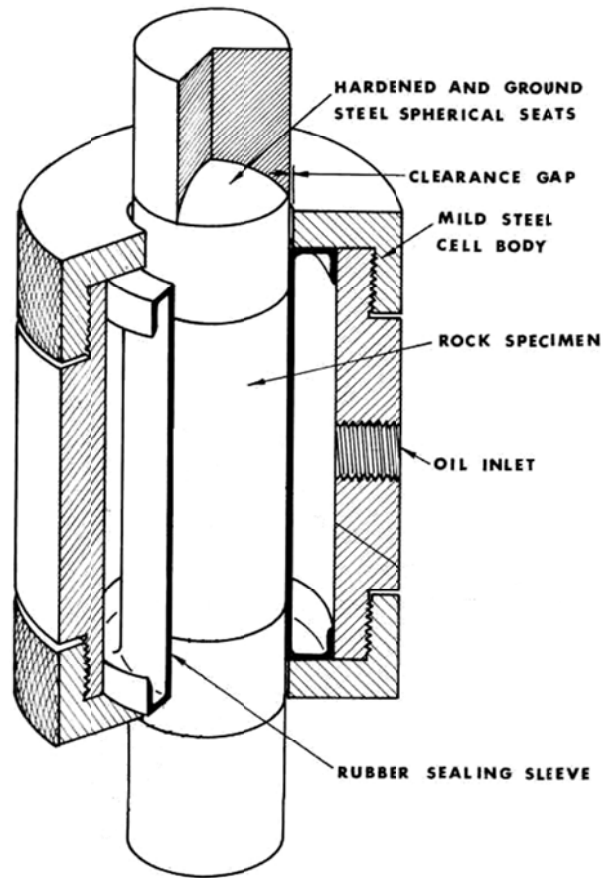


Figure 3.2: Details of Hoek Cell

Referenced and Revised: Simple triaxial cell for field or laboratory testing of rock, *E. Hoek & J. A. Franklin (1968)*

Step 1) The membrane jacket is inserted into the cell. Then, the Hoek Cell is assembled by attaching other cell parts together. The caps on both couplings are unscrewed, so that a hydraulic pump can be connected to one of the couplings through a hose. The hydraulic pump is operated to push the oil into the cell. The valve in the other coupling must be pressed inward to bleed the air out of the cell while pumping. The air-releasing

coupling should face upward to ensure all air can be removed from the cell. When the oil comes out from the air-releasing coupling, the valve is released and covered with its cap.

[Note] This first step is only necessary for preparing the cell at the beginning of the testing program. Once the cell is filled with hydraulic oil, each load test can start from Step 2 described below.

Step 2) A test rock specimen is inserted into the membrane jacket opening of the cell that is lying flat on its side. It is then adjoined by the steel cylinder seat at the bottom and by the steel spherical seat at the top. It is important that the horizontal line marked on the spherical seat is flush with the top surface of the cell. While keeping the specimen and steel seats in their respective positions, the hydraulic pump is operated to build up just enough oil pressure (ex. 15-20 psi) to grip all three components and hold them together. The cell can now be held upright on top of a self-adjusting loading platen. At the top of the cell, the mating piece for the steel spherical seat is added to close the gap. Then, the hydraulic pump is operated again to make the confining pressure reach exactly the desired level (25 psi or 50 psi).

Step 3) Steps 1 through 4 previously given in Section 3.2 are executed to compress the rock specimen to failure. During the period of compression, the confining pressure should be under surveillance to ensure it will not change by more than $\pm 1\%$. If the confining pressure does deviate, the pump can be operated to adjust the confining pressure. Somewhat weak rock specimens tend to dilate laterally while being compressed axially, which can increase the confining pressure significantly.

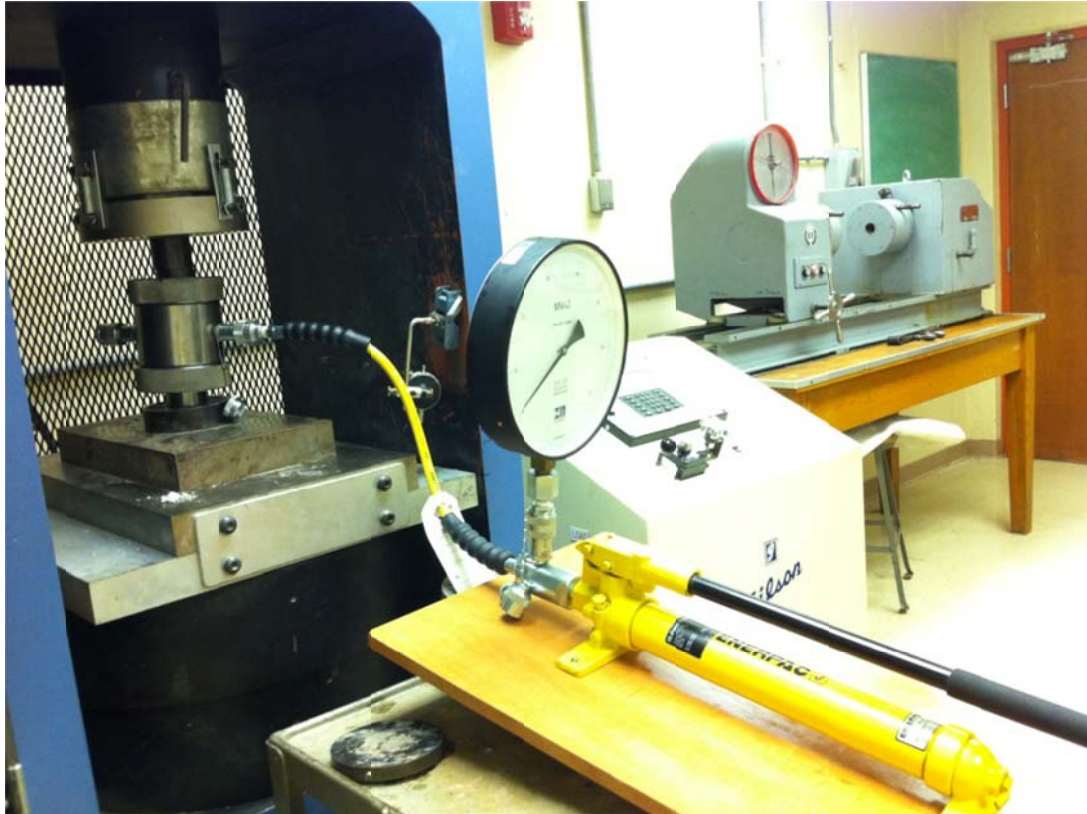


Figure 3.3: Strong Rock Specimen Undergoing Hoek Cell Triaxial Compression Test

3.3.2 Triaxial Test on Weak Rock Samples

In the current study, claystone and highly weathered shale were both classified as weak rock materials. Soil-like characteristics of these rock samples were easily noticeable, as they possess somewhat soft surface texture, and they can be cut very quickly without much pressure. The compression strength of weak rock is much lower than that of strong rock but a little higher than that of pure soil. Since weak rock is very common at the shallow depths, the confining pressure of only 10 psi or 20 psi is more than adequate in the triaxial cell testing. The test equipment used to run the weak rock triaxial test was “GEOTEC Sigma-1”, whose maximum load is 5,000 pounds and the accuracy is 0.01 pound. This machine was designed to perform triaxial compression tests on soil samples. The Hoek Cell cannot be used to test any weak rock specimen, as it can become

compressed without showing any signs of failure in the axial direction and it can dilate significantly in the lateral direction and keep increasing the confining pressure.

The following steps were taken to perform the triaxial compression test on each weak rock specimen:

Step 1) One porous stone disc is added on the bottom loading platen, and then the rock specimen is placed on top of the porous stone. Another porous stone disc and the top load platen are positioned over the top end of the test specimen. A rubber membrane is stretched over the inside of the membrane stretcher. The membrane's edges are folded over the stretcher ends. Small vacuum pressure is applied to the port on the side of the stretcher to stick the membrane tightly against the inner surface of the stretcher. The membrane stretcher, with the membrane held inside, is lowered over the top load platen, porous stone disc, and then test specimen until it reaches the bottom load platen. The vacuum pressure is cut off so that the membrane will wrap around the rock specimen. There should be one o-ring on the top platen and another on the bottom plastic platen. They can be each rolled up over the unfolded edge of the rubber membrane to form a water/pressure-tight seal over the platens.

Step 2) Saturation tubes are connected to the top platen, with the ends of tubes covered with vacuum grease. The valves for the saturation tubes are closed. Then, the triaxial cell chamber is installed over the membrane-encased test specimen. Each end of the chamber should be coated with vacuum grease and pressed against an o-ring that is seated in a circular groove cut into the bottom or top assembly. Three steel rods are attached to the slots on the top and bottom assemblies, and they are tightened by hand to ensure that the interface between the cell and each assembly is water/pressure-tight. There is a piston located at the center of the top assembly. The piston is unlocked and lowered slowly until its tip goes gently into a small cone depression existing at the center of the top load platen. Once this is achieved, the piston should be locked.

Step 3) The bottom assembly and de-aired water tank are connected through a tube with two end couplings. Another tube is attached to a port on the top assembly for drainage. Then, the water is pushed into the bottom of the chamber by applying a small positive air pressure on top of the water in the water tank. As the water level rises inside the chamber, the air is pushed out through the drainage tube. This process is continued until the water starts flowing out of the drainage line. When the water level is just below the top of the chamber, the chamber may be tilted to bleed most of the remaining air out. Once the cell is filled with water, the tube attached to the bottom assembly is disconnected from the water tank and hooked to the chamber pressure port on the panel. The drainage line attached to the top assembly is disconnected and replaced with another tubing that connects the top chamber to pressure pipette through the two-end couplings.

Step 4) The chamber is picked up and placed/centered on top of the platform on the loading machine. The pressure pipette is filled with water, and then a specified level of positive air pressure is dialed to apply the confining pressure to the rock specimen. The platform is raised slowly to decrease the gap between the tip of the locked loading piston and a cone-shaped seating on the upper cross-head of the compression machine. The piston is unlocked, and the axial load can be applied to the test specimen by allowing the platform to rise at a small constant strain rate. The software bundled with GEOTEC Sigma-1 automatically records the axial load reading every second via an electric load cell attached to the upper cross-head. The failure of the rock sample is set as the strain of the sample reaches an axial strain of 15%. This means that the loading rate is set at 90% strain per hour (15% strain per 10 minutes).

Step 5) When the rock specimen is compressed to 15% strain, the compression machine stops advancing the chamber automatically. The loading piston is then manually locked, and the loading platform is lowered to unload the specimen. The chamber is removed from the compression machine. The chamber is drained by connecting one tube to the bottom assembly (to form a drainage line) and connecting the top assembly port to the

pressure source. Once the cell is drained, all the valves are closed. The cell unit is disassembled by removing the top assembly first. A few photographs should be taken on the specimen with and without the rubber membrane to document its failure mode. Step 3 outlined in Section 3.1 is followed to calculate the compressive strength. Conduct Step 4 of Section 3.1 to measure the moisture content of the rock specimen. All the data stored in the computer can be accessed to produce several graphical plots.



Figure 3.4: Weak rock Specimen Failing During Soil Triaxial Test

3.4 Calculation of m_i values

Material constant m_i is a critical parameter in GSI system, because it is the indicator for expressing the strength of the intact rock sample. However, the m_i can only be determined by the peak triaxial strength and the peak unconfined compression strength. Hence, results from the triaxial compression and unconfined compression test methods described in the previous sections must be used in the m_i calculation. Once the laboratory experiments are completed, the m_i value can be determined through two computational methods, which are Hoek method and the LMA method. Each of these methods is described below.

3.4.1 The Hoek Method

Hoek presented his method in his 1997 paper “Practical Estimates of Rock Mass Strength,” which he coauthored with Brown. The regression equations for determining σ_{ci} and m_i are:

$$\sigma_{ci}^2 = \frac{\sum y}{n} - \frac{\sum x}{n} \cdot \frac{n \sum xy - \sum x \sum y}{n \sum x^2 - (\sum x)^2}$$

$$m_i = \frac{1}{\sigma_{ci}} \cdot \frac{n \sum xy - \sum x \sum y}{n \sum x^2 - (\sum x)^2}$$

where $x = \sigma'_3$; and $y = (\sigma'_1 - \sigma'_3)^2$.

The coefficient of determination (r) is calculated as:

$$r = \frac{(n \sum xy - \sum x \sum y)^2}{[n \sum x^2 - (\sum x)^2][n \sum y^2 - (\sum y)^2]}$$

This method is easy to understand and apply. However, the method comes with the prerequisite that the confining pressure applied should reach about half of the uniaxial compression strength. Otherwise, the resulting m_i value could be extremely large (more than hundreds) or negative.

3.4.2 The LMA Method

The LMA (Levenberg–Marquardt Algorithm) method was developed by Levenberg (1944) and Marquadt (1963). This method is an iterative approach, based on the Gauss-Newton algorithm. It may be superior to other regression methods, as it is very stable and converges swiftly. To estimate the accuracy of the function, the sum of square error (SSE) is the best way to tell the difference between the function and the actual curve. The equation for SSE is given by:

$$E(x, w) = \frac{1}{2} \sum_{p=1}^p e_{p,m}^2$$

where x = input vector; w = weight vector; $e_{p,m}$ = training error at output m when applying pattern p ;

$$e_{p,m} = d_{p,m} - o_{p,m}$$

d = desired output vector; and o = actual output vector.

The application of the LMA method is to continuously decrease SSE during the iteration process. The general equation of the LMA method is:

$$w_{k+1} = w_k - (J_k^T J_k + \mu I)^{-1} J_k e_k$$

where J = Jacobian matrix; I = identity matrix; and μ = combination coefficient which is always positive.

In this project, the LMA method is applied through “RocLab 1.0”, which is a free-download software created by Rocscience Inc. in 2003. In RocLab 1.0, the range of m_i value is restricted from 1 to 50. This is because according to Hoek the typical m_i value is up to 35 for strong brittle rocks and is as low as 5 for weak ductile rocks.

3.5 Statistical Analysis

To explore the characteristics of the rock types among different geological regions in Ohio, a set of statistical analyses was performed on the basic rock property data assembled in this project. The data pool combined the rock properties taken from ODOT's Material Testing Laboratory, ODOT database FALCON GDMS, and Ohio University's geotechnical laboratory testing. Each set of the basic rock properties was analyzed to determine its confidence interval. Rock properties in various geological regions were compared by conducting t-tests. And, the correlation between RMR and GSI was explored using regression methods.

The operations of any statistical method have some prerequisites that is that the data sample must meet certain conditions concerning the sample's normality and homogeneity. The normality means that the sample is normally distributed. The common methods to check the sample normality are Shapiro-Wilk Statistic (S-W) and Kolmogorov-Smirnov Statistic (K-S). Assuming the confidence level is 95%, the sample is said to be normally distributed if its values of S-W and K-S are greater than 0.05. If the sample is not initially normally distributed, the following actions should be taken:

- 1) There are too many extreme data points in the sample. The frequency of the data in the sample should distribute as a bell curve if the sample meets normality. An excessive amount of extreme data will make the distribution curve flat or skewed to one side. If that is the case, some of the extreme data must be removed to resolve the problem.
- 2) The sample is overlapped by several normal distribution sub-samples. If the plot of the sample frequency has several independent peaks, the sample has to be separated into several sub-samples with each having its own normal distribution.
- 3) The data in the sample is not sufficient to build up a normal distribution. The bell curve is not smooth along the whole sample since parts of the data are missing. If this is the case, additional data must be collected to fill the voids in the sample.

The homogeneity means that the variances of two samples are identical. The Levene's test (F-test) is the method of choice to check homogeneity. Assuming the confidence level is 95%, the variance of two sample are the same if the significance of Levene's test is greater than 0.05.

In the current study, the normality test, homogeneity test, and t-test were all performed by SPSS (Statistical Product and Service Solutions), which is a powerful statistical software package developed by IBM Company.

3.5.1 Confidence Interval of Basic Rock Properties

In this study, unit weight and unconfined compression strength constituted basic rock properties of each rock type in each geological region. ODOT provided the ranges of these basic rock properties in their 2011 document "Rock Slope Design Guide." For the data pool assembled, the confidence interval approach was adopted to examine the ranges of each property type accurately. A confidence interval should meet the assumption of normality. The equation of confidence interval is:

$$\bar{x} - z \frac{s}{\sqrt{n}} \leq x \leq \bar{x} + z \frac{s}{\sqrt{n}}$$

where \bar{x} = the average of the sample; s = the standard deviation of the sample; n = the number of the sample; z = the border in the cumulative normal distribution ($z = 1.64$ for 90% confidence level, $z = 1.96$ for 95% confidence level, and $z = 2.58$ for 99% confidence level).

3.5.2 t-Test Comparison between Geological Regions

The t-test was utilized to determine whether the basic rock properties can be treated as the same between any two different geological regions. The samples in the t-test should

be normally distributed. If two samples in the t-test meet homogeneity, the key equation of t-test is given by:

$$t = \frac{\bar{x}_1 - \bar{x}_2}{\sqrt{\left(\frac{1}{n_1} + \frac{1}{n_2}\right) \cdot \frac{(n_1-1)s_1^2 + (n_2-1)s_2^2}{n_1+n_2-2}}}$$

where \bar{x}_1, \bar{x}_2 = the average of sample 1 and sample 2, respectively; s_1, s_2 = the standard deviation of sample 1 and sample 2, respectively; and n_1, n_2 = the number of sample 1 and sample 2, respectively.

If the samples do not meet homogeneity, the t-test should be based on the following t statistics:

$$t = \frac{\bar{x}_1 - \bar{x}_2}{\sqrt{\frac{s_1^2}{n_1} + \frac{s_2^2}{n_2}}}$$

3.5.3 Correlation between RMR and GSI

Before exploring the correlation between RMR and GSI, the values of RMR and GSI should be determined first. The RMR is the sum of ratings of six parameters, which are unconfined compression strength, RQD, spacing of joints, condition of joints, groundwater conditions, and joint orientations. Hence, the triaxial compression test results will be excluded in seeking the correlation. Furthermore, based on Hoek's research, the groundwater conditions may be initially assumed to be "Completely Dry" (rating = 10 for groundwater conditions) and the joint orientations may be assumed to be "Very Favorable" (rating = 0 for joint orientations).

For each unconfined compression test performed, the GSI value was first estimated by consulting Table 2.11. Subsequently, the value was verified through a back-calculation technique. The equation used in the GSI back-calculation was:

$$\sigma'_1 = \sigma'_3 + \sigma_{ci} \left(m_b \frac{\sigma'_3}{\sigma_{ci}} + s \right)^a$$

where σ'_1 = the effective major principle stress, which is treated as unconfined compression strength; σ'_3 = the effective minor principle stress, which is determined by $\mu\gamma H/(1 - \mu)$; μ = Poisson's ratio; γ = the unit weight of rock sample; H = the depth below the ground surface;

$$m_b = m_i \exp\left(\frac{GSI - 100}{28 - 14D}\right)$$

$$s = \exp\left(\frac{GSI - 100}{9 - 3D}\right)$$

$$a = \frac{1}{2} + \frac{1}{6} \left[\exp\left(\frac{GSI}{-15}\right) - \exp\left(\frac{20}{-3}\right) \right]$$

and D = the disturbance factor during the excavation, which is assumed to be 0.

Once all the GSI values were finalized, the correlation between RMR and GSI was explored using the regression techniques, which included will linear, quadratic, exponential, logarithmic, and power functions. For generalizing the RMR-GSI relationship somewhat, three different groundwater conditions (very dry, moist, under moderate pressure) and four types of joint orientations (very favorable, favorable, fair, unfavorable) were considered. Variations in RQD were not addressed as a separate variable, as they are embedded within RMR.

CHAPTER 4 : RESULTS

4.1 Literature Review Results

An extensive literature review was conducted to collect information on the geology of Ohio rock, the Rock Mass Rating (RMR) system, the Geological Strength Index (GSI) system, the AASHTO LRFD highway bridge foundation design specifications, and basic/strength properties of Ohio rock samples. Information on Ohio rock was found mainly in the ODOT report – Rock Slope Design Guide (2011).

4.2 Ohio Rock Property Data Assembled

Ohio rock property data assembled in the project all came from three sources – a data file assembled by the ODOT’s Material Testing Laboratory, ODOT database FALCON GDMS (Geotechnical Document Management System), and Ohio University team’s laboratory testing. Contrary to the initial hope, no useful data on Ohio regional rocks was available from the US Army Corps of Engineers, private firms (ex. Advanced Terra Testing, Golder Associates), and the Colorado School of Mines. The US Army Corps of Engineers had a limited amount of rock mass shear strength data, but not unconfined and triaxial compression test data. Advanced Terra Testing possessed a volume of Ohio rock strength test data, but they could not release the data unless specific project names/locations are provided.

4.3 Basic Rock Properties

4.3.1 Statewide Ranges of Basic Rock Properties

A summary on the quantities of rock properties assembled in the current project showed that a total of 109 unit weights and 109 unconfined compression strength values were provided by the ODOT’s Material Testing Laboratory. During the exploration of the database FALCON, 61 unit weights and 203 unconfined compression strength values were located. In addition, the Ohio University team contributed 127 unit weights, 47

unconfined compression strength values, and 80 triaxial compression test results. The distribution of the basic rock property data is shown in Tables 4.1 and 4.2 for each major rock type in various Ohio geological regions (defined previously in Figure 2.1).

Table 4.1: Total Number of Ohio Rock Unit Weight Values Assembled

Region	Rock Type				
	Claystone	Limestone	Sandstone	Shale	Total
Central	0	31	4	10	45
East	0	N/A	32	10	42
Northeast	N/A	8	18	45	71
Northwest	N/A	14	N/A	N/A	14
Southeast	9	9	36	13	67
Southwest	N/A	13	N/A	45	58
Statewide	9	75	90	123	297

[Note] Number = 0 --- No rock samples were provided for the region.

N/A = The type of rock was not available in the region.

Table 4.2: Total Number of Ohio Rock Unconfined Compression Strength Values Assembled

Region	Rock Type				
	Claystone	Limestone	Sandstone	Shale	Total
Central	0	24	1	5	30
East	0	N/A	27	6	33
Northeast	N/A	3	17	90	110
Northwest	N/A	15	N/A	N/A	15
Southeast	4	6	43	13	66
Southwest	N/A	37	N/A	68	105
Statewide	4	85	88	182	359

[Note] Number = 0 --- No rock samples were provided for the region.

N/A = The type of rock was not available in the region.

Among these data, nearly forty percent are from unconfined compression tests and triaxial tests performed at Ohio University's geotechnical laboratory. The detail

information on the tests performed by the Ohio University team is listed below in Tables 4.3 and 4.4.

Table 4.3: Number of Unconfined Compression Strength Tests Performed by OU

Region	Rock Type				
	Claystone	Limestone	Sandstone	Shale	Total
Central	1	3	1	0	5
East	1	N/A	0	2	3
Northeast	N/A	3	11	3	17
Northwest	N/A	8	N/A	N/A	8
Southeast	4	0	3	2	9
Southwest	N/A	2	N/A	3	5
Statewide	6	16	15	10	47

[Note] Number = 0 --- No rock samples were provided for the region.

N/A = The type of rock was not available in the region.

Table 4.4: Number of Triaxial Compression Tests Performed by OU

Region	Rock Type				
	Claystone	Limestone	Sandstone	Shale	Total
Central	0	7 (7H)	3 (3H)	5 (4H+1S)	15 (14H+1S)
East	0	N/A	5 (5H)	4 (4S)	9 (5H+4S)
Northeast	N/A	5 (5H)	5 (5H)	5 (5H)	15 (15H)
Northwest	N/A	1 (1H)	N/A	N/A	1 (1H)
Southeast	5 (5S)	5 (5H)	6 (6H)	8 (7H+1S)	24 (18H+6S)
Southwest	N/A	6 (6H)	N/A	10 (4H+6S)	16 (10H+6S)
Statewide	5 (5S)	24 (24H)	19 (19H)	32 (20H+12S)	80 (63H+17S)

[Note] Number = 0 --- No rock samples were provided for the region.

N/A = The type of rock was not available in the region.

H = The quantity of samples tested in Hoek Cell.

S = The quantity of samples tested in soil triaxial test.

Some limestone cores taken in the northwest region came with a 2.5-inch diameter. A few different techniques were applied to reduce their diameters to 2 inches (so that they would fit into the Hoek Cell). However, all attempts failed. The core samples

disintegrated badly in the process. Thus, these larger-diameter limestone samples could not be tested by the Hoek Cell triaxial compression test method.

The statewide basic rock properties of each Ohio rock type are provided in “Rock Slope Design Guide” published by ODOT 2011, as listed in Table 4.5.

Table 4.5: Basic Rock Properties of Ohio Rocks Provided by ODOT

Rock Type	Unit Weight (pcf)	Unconfined Compressive Strength (psi)
Limestone	155-165	3500-16400
Sandstone	155-160	2000-7800
Shale	160-165	1900-2500
Claystone	160-165	50-1400

In this study, basic properties of each major rock type were derived by applying the confidence interval method to the statewide data set assembled. They are listed in Tables 4.6 through 4.10. Figures 4.1 through 4.5 plot the unit weight-strength properties of the rock samples tested by the Ohio University team, ODOT, and others. The properties of shale found in Ohio vary a lot from region to region and according to the degree of weathering. If the shale in the entire state is treated as one sample in the statistical analysis, the overlap problem will appear and violate the sample’s normality. So, the shale group was separated into unweathered shale and weathered shale. The separation between the two classes of shale was found generally at unconfined compression strength of 1 ksi.

Table 4.6: Basic Properties of Limestone in Ohio

	No	Min	Max	Ave	SD	CI (90%)		CI (95%)		CI (99%)	
UW (pcf)	54	157	180	167	5	166	168	166	168	166	169
UCS (psi)	65	3659	19065	10159	3261	9496	10823	9367	10952	9116	11203

[Note] UW = Unit Weight; UCS = Unconfined Compression Strength; SD = Standard Deviation; and CI (95%) = 95% Confidence Interval.

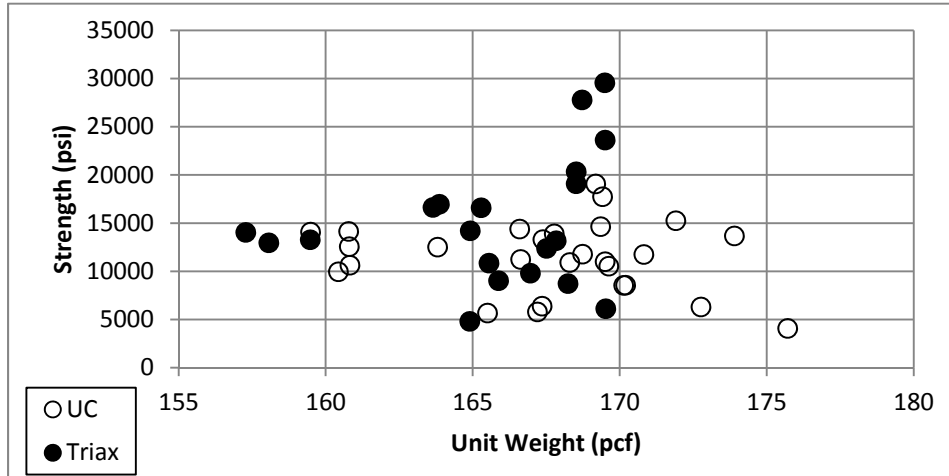


Figure 4.1: Plot of Ohio Limestone Properties (OU Data)

Table 4.7: Basic Properties of Sandstone in Ohio

	No	Min	Max	Ave	SD	CI (90%)		CI (95%)		CI (99%)	
UW (pcf)	45	149	171	160	5	159	162	159	162	158	162
UCS (psi)	63	456	7655	3719	1885	3329	4108	3253	4184	3106	4332

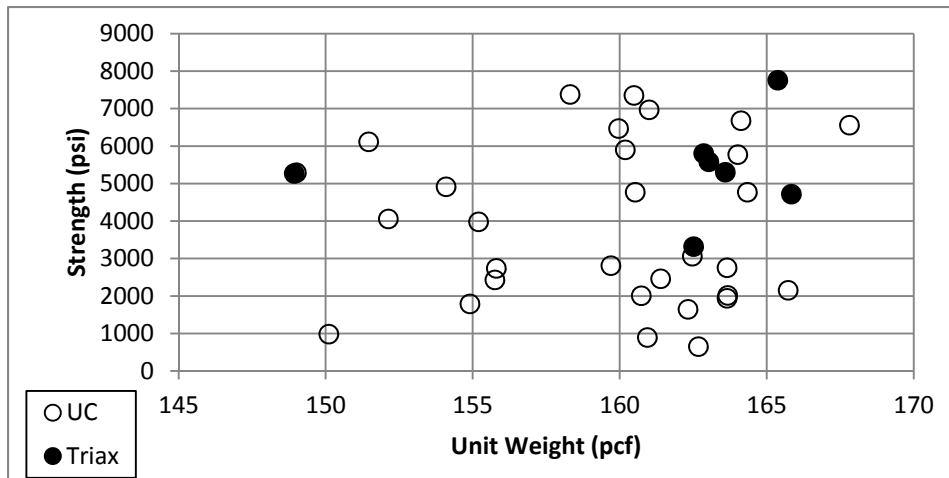


Figure 4.2: Plot of Ohio Sandstone Properties (OU Data)

Table 4.8: Basic Properties of Unweathered Shale in Ohio

	No	Min	Max	Ave	SD	CI (90%)		CI (95%)		CI (99%)	
UW (pcf)	62	145	172	159	6	158	160	157	160	157	161
UCS (psi)	36	1628	5890	3326	1234	2988	3663	2922	3729	2795	3856

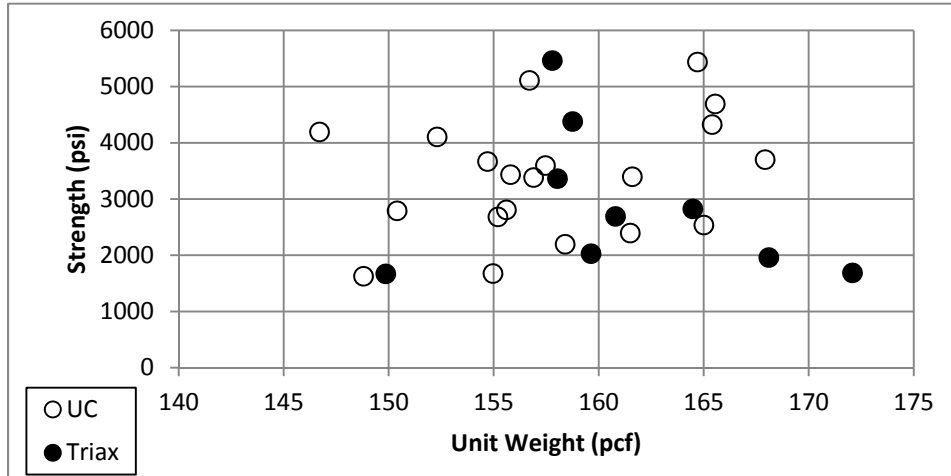


Figure 4.3: Plot of Ohio Unweathered Shale Properties (OU Data)

Table 4.9: Basic Properties of Weathered Shale in Ohio

	No	Min	Max	Ave	SD	CI (90%)	CI (95%)	CI (99%)			
UW (pcf)	56	144	166	156	5	154	157	154	157	154	158
UCS (psi)	77	32	499	263	124	239	286	235	290	226	299

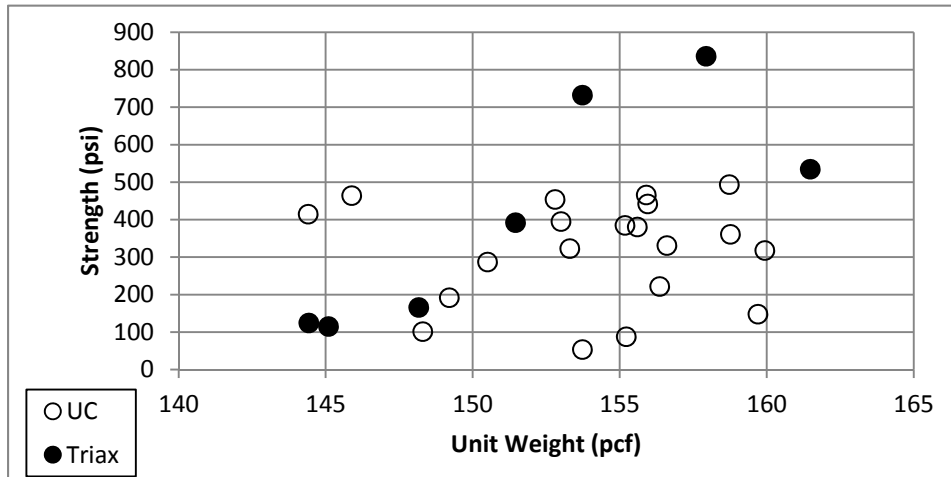


Figure 4.4: Plot of Weathered Shale Properties in Ohio (OU Data)

Table 4.10: Basic Properties of Claystone in Southeast Region

	No	Min	Max	Ave	SD	CI (90%)	CI (95%)	CI (99%)			
UW (pcf)	9	129	157	140	10	135	145	134	146	132	148
UCS (psi)	4	16	43	26	13	16	36	14	38	10	42

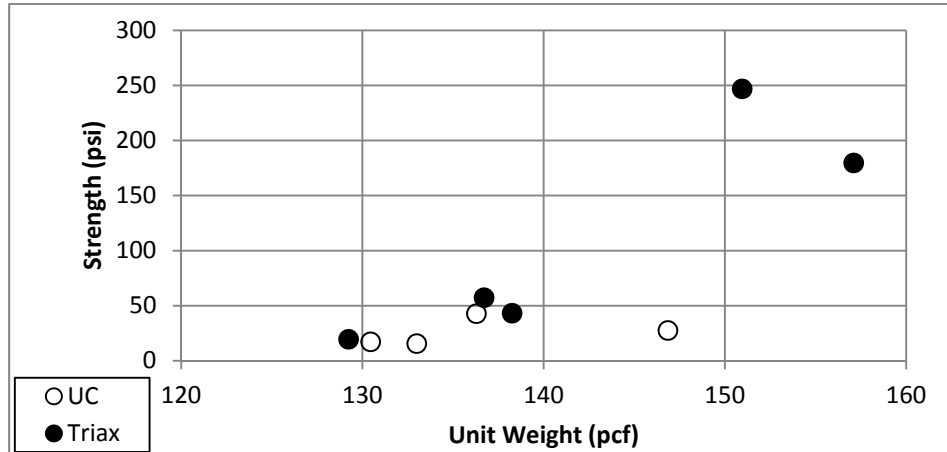


Figure 4.5: Plot of Claystone Properties in Ohio (OU Data)

As seen in Figures 4.1 through 4.3, larger unit weight does not necessarily equate to higher compressive strength for strong rock materials. Figures 4.4 and 4.5 indicate that weathered shale and claystone samples exhibited the unit weight-strength proportionality. Examinations of these plots also show that the confining pressure levels of up to 50 psi had little to a marginal effect on the compressive strength of strong rock materials such as limestone, sandstone, and unweathered shale. On the contrary, the confining pressure often propelled the compressive strength to slightly higher levels for weathered shale and claystone samples, since these specimens behave more like soil samples.

Table 4.11 combines the information contained in Tables 4.5 through 4.10 to show graphically how basic rock property ranges compare between the 2011 ODOT report and the current project (95% confidence interval). The following observations are made:

- For each major Ohio rock type, the range of unit weight is generally narrower than the range listed in the ODOT 2011 report.
- Limestone and sandstone are both heavier than what the ODOT 2011 report indicated.

Table 4.11: Comparison of Basic Rock Properties between ODOT Report and Current Study

		Unit Weight (pcf)																						
		150	151	152	153	154	155	156	157	158	159	160	161	162	163	164	165	166	167	168				
Limestone	ODOT						155-165																	
	Study																	166-168						
Sandstone	ODOT						155-160																	
	Study										159-162													
Shale (UW)	ODOT												160-165											
	Study								157-160															
Shale (W)	ODOT												160-165											
	Study				154-157																			
Claystone	ODOT											160-165												
	Study	134-146																						

		Unconfined Compression Strength (ksi)																						
		0	1	2	3	4	5	6	7	8	9	10	11	12	13	14	15	16	17	18				
Limestone	ODOT				3.5-16.4																			
	Study											9.4-11.0												
Sandstone	ODOT			2.0-7.8																				
	Study			3.3-4.2																				
Shale (UW)	ODOT			1.9-2.5																				
	Study			2.9-3.7																				
Shale (W)	ODOT			1.9-2.5																				
	Study	0.2-0.3																						
Claystone	ODOT	< 0.14																						
	Study	< 0.04																						

- Shale (unweathered; weathered) is lighter than what the ODOT 2011 report indicated.
- Claystone is much lighter than what the ODOT 2011 report indicated.
- The ranges of unconfined compression strength are also much narrower than those reported in the 2011 ODOT report for limestone and sandstone.

- Unconfined compression strength of shale (unweathered) is slightly higher than what the ODOT 2011 report indicated.
- Shale (weathered) and claystone are each much weaker than what the ODOT 2011 report indicated.

4.3.2 Regional Comparisons of Basic Rock Properties

Now that the statewide rock properties have been examined, we can look at the basic rock properties regionally to find out if any regional differences exist. Claystone was excluded from this regional examination due to its isolated occurrences and the general lack of data. Tables 4.12 through 4.16 list basic properties of limestone found in various geological regions in the state. The confidence interval concept was again applied to establish the statistically sound rock property ranges. Figures 4.6 through 4.10 plot the same data. And, Figure 4.11 summarizes the 95% confidence interval ranges of the regional limestone properties on the Ohio map.

Table 4.12: Limestone in Northwest Region

	No	Min	Max	Ave	SD	CI (90%)		CI (95%)		CI (99%)	
UW (pcf)	14	147	176	168	7	165	171	164	172	163	173
UCS (psi)	14	4083	15257	9063	3531	7516	10611	7214	10913	6629	11498

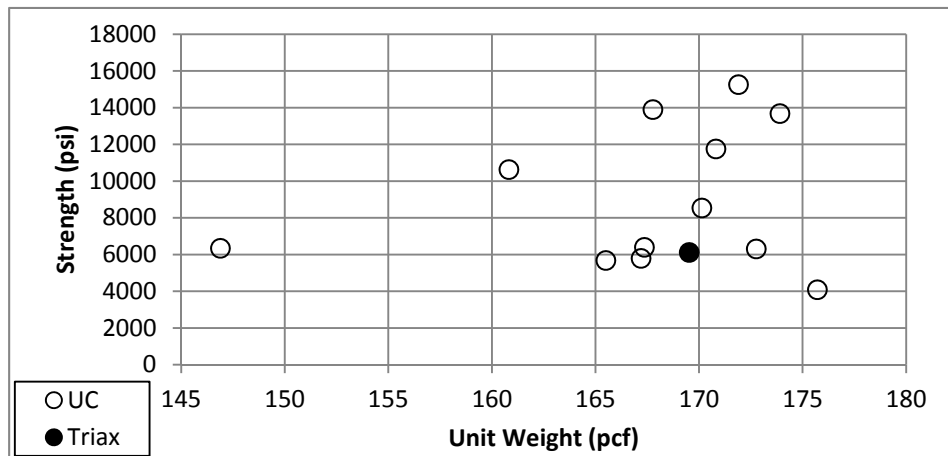


Figure 4.6: Plot of Limestone Properties in Northwest Region (OU Data)

[Note] UC = Unconfined Compression; and Triax = Triaxial Compression.

Table 4.13: Basic Properties of Limestone in Northeast Region

	No	Min	Max	Ave	SD	CI (90%)		CI (95%)		CI (99%)	
UW (pcf)	8	169	170	169	1	169	169	169	169	169	170
UCS (psi)	3	11776	25448	18763	6841	12286	25241	11022	26504	8573	28953

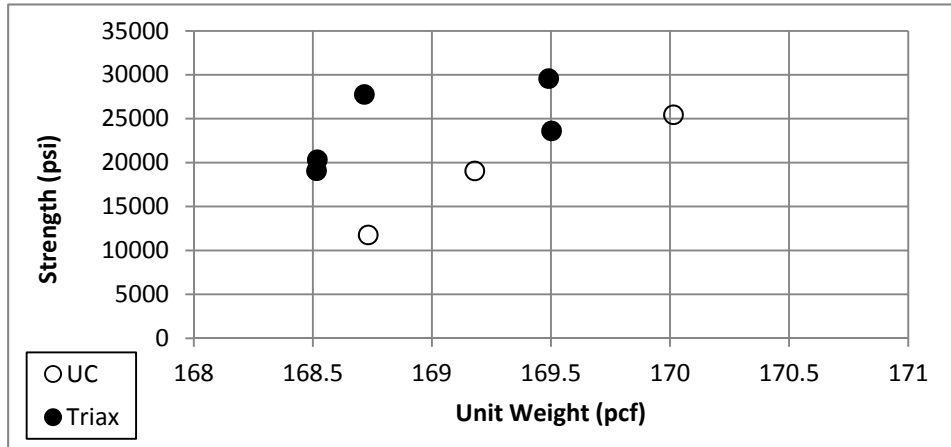


Figure 4.7: Plot of Limestone Properties in Northeast Region (OU Data)

Table 4.14: Basic Properties of Limestone in Central Region

	No	Min	Max	Ave	SD	CI (90%)		CI (95%)		CI (99%)	
UW (pcf)	31	143	170	156	7	154	158	154	159	153	160
UCS (psi)	18	2222	14140	7609	4279	5955	9263	5632	9586	5007	10211

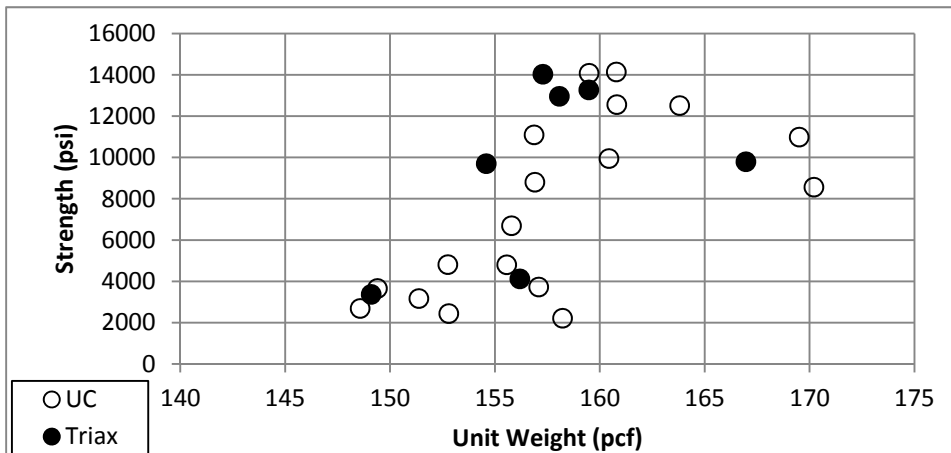


Figure 4.8: Plot of Limestone Properties in Central Region (OU Data)

Table 4.15: Basic Properties of Limestone in Southeast Region

	No	Min	Max	Ave	SD	CI (90%)	CI (95%)	CI (99%)			
UW (pcf)	9	153	180	165	7	161	169	160	170	159	172
UCS (psi)	6	3303	30947	15796	11200	8297	23294	6834	24757	3999	27592

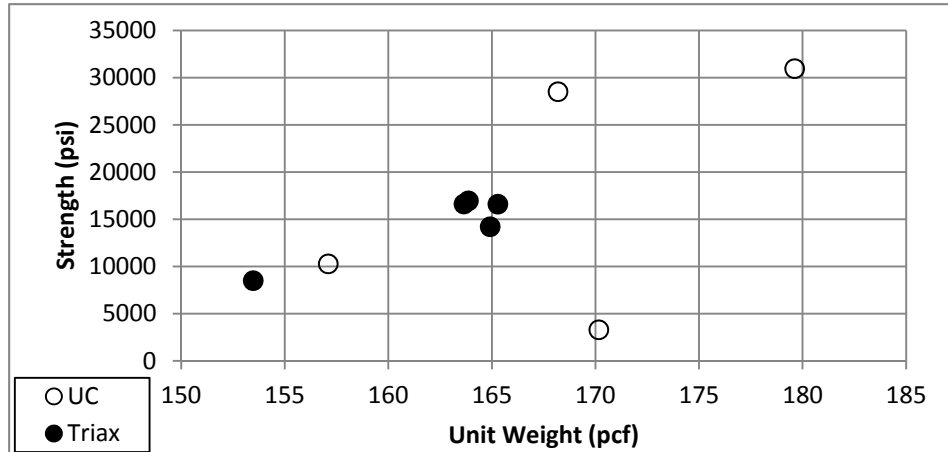


Figure 4.9: Plot of Limestone Properties in Southeast Region (OU Data)

Table 4.16: Basic Properties of Limestone in Southwest Region

	No	Min	Max	Ave	SD	CI (90%)	CI (95%)	CI (99%)			
UW (pcf)	13	165	170	167	2	167	168	167	168	166	169
UCS (psi)	29	6250	14630	10900	1824	10344	11455	10236	11564	10026	11774

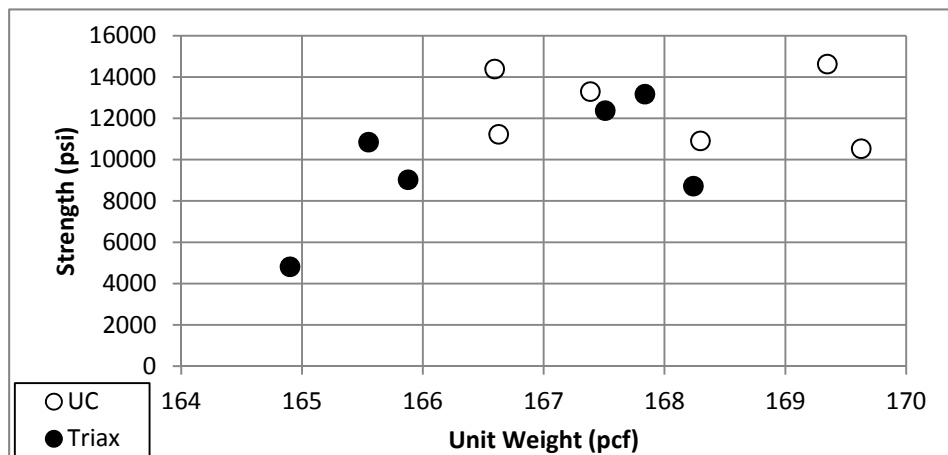


Figure 4.10: Plot of Limestone Properties in Southwest Region (OU Data)

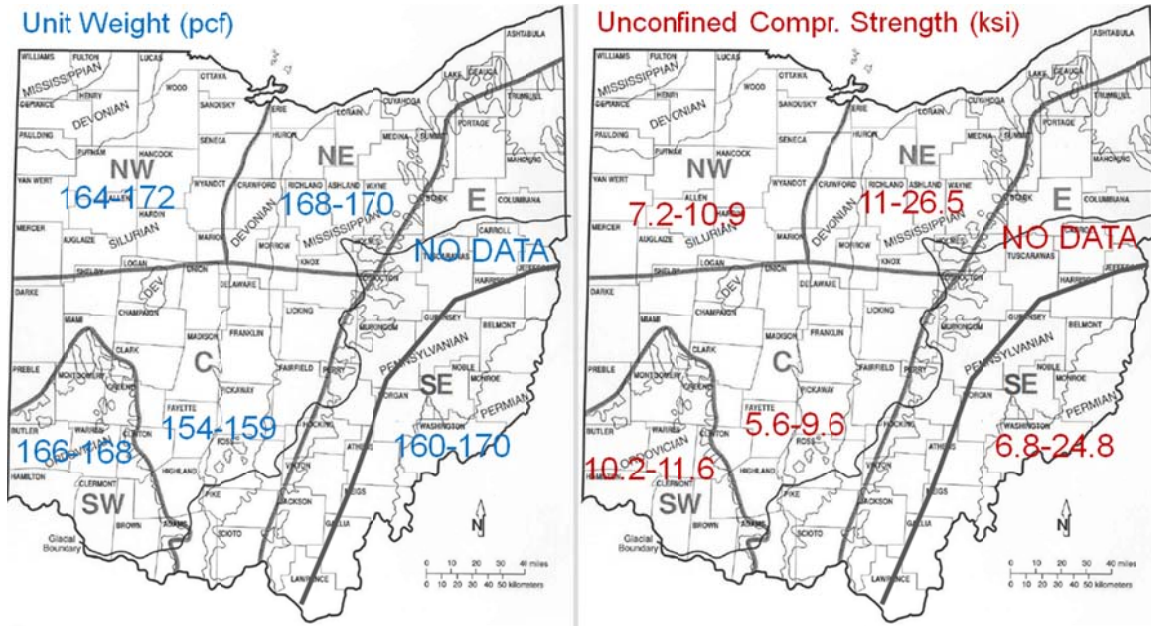


Figure 4.11: Basic Properties of Ohio Limestone Mapped

[Note] No Data = Not enough data to determine confidence intervals

Tables 4.17 through 4.19 list basic properties of limestone found in various geological regions in the state. Figures 4.12 through 4.14 plot the same data. And, Figure 4.15 summarizes the 95% confidence interval ranges of the regional sandstone properties on the Ohio map.

Table 4.17: Basic Properties of Sandstone in Northeast Region

	No	Min	Max	Ave	SD	CI (90%)	CI (95%)	CI (99%)			
UW (pcf)	18	135	151	141	4	140	143	139	144		
UCS (psi)	17	4274	13182	7961	2940	6791	9130	6563	9358	6121	9800

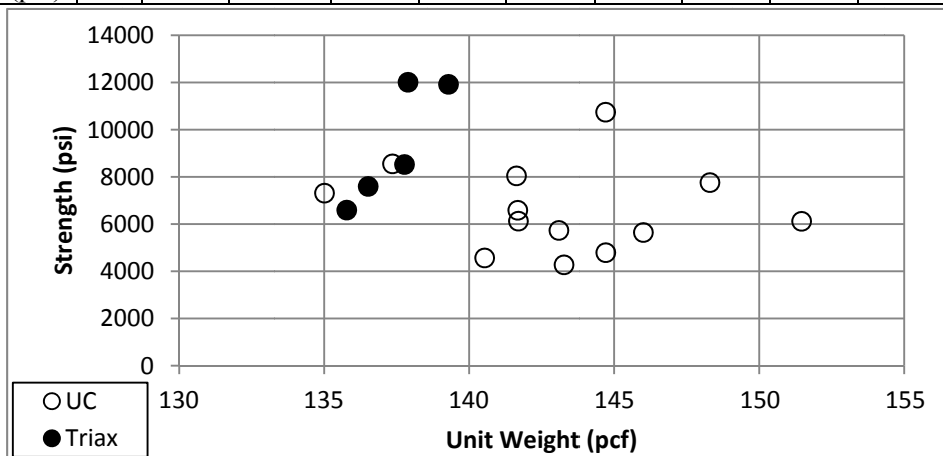


Figure 4.12: Plot of Sandstone Properties in Northeast Region (OU Data)

Table 4.18: Basic Properties of Sandstone in Eastern Region

	No	Min	Max	Ave	SD	CI (90%)		CI (95%)		CI (99%)	
UW (pcf)	32	125	161	142	10	140	145	139	146	138	147
UCS (psi)	27	986	9050	4131	1825	3555	4707	3442	4819	3224	5037

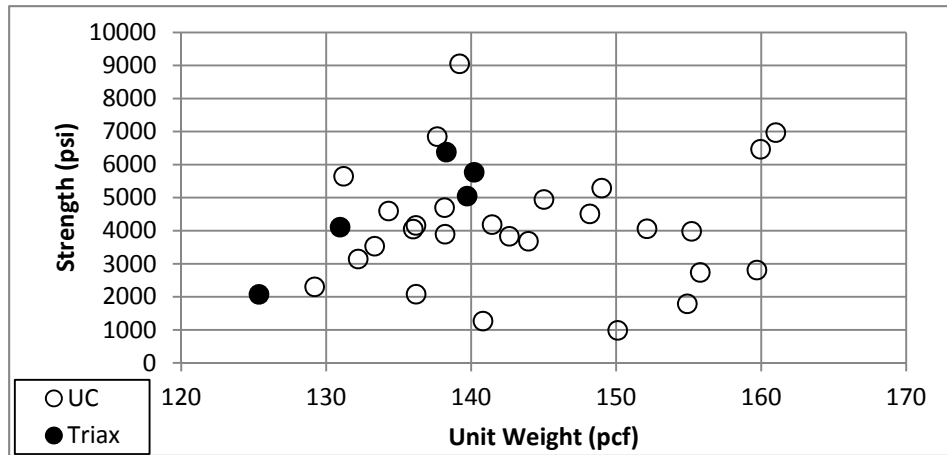


Figure 4.13: Plot of Sandstone Properties in Eastern Region (OU Data)

Table 4.19: Basic Properties of Sandstone in Southeast Region

	No	Min	Max	Ave	SD	CI (90%)		CI (95%)		CI (99%)	
UW (pcf)	33	154	171	162	4	161	163	161	164	161	164
UCS (psi)	26	2434	10980	6194	2705	5324	7064	5154	7234	4825	7563

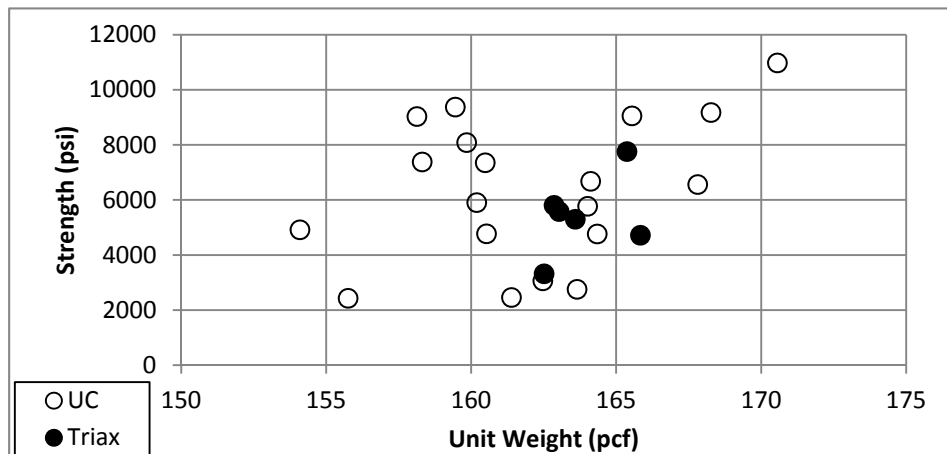


Figure 4.14: Plot of Sandstone Properties in Southeast Region (OU Data)

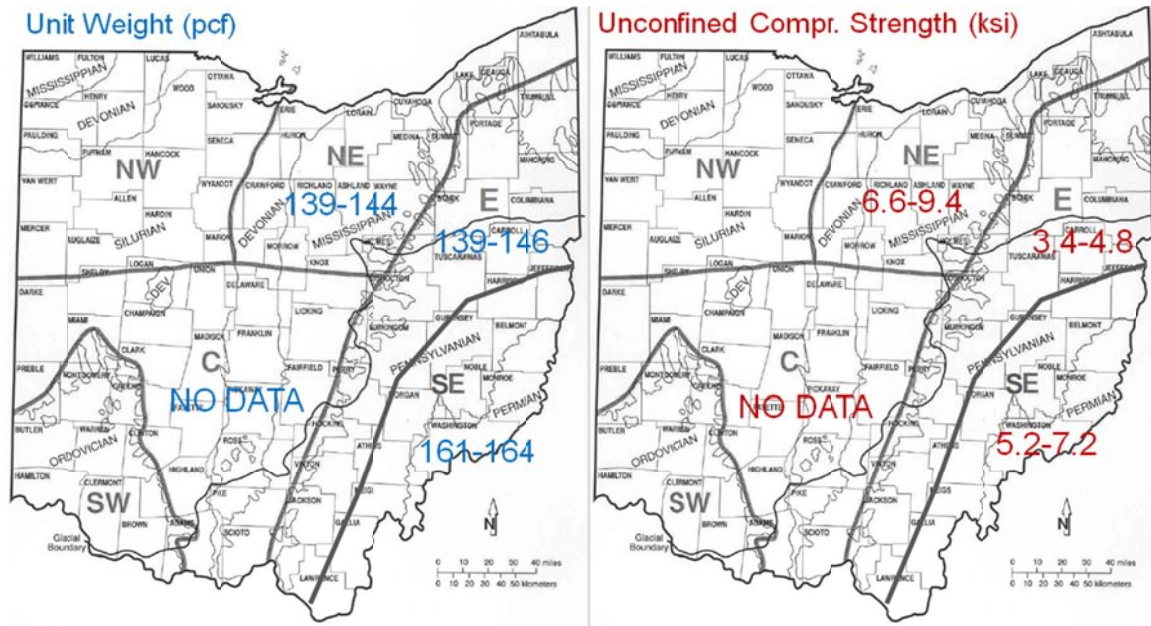


Figure 4.15: Basic Properties of Sandstone in Ohio Mapped
 [Note] No Data = Not enough data to determine confidence intervals

Tables 4.20 through 4.24 list basic properties of unweathered shale found in various geological regions in the state. Figures 4.16 through 4.20 plot the same data. And, Figure 4.21 summarizes the 95% confidence interval ranges of the regional unweathered shale properties on the Ohio map.

Similarly, Tables 4.25 through 4.29 list basic properties of weathered shale found in various geological regions in the state. Figures 4.22 through 4.26 plot the same data. And, Figure 4.27 summarizes the 95% confidence interval ranges of the regional weathered shale properties on the Ohio map.

Table 4.20: Basic Properties of Unweathered Shale in Northeast Region

	No	Min	Max	Ave	SD	CI (90%)		CI (95%)		CI (99%)	
UW (pcf)	27	149	165	158	4	156	159	156	159	155	160
UCS (psi)	18	1508	5437	2921	1262	2434	3409	2338	3504	2154	3689

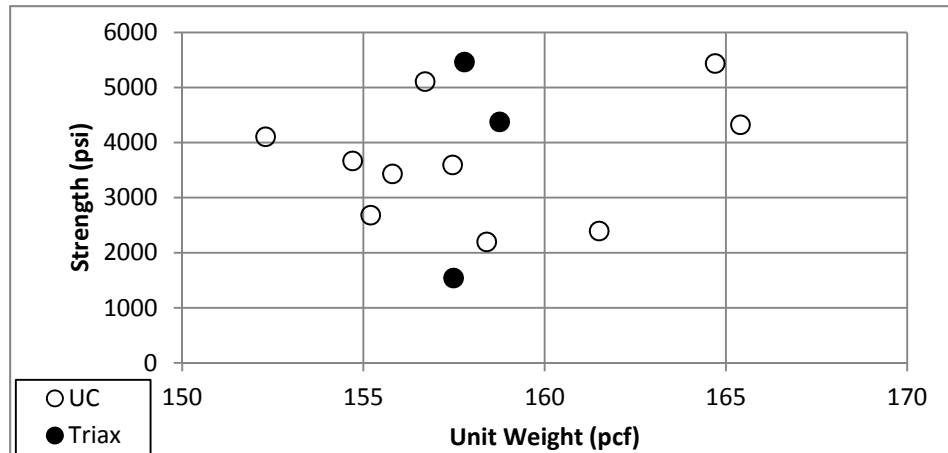


Figure 4.16: Plot of Unweathered Shale in Northeast Region (OU Data)

Table 4.21: Basic Properties of Unweathered Shale in Central Region

	No	Min	Max	Ave	SD	CI (90%)		CI (95%)		CI (99%)	
UW (pcf)	5	152	168	160	8	154	165	153	166	151	168
UCS (psi)	5	8018	13970	10283	2395	8527	12040	8184	12383	7520	13047

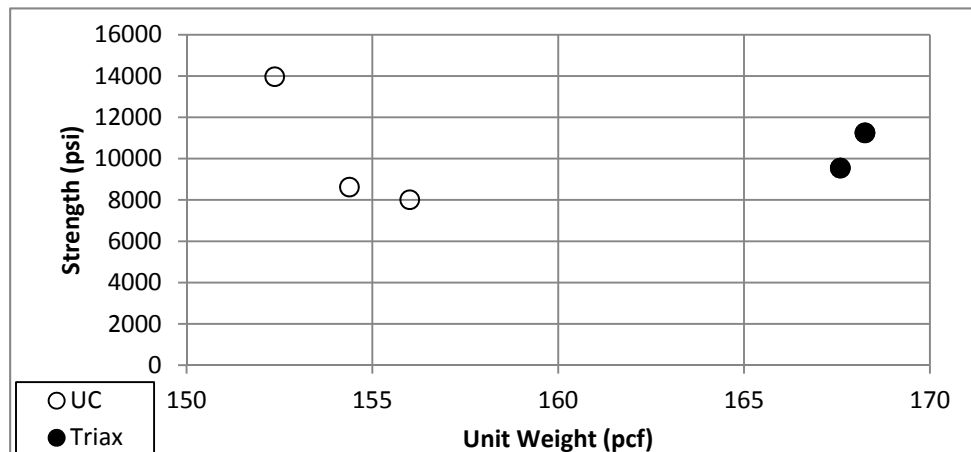


Figure 4.17: Plot of Unweathered Shale Properties in Central Region (OU Data)

Table 4.22: Basic Properties of Unweathered Shale in Eastern Region

	No	Min	Max	Ave	SD	CI (90%)		CI (95%)		CI (99%)	
UW (pcf)	3	156	162	158	3	155	161	154	162	153	163
UCS (psi)	3	2807	3397	3196	337	2877	3515	2815	3577	2694	3697

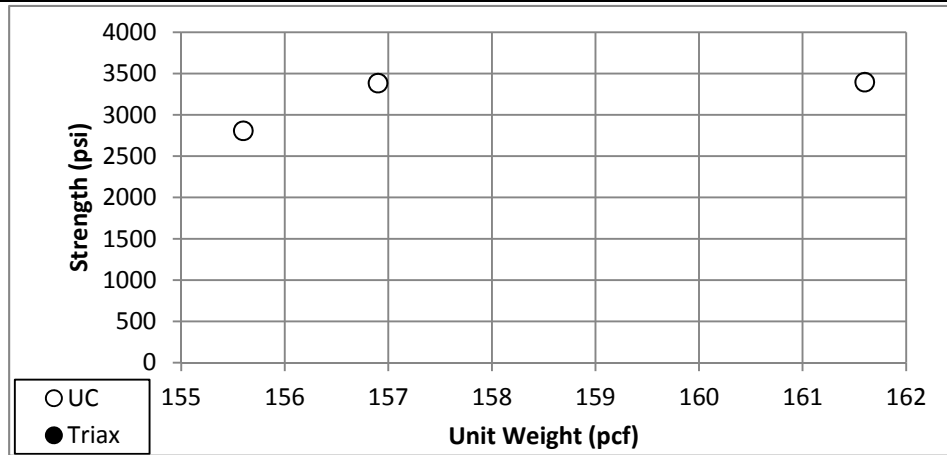


Figure 4.18: Plot of Unweathered Shale Properties in Eastern Region (OU Data)

Table 4.23: Basic Properties of Unweathered Shale in Southeast Region

	No	Min	Max	Ave	SD	CI (90%)		CI (95%)		CI (99%)	
UW (pcf)	10	155	172	165	5	162	167	162	168	161	169
UCS (psi)	7	1312	4779	2919	1448	2022	3817	1847	3992	1507	4331

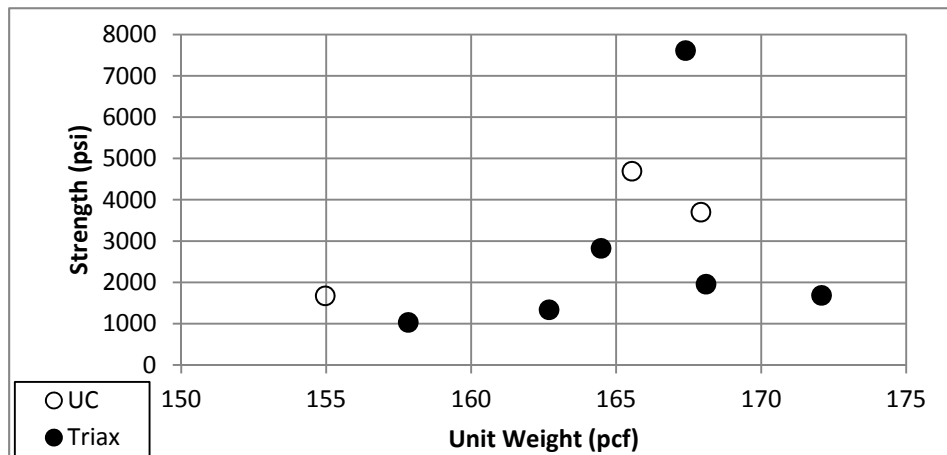


Figure 4.19: Plot of Unweathered Shale Properties in Southeast Region (OU Data)

Table 4.24: Basic Properties of Unweathered Shale in Southwest Region

	No	Min	Max	Ave	SD	CI (90%)		CI (95%)		CI (99%)	
UW (pcf)	14	117	166	146	17	138	153	137	154	134	157
UCS (psi)	14	1628	5890	3302	1493	2648	3956	2520	4084	2273	4331

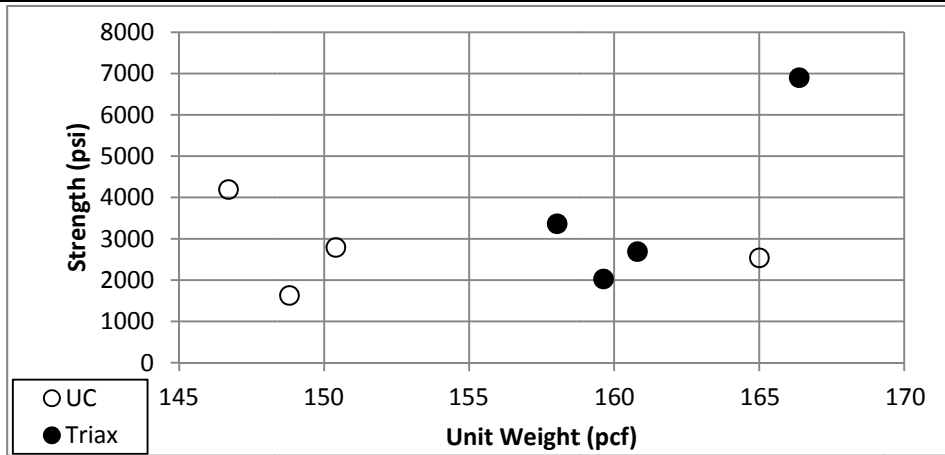


Figure 4.20: Plot of Unweathered Shale Properties in Southwest Region (OU Data)

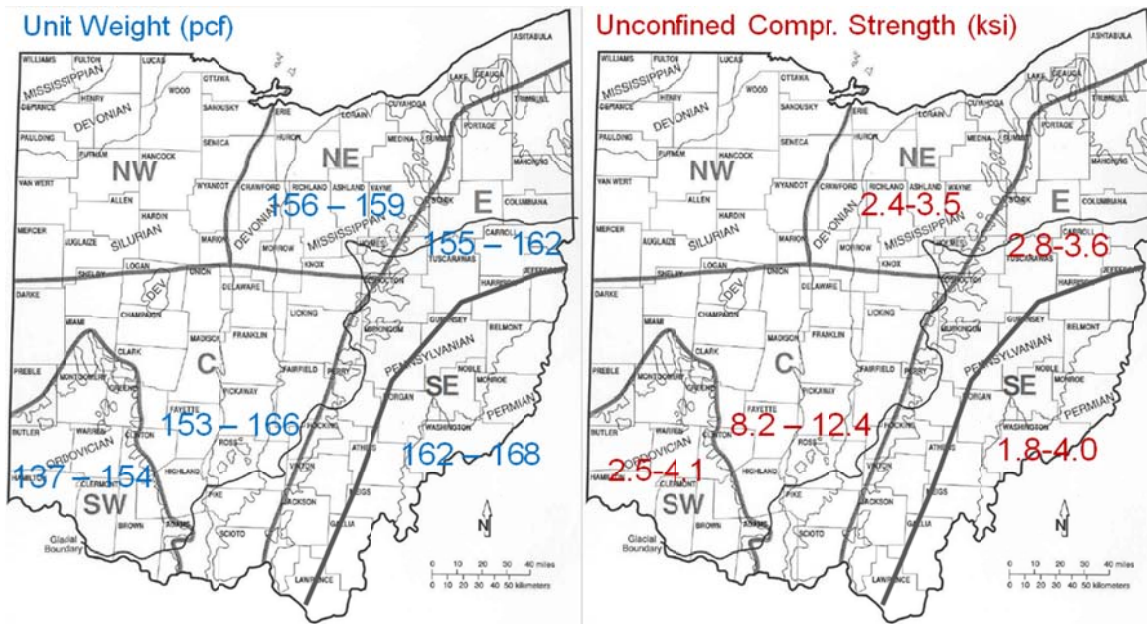


Figure 4.21: Basic Properties of Unweathered Shale in Ohio Mapped

Table 4.25: Basic Properties of Weathered Shale in Northeast Region

	No	Min	Max	Ave	SD	CI (90%)		CI (95%)		CI (99%)	
UW (pcf)	22	149	164	156	4	155	158	155	158	154	159
UCS (psi)	25	262	678	453	121	413	493	406	501	391	516

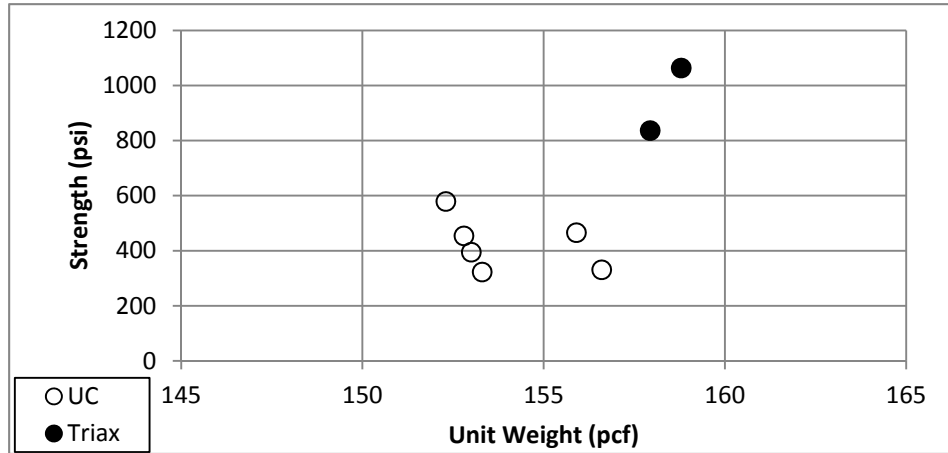


Figure 4.22: Plot of Weathered Shale Properties in Northwest Region (OU Data)

Table 4.26: Basic Properties of Weathered Shale in Central Region

	No	Min	Max	Ave	SD	CI (90%)		CI (95%)		CI (99%)	
UW (pcf)	5	140	155	149	6	144	154	143	154	142	156
UCS (psi)	5	93	1671	866	648	391	1341	298	1434	119	1614

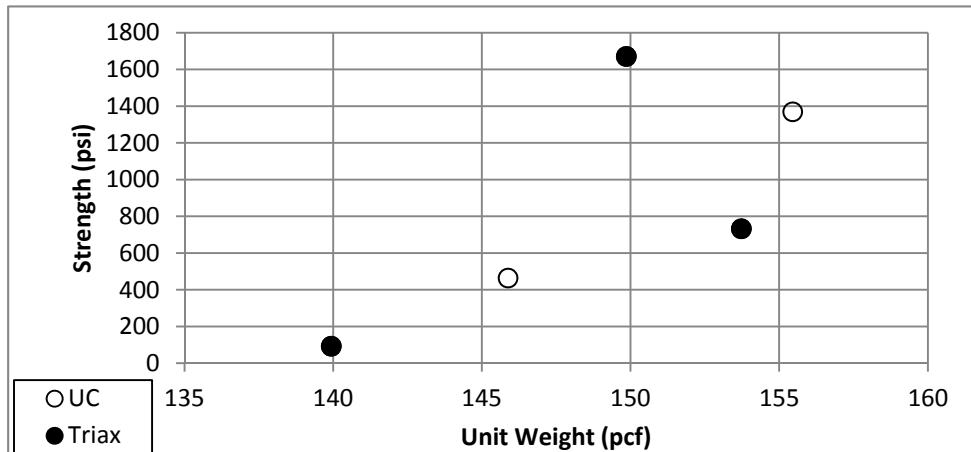


Figure 4.23: Plot of Weathered Shale Properties in Central Region (OU Data)

Table 4.27: Basic Properties of Weathered Shale in Eastern Region

	No	Min	Max	Ave	SD	CI (90%)		CI (95%)		CI (99%)	
UW (pcf)	7	142	155	148	5	144	151	144	151	143	153
UCS (psi)	3	54	102	81	25	58	104	53	109	44	118

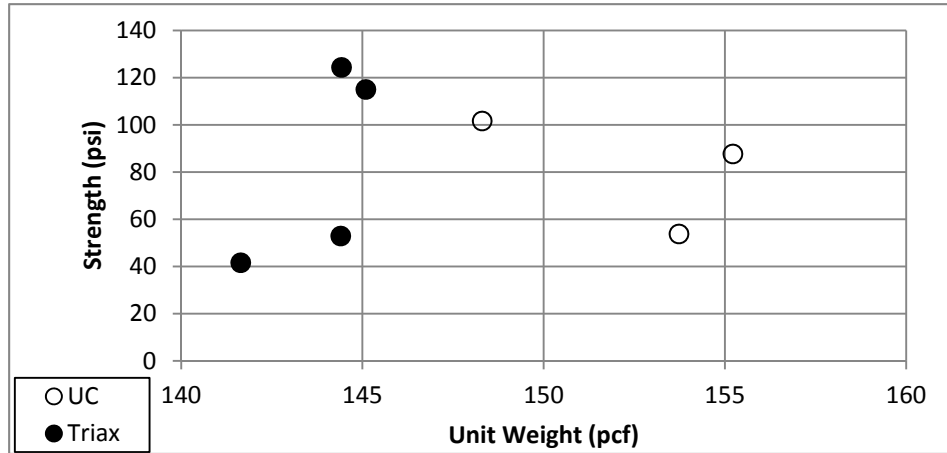


Figure 4.24: Plot of Weathered Shale Properties in Eastern Region (OU Data)

Table 4.28: Basic Properties of Weathered Shale in Southeast Region

	No	Min	Max	Ave	SD	CI (90%)		CI (95%)		CI (99%)	
UW (pcf)	4	151	166	161	7	156	166	154	167	152	169
UCS (psi)	5	226	874	617	238	443	792	409	826	343	892

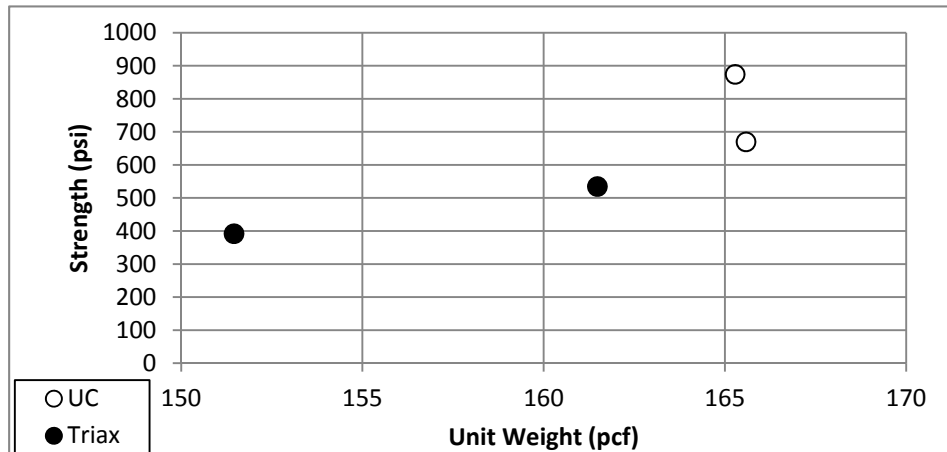


Figure 4.25: Plot of Weathered Shale Properties in Southeast Region (OU Data)

Table 4.29: Basic Properties of Weathered Shale in Southwest Region

	No	Min	Max	Ave	SD	CI (90%)	CI (95%)	CI (99%)			
UW (pcf)	27	117	158	142	12	138	145	137	146	136	148
UCS (psi)	43	110	946	439	214	385	492	375	503	355	523

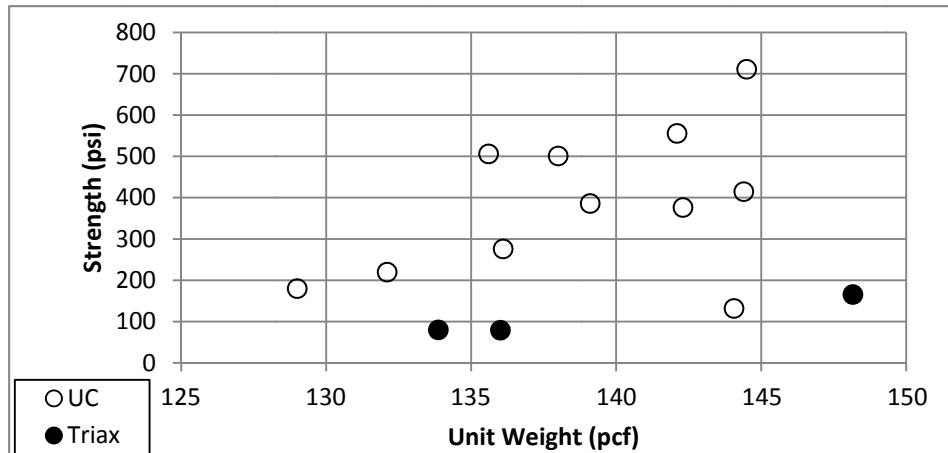


Figure 4.26: Plot of Weathered Shale Properties in Southwest Region (OU Data)

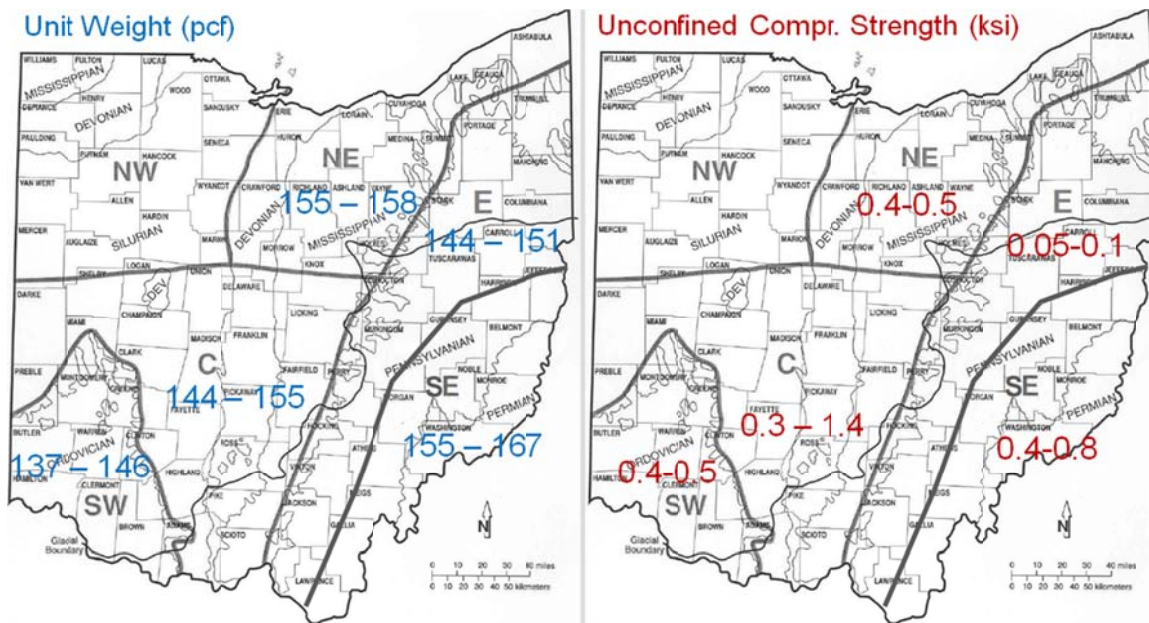


Figure 4.27: Basic Properties of Weathered Shale in Ohio Mapped

To examine possible geographical differences in the basic rock properties among Ohio regions more scientifically, t-test analysis was carried out using SPSS to the regional unit

weight and unconfined compression strength data sets belonging to each major rock type. Claystone was again excluded from the t-test analysis due to its isolated occurrences and the general lack of data. The results of the t-tests are summarized in Tables 4.30, 4.32, 4.34, 4.36, 4.38, 4.40, 4.42, and 4.44. To further make sense of the data, the regional 95% confidence intervals are also laid out against the ODOT 2011 report range in Tables 4.31, 4.33, 4.35, 4.37, 4.39, 4.41, and 4.43.

Tables 4.30 and 4.31 present regional examinations of the unit weight of Ohio limestone. The t-test results show that limestone’s unit weight is different in the central region and that the unit weight in the southwest region is not the same as that in the northeast region. They also indicate that the limestone’s unit weight is about the same among the northeast, northwest, southeast, and southwest regions. These somewhat confusing results might have emerged due to limited amounts of data available in some regions.

Table 4.30: T-Test Results for Unit Weight of Limestone in Ohio Regions

	Central	Northwest	Southeast	Southwest	Northeast
Central		Different	Different	Different	Different
Northwest	Different		Same	Same	Same
Southeast	Different	Same		Same	Same
Southwest	Different	Same	Same		Different
Northeast	Different	Same	Same	Different	

Table 4.31: Ranges of Unit Weight of Limestone in Ohio Regions

		Unit Weight (pcf)																	Data			
		15	15	15	15	15	15	16	16	16	16	16	16	16	16	16	16	17		17	17	
Limestone	ODO	155-165																				
	NW												164-172						14			
	NE																169-170				8	
	C	154-159																			31	
	SW															167-168					13	
	SE							160-170													9	

[Note] NW = northwest; NE = northeast; C = central; SW = southwest; and SE = southeast.

According to Table 4.31, none of the regions has a range that matches the ODOT’s unit weight range. Limestone in the central region is definitely lightest in the state. The unit weight range in the northwest region is slightly different from that in the southeast region. And, the unit weight ranges in the northeast and southwest regions are very narrow, and they could be subsets of the range existing in either the northwest or southwest region. Additional data will be needed to clarify some of these conflicting results.

Tables 4.32 and 4.33 present regional examinations of the unconfined compression strength of Ohio limestone. The t-test results show that limestone’s compressive strength is about the same between the central and southeast regions and it is different in the northeast, northwest, and southwest regions. Table 4.33 shows that the strength ranges in the northwest and central regions are within the ODOT range. Table 4.33 suggests that Ohio limestone’s compressive strength may be about the same among the northwest, central, and southwest regions. It also indicates that the strength varies more widely in the northeast and southeast regions. So, there appears to be a few discrepancies between the two tables. Additional data will be needed to clarify this issue.

Table 4.32: T-Test Results for Unconfined Compression Strength of Limestone among Ohio Regions

	Central	Northwest	Southeast	Southwest	Northeast
Central		Same	Same	Different	Different
Northwest	Same		Same	Same	Different
Southeast	Same	Same		Same	Same
Southwest	Different	Same	Same		Same
Northeast	Different	Different	Same	Same	

Table 4.33: Ranges of Unconfined Compression Strength of Limestone in Ohio Regions

		Unconfined Compression Strength (ksi)																				Data												
		3	4	5	6	7	8	9	10	11	12	13	14	15	16	17	18	19	20	21	22													
Limestone	ODO	3.5-16.4																																
	NW					7.2-10.9																							14					
	NE										11.0-26.5																						3	
	C			5.6-9.6																									18					
	SW									10.2-																			29					
	SE					6.8-24.8																												

Tables 4.34 and 4.35 present regional examinations of the unit weight of Ohio sandstone. The t-test results state that sandstone’s unit weight is about the same between the eastern and northeast regions and that the sandstone in the southeast region is different from the other regions. Table 4.35 agrees with the t-test results. There are no ambiguities that will need to be studied further. Table 4.35 shows that none of the regions has a range that matches the ODOT’s unit weight range.

Table 4.34: T-Test Results for Unit Weight of Sandstone among Ohio Regions

	Eastern	Northeast	Southeast
Eastern		Same	Different
Northeast	Same		Different
Southeast	Different	Different	

Table 4.35: Ranges of Unit Weight of Sandstone in Ohio Regions

		Unit Weight (pcf)														Data
		140	142	144	146	148	150	152	154	156	158	160	162	164		
Sandstone	ODOT									155-160						
	NE	139-144													18	
	E	139-146													32	
	SE											161-164			33	

Tables 4.36 and 4.37 present regional examinations of the unconfined compression strength of Ohio sandstone. The t-test results show that sandstone’s compressive strength is different in each of the three regions. And, Table 4.37 appears to support this statistical analysis outcome. This table also shows that the strength ranges in the eastern and southeastern regions are within the ODOT range.

Table 4.36: T-Test Results for Unconfined Compression Strength of Sandstone among Ohio Regions

	Eastern	Northeast	Southeast
Eastern		Different	Different
Northeast	Different		Different
Southeast	Different	Different	

Table 4.37: Ranges of Unconfined Compression Strength of Sandstone among Ohio Regions

		Unconfined Compression Strength (ksi)									Data
		2	3	4	5	6	7	8	9		
Sandstone	ODOT	2.0-7.8									
	NE					6.5-9.4				17	
	E		3.4-4.8							27	
	SE				5.2-7.2					26	

Tables 4.38 and 4.39 present regional examinations of the unit weight of Ohio’s unweathered shale. The t-test results show that unweathered shale’s unit weight is about the same among all the regions. The t-test results also point out that the unweathered shale’s unit weights in the southeast and southwest regions may have some distinctions. So, there seem to be unresolved issues. Table 4.39 appears to state that unweathered shale may be the lightest in the southwest, heaviest in the southeast, and in the mid-range in the northeast, eastern, and central regions. Additional data will be welcome to clarify these lightly contradictory outcomes. Table 4.39 also shows that none of the regions has a range of unit weight that matches the ODOT range.

Table 4.38: T-Test Results for Unit Weight of Unweathered Shale among Ohio Regions

	Central	Eastern	Northeast	Southeast	Southwest
Central		Same	Same	Same	Same
Eastern	Same		Same	Same	Different
Northeast	Same	Same		Different	Different
Southeast	Same	Same	Different		Different
Southwest	Same	Different	Different	Different	

Table 4.39: Ranges of Unit Weight of Unweathered Shale among Ohio Regions

		Unit Weight (pcf)																Data					
		148	149	150	151	152	153	154	155	156	157	158	159	160	161	162	163	164	165	166	167	168	
Shale (uw)	ODOT														160-165								
	NE									156-159													27
	E									155-162													3
	C									153-166													5
	SW									137-154													14
	SE																			162-168			10

Tables 4.40 and 4.41 present regional examinations of the unconfined compression strength of Ohio shale (unweathered). The t-test results show that unweathered shale’s compressive strength is fairly uniform outside the central region. Table 4.41 does not appear to refute this statistical outcome, clearly showing the heaviest unweathered shale in the central region. Table 4.41 also shows that none of the regions has a range of compressive strength that matches the ODOT range.

Next, Tables 4.42 and 4.43 present regional examinations of the unit weight of Ohio’s weathered shale. The t-test results show that weathered shale’s unit weight is about the same among the central, eastern, and southwest regions. The t-test results also point out that the weathered shale’s unit weights in the northeast and southeast regions may have some distinctions. Table 4.43 appears to support these statistical outcomes. Table 4.43 also shows that none of the regions has a range of unit weight that matches the ODOT range.

Table 4.40: T-Test Results for Unconfined Compression Strength of Unweathered Shale among Ohio Regions

	Central	Eastern	Northeast	Southeast	Southwest
Central		Different	Different	Different	Different
Eastern	Different		Same	Same	Same
Northeast	Different	Same		Same	Same
Southeast	Different	Same	Same		Same
Southwest	Different	Same	Same	Same	

Table 4.41: Ranges of Unconfined Compression Strength of Unweathered Shale among Ohio Regions

		Unconfined Compression Strength (ksi)																			Data
		2	2.5	3	3.5	4	4.5	5	5.5	6	6.5	7	7.5	8	8.5	9	9.5	10	10.5	11	
Shale (uw)	ODOT	1.9-2.5																			
	NE	2.3-3.5																			18
	E	2.8-3.6																			3
	C																				5
	SW	2.5-4.0																			14
	SE	1.8-4.0																			7

Table 4.42: T-Test Results for Unit Weight of Weathered Shale among Ohio Regions

	Central	Eastern	Northeast	Southeast	Southwest
Central		Same	Different	Different	Same
Eastern	Same		Different	Different	Same
Northeast	Different	Different		Same	Different
Southeast	Different	Different	Same		Different
Southwest	Same	Same	Different	Different	

Table 4.43: Ranges of Unit Weight of Weathered Shale among Ohio Regions

		Unit Weight (pcf)																Data							
		145	146	147	148	149	150	151	152	153	154	155	156	157	158	159	160		161	162	163	164	165	166	167
Shale (w)	ODOT																								160-165
	NE																								155-158
	E																								141-151
	C																								144-155
	SW																								137-146
	SE																								155-167

Finally, Tables 4.44 and 4.45 present regional examinations of the unconfined compression strength of Ohio shale (weathered). One part of the T-test results show that

weathered shale’s compressive strength is fairly uniform among all the regions. Another part of the t-test results indicate that weathered shale’s strength is different at least in the eastern region. According to Table 4.45, weathered shale’s compressive strength is the same between the northeast and southwest regions. Table 4.45 also indicates that the weathered shale’s strength varies widely in the central region and that the eastern region may have the weakest weathered shale. Additional data will be welcome to clarify theseslightly contradicting outcomes. Table 4.45 also shows that none of the regions has a range of compressive strength that matches the ODOT range.

Table 4.44: T-Test Results for Unconfined Compression Strength of Weathered Shale among Ohio Regions

	Central	Eastern	Northeast	Southeast	Southwest
Central		Same	Same	Same	Same
Eastern	Same		Different	Different	Different
Northeast	Same	Different		Different	Same
Southeast	Same	Different	Different		Same
Southwest	Same	Different	Same	Same	

Table 4.45: Ranges of Unconfined Compression Strength of Weathered Shale among Ohio Regions

		Unconfined Compression Strength (ksi)																				Data					
		0	0.1	0.2	0.3	0.4	0.5	0.6	0.7	0.8	0.9	1	1.1	1.2	1.3	1.4	1.5	1.6	1.7	1.8	1.9	2	2.1	2.2			
Shale (w)	ODOT																								1.9-2.5		
	NE					0.4-0.5																				25	
	E	0.05-0.1																								3	
	C				0.3-1.4																						5
	SW					0.4-0.5																				43	
	SE					0.4-0.8																				5	

4.4 Calculations of GSI Parameters

The critical parameters in the GSI system are the material coefficient (m_i) and uniaxial compression strength of intact rock (σ_{ci}). Once these parameter values are determined, one can proceed and compute engineering properties of rock masses that are essential for bridge foundation design.

These two parameters can be calculated through the Hoek's method or the LMA method. In this project, it was observed that the m_i values determined by the Hoek's linear regression method had a tendency to be extreme and very different from the values he provided himself. Sometimes, these m_i values were outside the permissible zone, higher than 100 or lower than 0. This situation frequently occurred due to the fact that low confining pressure levels were used in the laboratory testing. Hoek stated that ideally confining pressure needs to be half of the uniaxial compressive strength. In contrast, the LMA (Levenberg–Marquardt Algorithm) method converged efficiently, and its m_i values were always within the range provided by Hoek. According to Hoek's research, the typical m_i value of weak ductile rock is 5 and that of very strong brittle rock is 35, RocLab sets the m_i value from 1 to 50 to cover this range.

Table 4.46 summarizes the amount of laboratory test results that went into calculating the regional GSI parameter values for each major rock type. Tables 4.47 and 4.48 tabulate the results. Most of the calculate m_i ranges are in agreement with the Hoek's ranges. But, the upper limits of m_i ranges for limestone and unweathered shale are much higher than those provided by Hoek. In Hoek's research, sandstone is stronger than limestone, and shale is as weak as claystone. In this project, limestone was often stronger than sandstone, and unweathered shale is sometimes embedded with limestone (this is particularly true in the southwest region). Therefore, the m_i ranges of limestone and unweathered shale in Ohio tend to be higher than the Hoek's ranges. Furthermore, Hoek did not provide any ranges for the σ_{ci} values. If more samples are provided in some regions, such as claystone in the central and eastern regions, limestone in the northeast

and northwest regions, sandstone in the central region, the m_i ranges and σ_{ci} values for these rock types in the said regions may become more accurate and reasonable.

Table 4.46: Quantity of Data Used in m_i and σ_{ci} Calculations

Region	Rock Type				
	Claystone	Limestone	Sandstone	Shale (weathered)	Shale (unweathered)
Central	No	U2 + T5	No	U2 + T5	U3 + T5
Eastern	No	N/A	U5 + T4	U2 + T3	N/A
Northeast	N/A	U1+T4	U5 + T3	U2 + T5	U2 + T5
Northwest	N/A	No	N/A	N/A	N/A
Southeast	U2 + T5	U3 + T5	U3 + T6	U2 + T2	U3 + T3
Southwest	N/A	U2 + T4	N/A	U2 + T6	N/A

[Note] U = Number of unconfined compression test results used.

T = Number of triaxial compression test results used.

No = The calculated m_i value isn't reasonable, but no more samples are left.

N/A = This type of rock is not available from the region.

Table 4.47: Calculated m_i Ranges

Region	Claystone	Limestone	Sandstone	Shale (weathered)	Shale (unweathered)
Central	No	9.77 – 17.49	No	3.09 – 14.02	22.25 – 30.08
Eastern	No	N/A	15.12 – 19.68	3.01 – 5.75	N/A
Northeast	N/A	36.29*	16.25 – 22.28	4.55 – 9.32	26.22
Northwest	N/A	No	N/A	N/A	N/A
Southeast	1.65 – 7.95	17.75 – 29.76	13.02 – 18.16	6.71 – 8.93	15.61 – 21.55
Southwest	N/A	7.42 – 15.51	N/A	1.30 – 7.71	N/A
Statewide	2 – 8	7 – 30	13 – 22	1 – 14	16 – 30
Hoek	2 – 6	7 – 15	13 – 21	4 – 8	4 – 8

[Note] No = The calculated m_i value isn't reasonable, but no more samples are left.

N/A = The type of rock is not available in the region.

* = This result may not be reasonable, since there are only a few data points.

Table 4.48: Calculated σ_{ci} Ranges (psi)

Region	Claystone	Limestone	Sandstone	Shale (weathered)	Shale (unweathered)
Central	No	11084 – 12969	No	814 – 886	6584 – 10063
Eastern	No	N/A	3687 – 5036	54 – 80	N/A
Northeast	N/A	No	7356 – 7838	1009 – 1021	2723
Northwest	N/A	No	N/A	N/A	N/A
Southeast	63 – 114	13204 – 14228	2013 – 6720	863 – 945	1114 – 1903
Southwest	N/A	11297 – 11516	N/A	73 – 86	N/A
Statewide	60 – 120	11000 - 14000	2000 – 8000	50 – 1000	1000 – 10000

[Note] No = The value of σ_{ci} is not good, but no more samples are left.

N/A = The type of rock is not available from the region.

4.5 Regression Correlation between RMR and GSI

For seeking the correlation between RMR and GSI, the triaxial test results were excluded since the RMR system relies only on the unconfined compression strength to derive the strength rating. For each unconfined compression test performed by the Ohio University team, GSI value was first visually estimated and subsequently evaluated through the back-calculation. In every case, the visual and back-calculated GSI values were close to each other. Thus, the back-calculation technique served as an effective way to verify the visual value.

As mentioned previously, RMR is a sum of relative ratings of five parameters (strength of intact rock, drill core RQD, joint spacing, joint conditions, and groundwater conditions) and one adjustment factor (joint orientations). Thus, assumptions must be made on the joint to establish RMR for any rock mass. Hoek conveniently assumed that the groundwater condition is “completely dry” and the joint orientations is “very favorable” to obtain his simple RMR-GSI correlation. In this study, for generalizing the RMR-GSI relationship somewhat, the Ohio University team considered four different groundwater

conditions (very dry, moist, under moderate pressure, severe water problems) and five types of joint orientations (very favorable, favorable, fair, unfavorable, very unfavorable). As for the remaining RMR parameters, the following guidelines should be adopted in order to enhance the correlation between RMR and GSI:

- 1) If GSI of a rock sample is between 80 and 100, the ratings of RQD, Joint Spacing, and Condition of Joints should be 20, 30 and 25, respectively;
- 2) If GSI of a rock sample is between 60 and 80, the ratings of RQD, Joint Spacing, and Condition of Joints should be 17, 25 and 20, respectively;
- 3) If GSI of a rock sample is between 45 and 60, the ratings of RQD, Joint Spacing, and Condition of Joints should be 13, 20 and 12, respectively;
- 4) If GSI of a rock sample is between 30 and 45, the ratings of RQD, Joint Spacing, and Condition of Joints should be 8, 10 and 6, respectively;
- 5) If GSI of a rock sample is between 0 and 30, the ratings of RQD, Joint Spacing, and Condition of Joints should be 3, 5 and 0, respectively.

Once the RMR and GSI values are determined for each set of rock materials, their correlation can be sought through the use of regression analysis. In this study, several mathematical functions (linear, quadratic, exponential, logarithmic, and power regression.) are utilized to identify the best form of the RMR-GSI correlation. Figures 4.28 through 4.47 present graphically the results of the regression analysis. And, Tables 4.49 through 4.52 summarize the RMR-GSI correlations under varied site conditions for each major Ohio rock type, borrowing the simple linear correlation form.

Examinations of the regression analysis plots can provide the following observations:

- In most cases, a simple linear function ($y = mx + c$) was sufficient to describe the relationship between RMR and GSI for Ohio rocks with a reasonably strong correlation ($r^2 = 0.7$ to 0.85).

- The slope (m) of the linear correlation is independent of the groundwater and joint orientation conditions. In contrast, the intercept (c) varies according to the groundwater and joint orientation conditions.
- The slope of the linear correlation between RMR and GSI differed among rock types. It appears that the slope becomes steeper for stronger rock material.

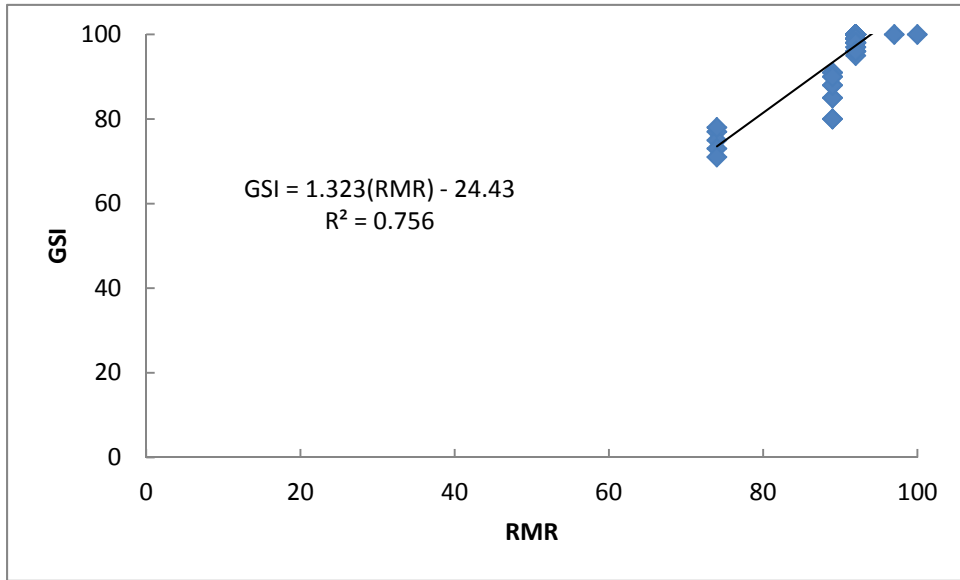


Figure 4.28: RMR-GSI Correlation for Limestone in Ohio (Linear)

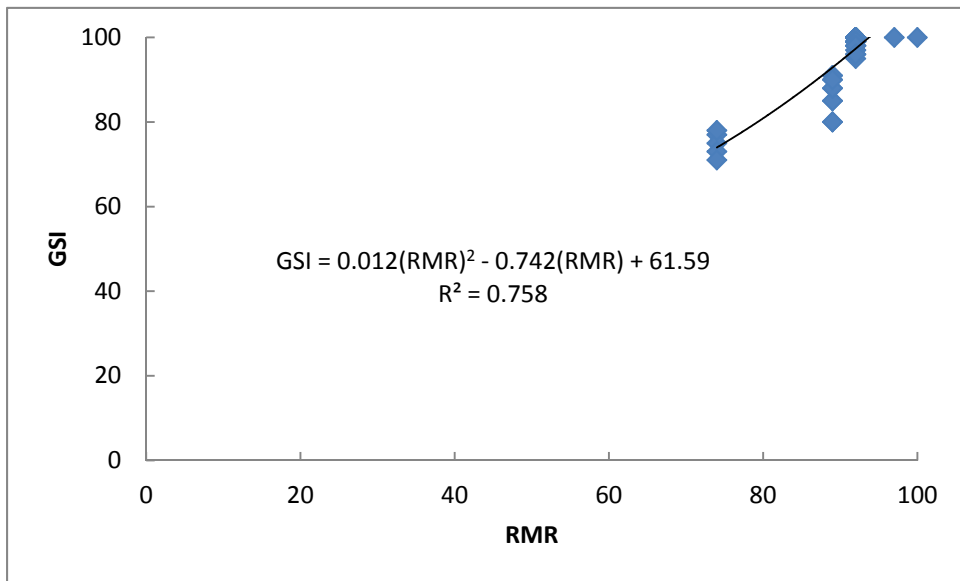


Figure 4.29: RMR-GSI Correlation for Limestone in Ohio (Quadratic)

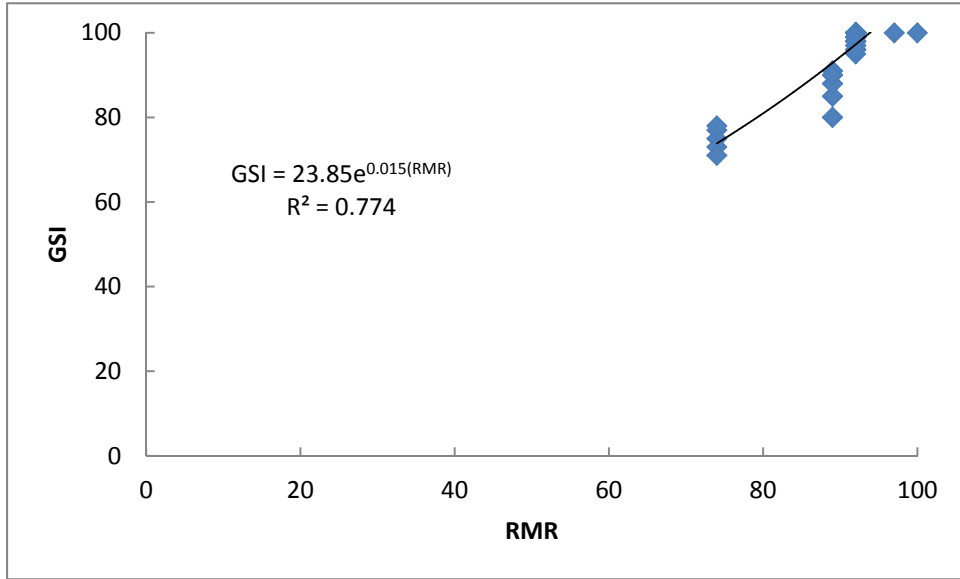


Figure 4.30: RMR-GSI Correlation for Limestone in Ohio (Exponential)

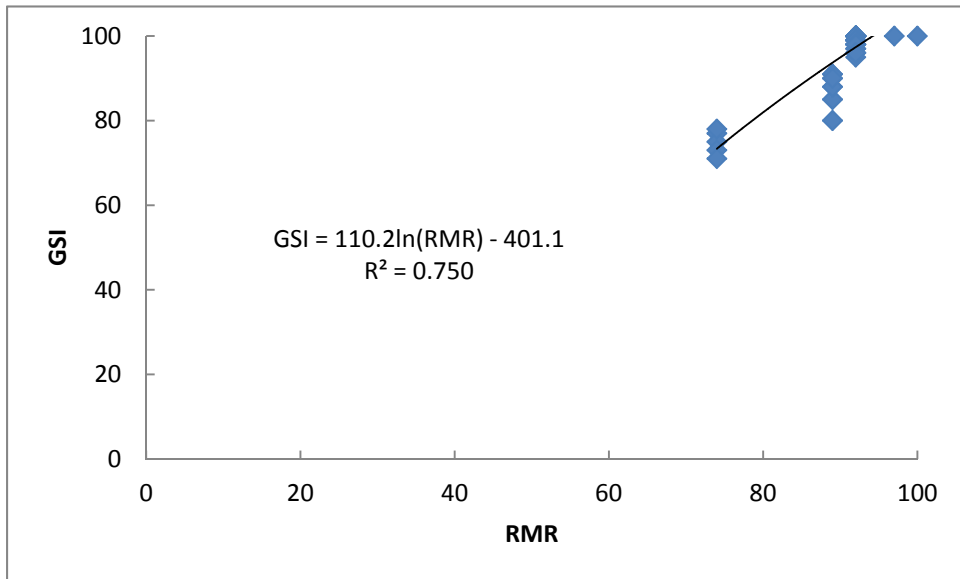


Figure 4.31: RMR-GSI Correlation for Limestone in Ohio (Logarithmic)

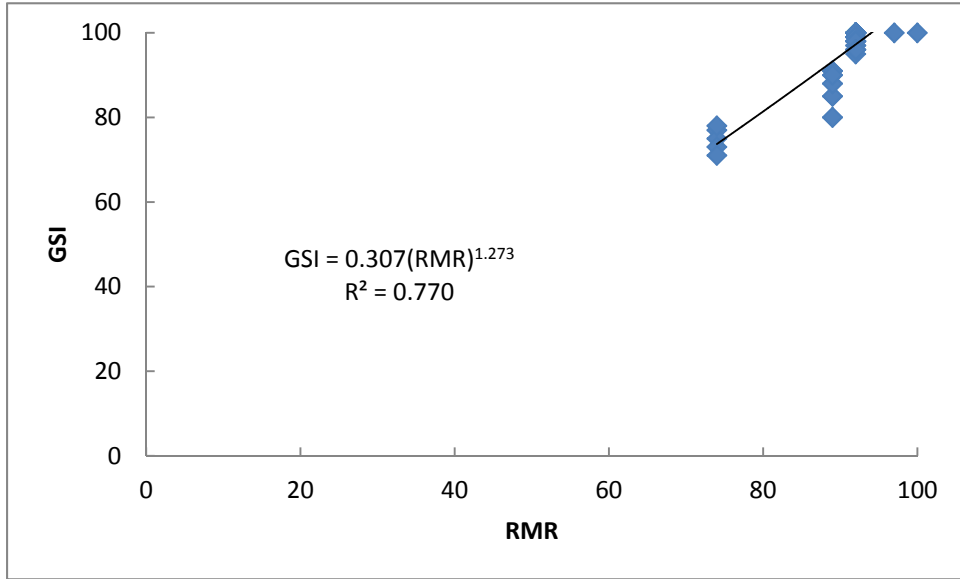


Figure 4.32: RMR-GSI Correlation for Limestone in Ohio (Power)

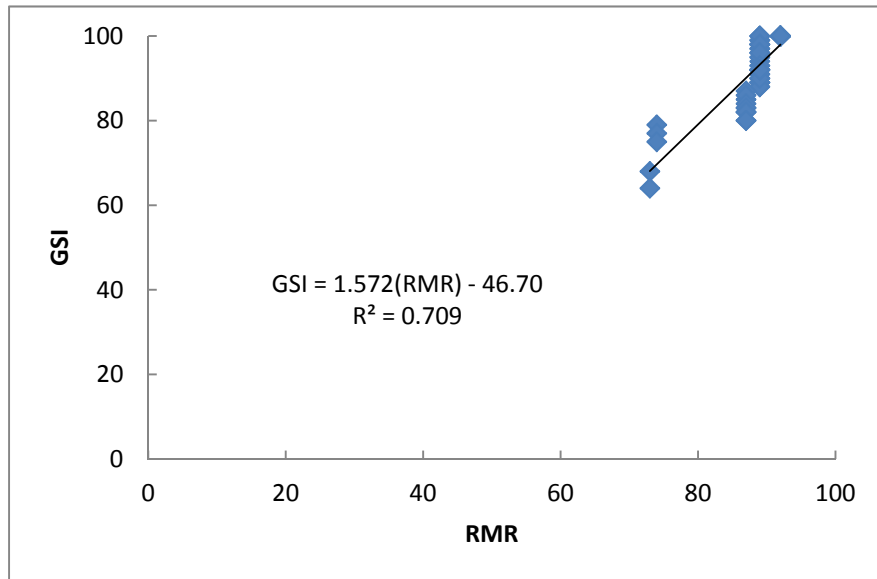


Figure 4.33: RMR-GSI Correlation for Sandstone in Ohio (Linear)

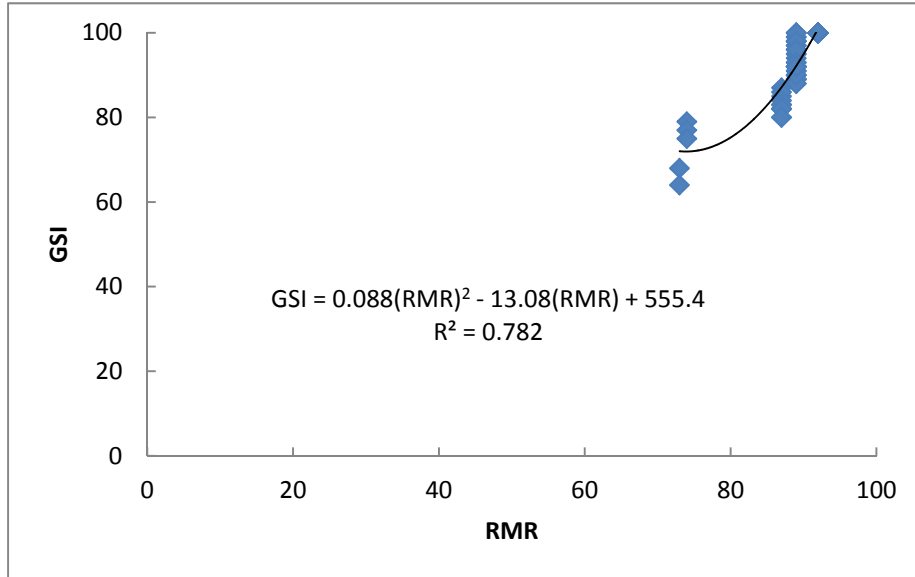


Figure 4.34: RMR-GSI Correlation for Sandstone in Ohio (Quadratic)

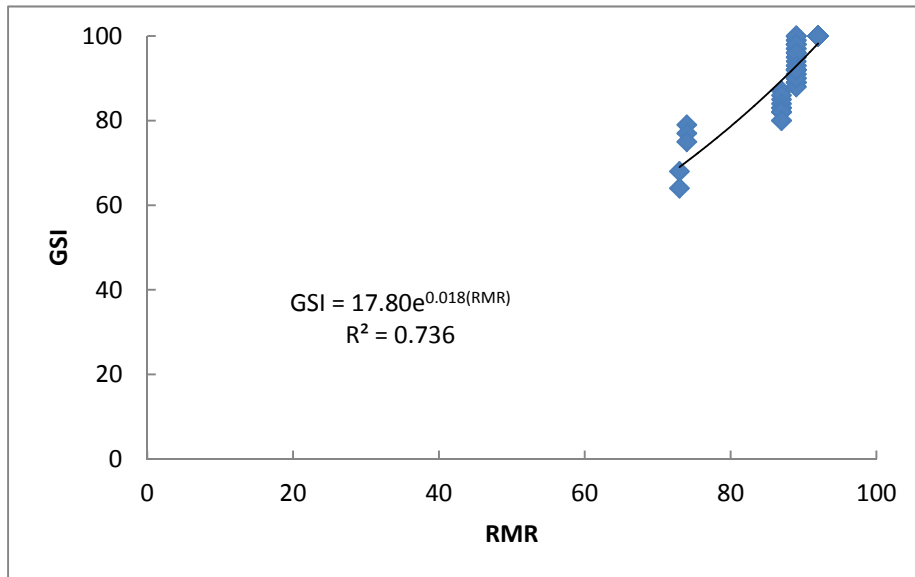


Figure 4.35: RMR-GSI Correlation for Sandstone in Ohio (Exponential)

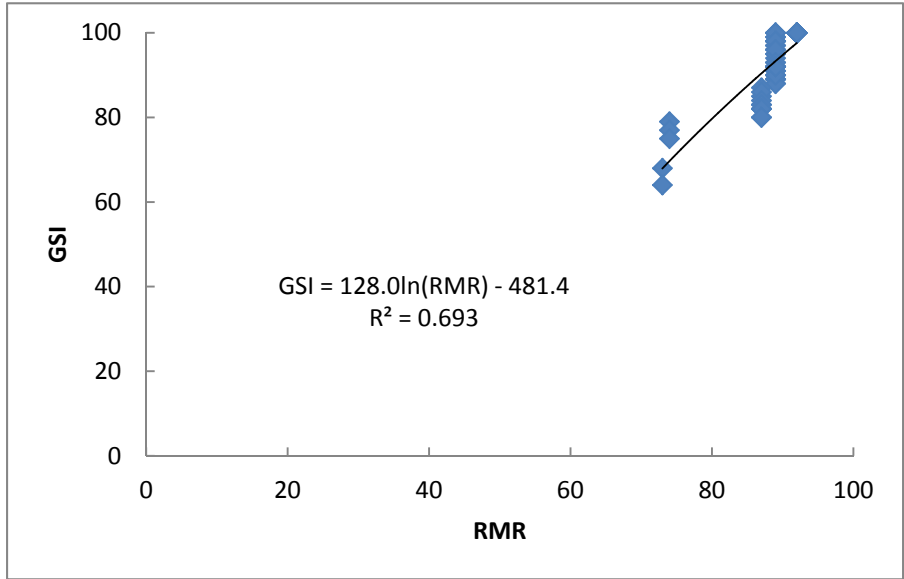


Figure 4.36: RMR-GSI Correlation for Sandstone in Ohio (Logarithmic)

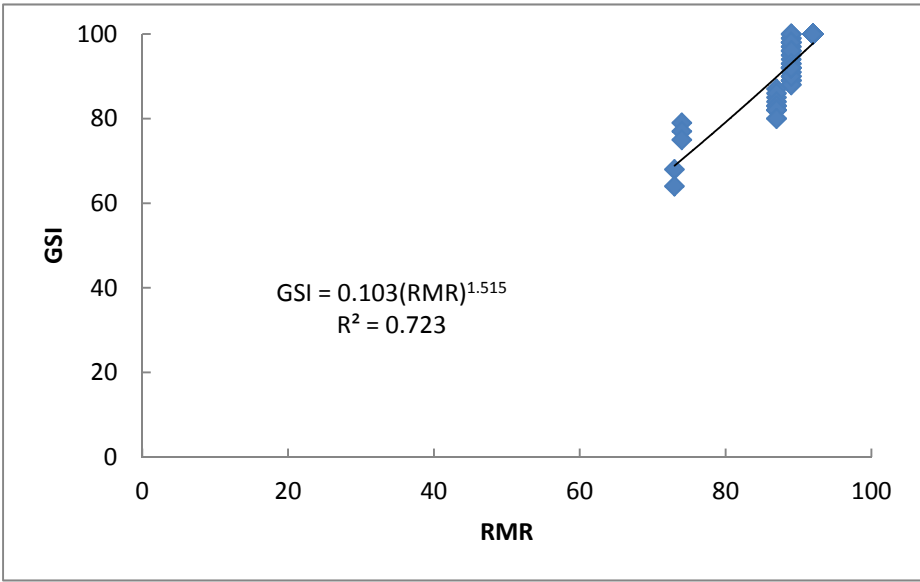


Figure 4.37: RMR-GSI Correlation for Sandstone in Ohio (Power)

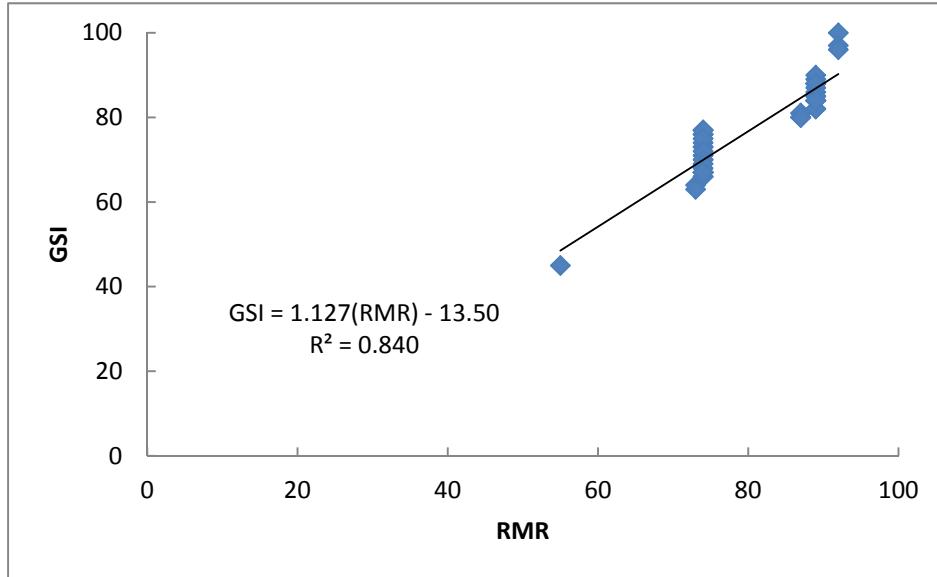


Figure 4.38: RMR-GSI Correlation for Unweathered Shale in Ohio (Linear)

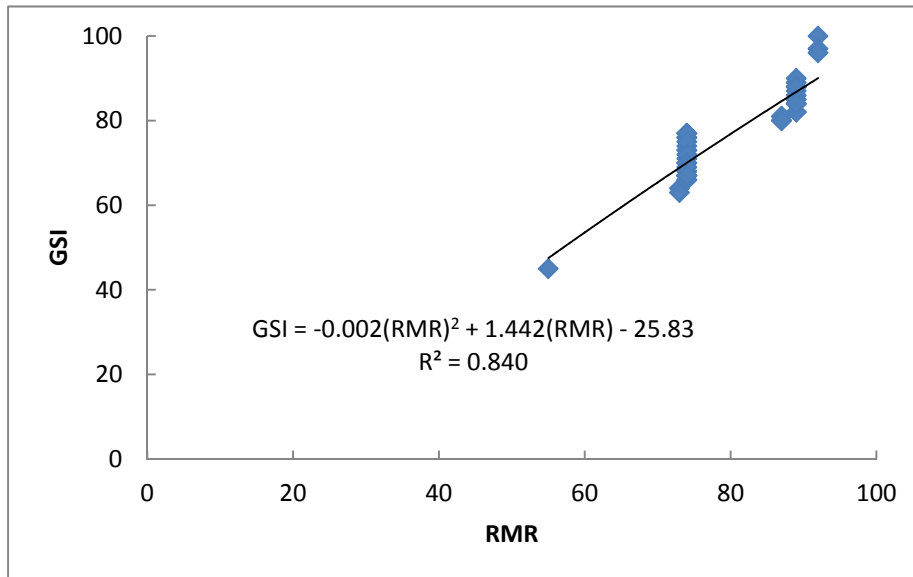


Figure 4.39: RMR-GSI Correlation for Unweathered Shale in Ohio (Quadratic)

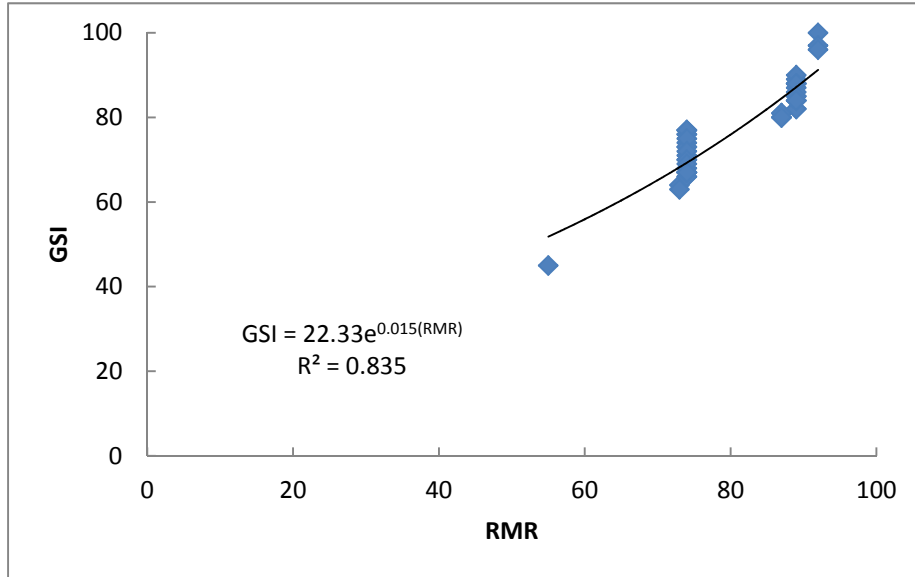


Figure 4.40: RMR-GSI Correlation for Unweathered Shale in Ohio (Exponential)

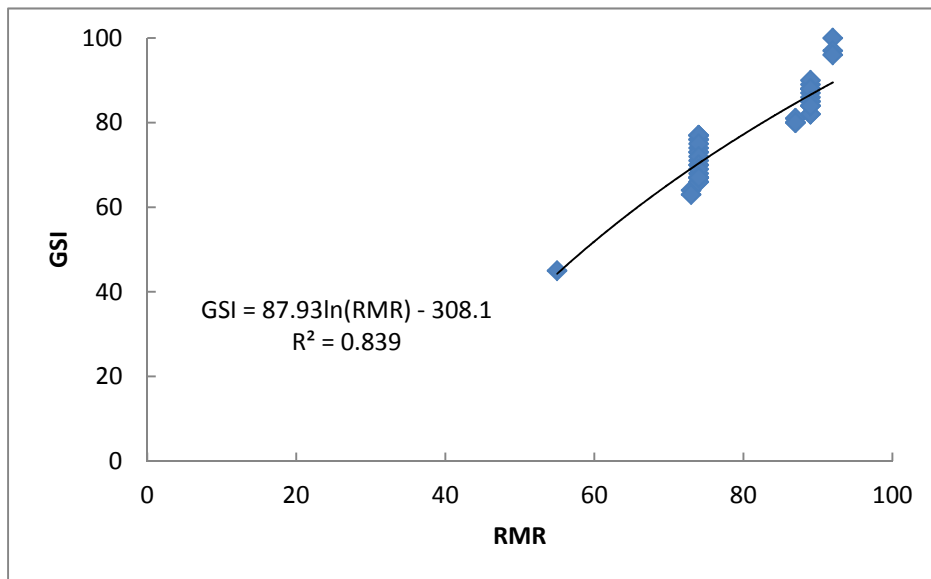


Figure 4.41: RMR-GSI Correlation for Unweathered Shale in Ohio (Logarithmic)

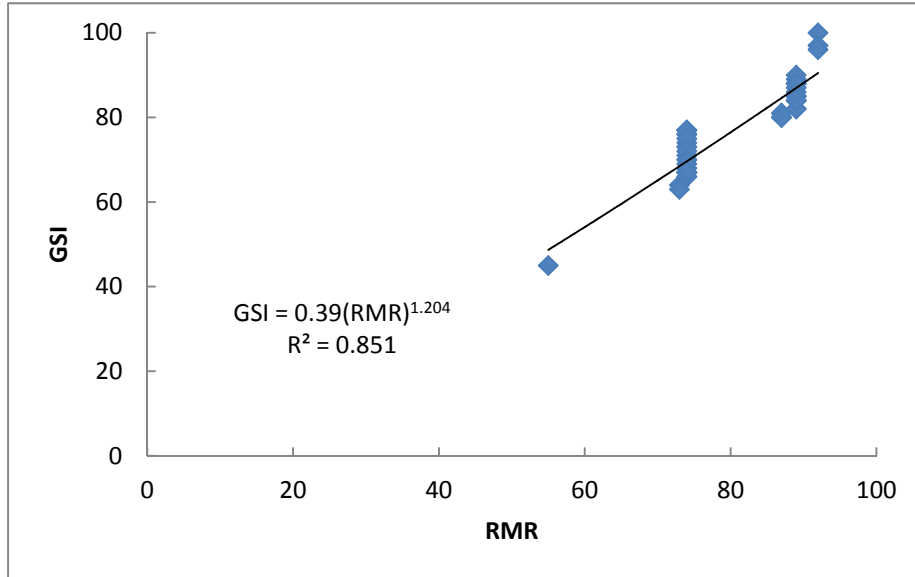


Figure 4.42: RMR-GSI Correlation for Unweathered Shale in Ohio (Power)

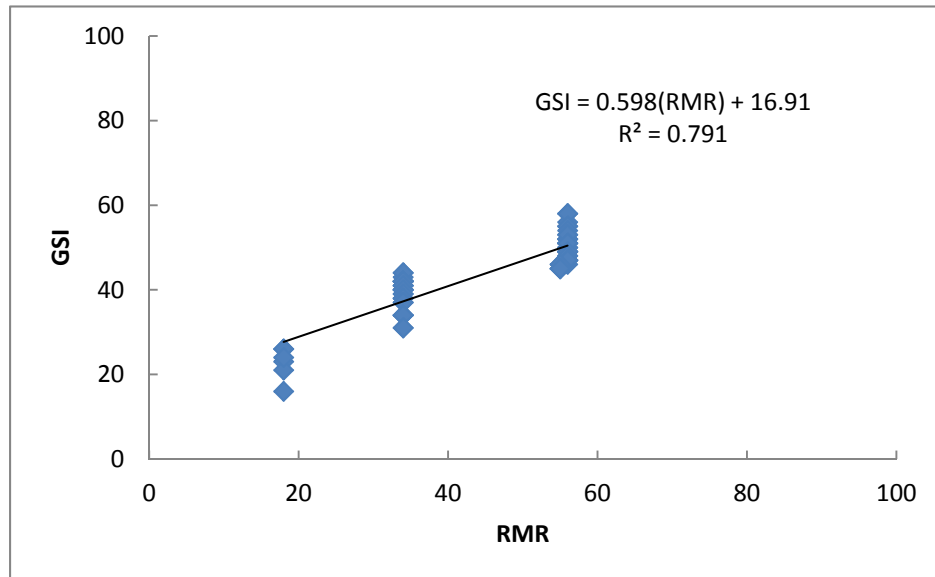


Figure 4.43: RMR-GSI Correlation for Weathered Shale in Ohio (Linear)

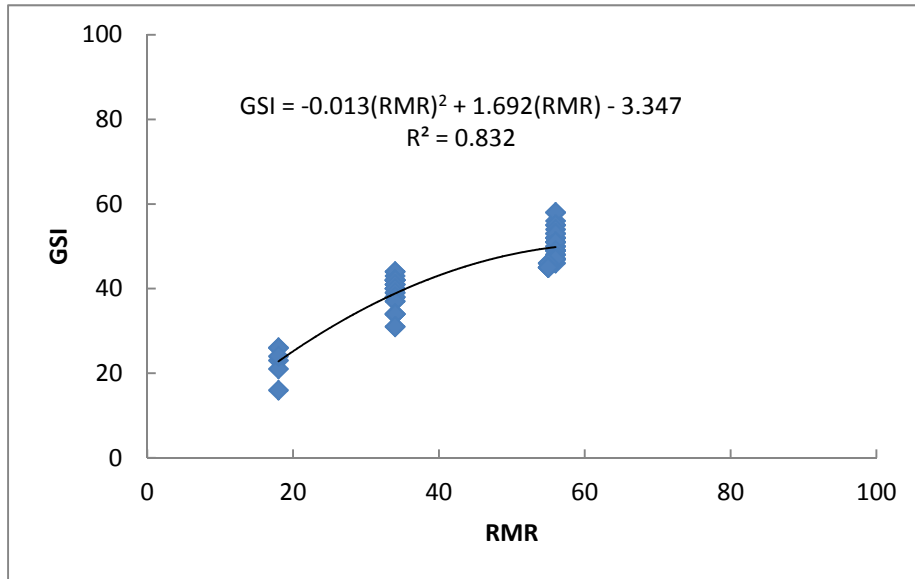


Figure 4.44: RMR-GSI Correlation for Weathered Shale in Ohio (Quadratic)

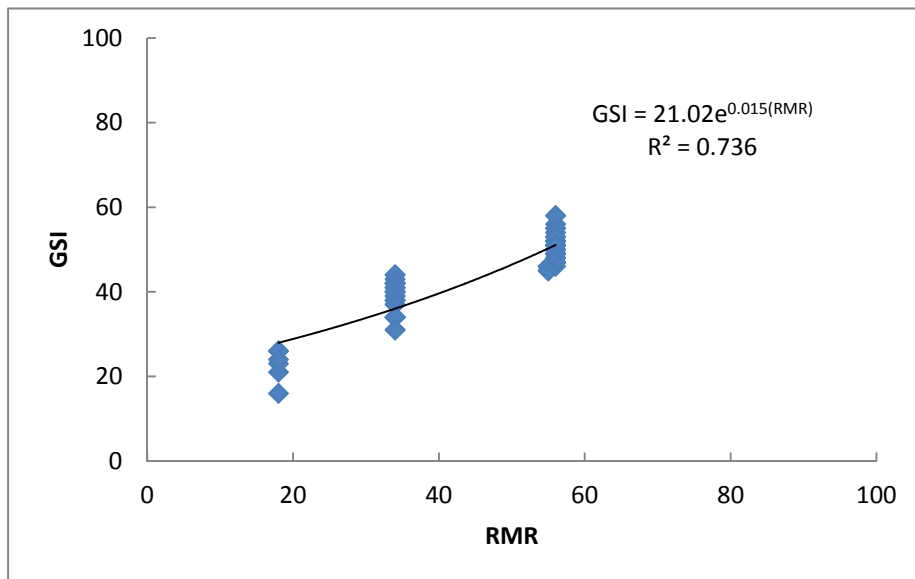


Figure 4.45: RMR-GSI Correlation for Weathered Shale in Ohio (Exponential)

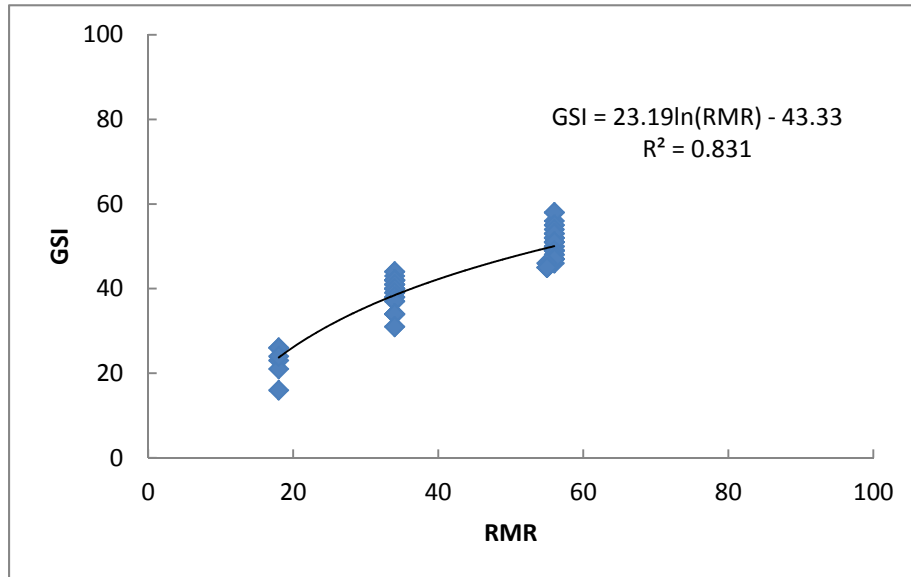


Figure 4.46: RMR-GSI Correlation for Weathered Shale in Ohio (Logarithmic)

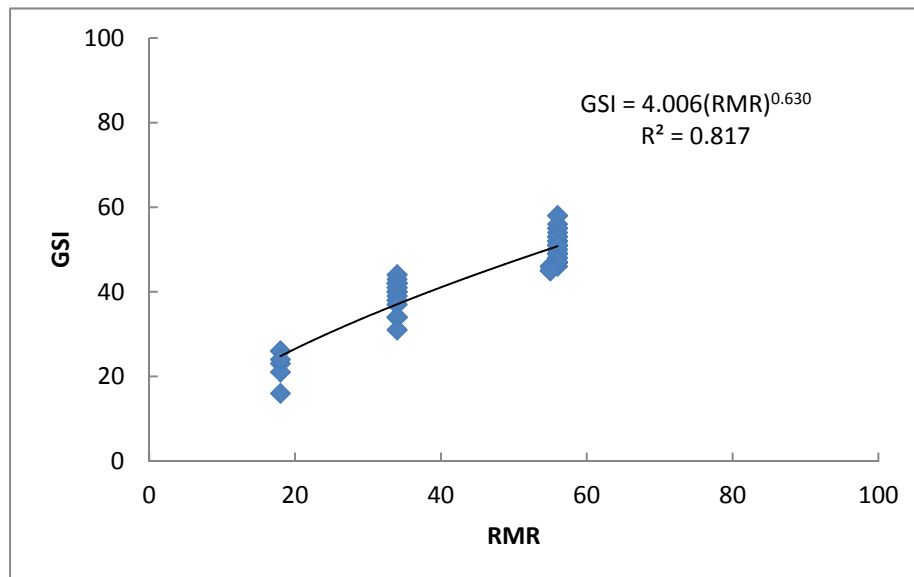


Figure 4.47: RMR-GSI Correlation for Weathered Shale in Ohio (Power)

Table 4.49: RMR-GSI Correlations for Limestone in Ohio

Groundwater Conditions	Joint Orientations	Correlation Eq.	r^2
Very Dry (10)	Very Favorable (0)	$GSI = 1.323(RMR) - 24.43$	0.756
	Favorable (-2)	$GSI = 1.323(RMR) - 21.78$	0.756
	Fair (-7)	$GSI = 1.323(RMR) - 15.16$	0.756
	Unfavorable (-15)	$GSI = 1.323(RMR) - 4.575$	0.756
	Very Unfavorable (-25)	$GSI = 1.323(RMR) + 8.662$	0.756
Moist (7)	Very Favorable (0)	$GSI = 1.323(RMR) - 20.46$	0.756
	Favorable (-2)	$GSI = 1.323(RMR) - 17.81$	0.756
	Fair (-7)	$GSI = 1.323(RMR) - 11.19$	0.756
	Unfavorable (-15)	$GSI = 1.323(RMR) - 0.604$	0.756
	Very Unfavorable (-25)	$GSI = 1.323(RMR) + 12.63$	0.756
Water under Moderate Pressure (4)	Very Favorable (0)	$GSI = 1.323(RMR) - 16.49$	0.756
	Favorable (-2)	$GSI = 1.323(RMR) - 13.84$	0.756
	Fair (-7)	$GSI = 1.323(RMR) - 7.223$	0.756
	Unfavorable (-15)	$GSI = 1.323(RMR) + 3.367$	0.756
	Very Unfavorable (-25)	$GSI = 1.323(RMR) + 16.60$	0.756
Severe Water Problems (0)	Very Favorable (0)	$GSI = 1.323(RMR) - 11.19$	0.756
	Favorable (-2)	$GSI = 1.323(RMR) - 8.547$	0.756
	Fair (-7)	$GSI = 1.323(RMR) - 1.928$	0.756
	Unfavorable (-15)	$GSI = 1.323(RMR) + 8.662$	0.756
	Very Unfavorable (-25)	$GSI = 1.323(RMR) + 21.90$	0.756

[Note] GSI value must be positive and rounded off to the nearest integer.

Table 4.50: RMR-GSI Correlations for Sandstone in Ohio

Groundwater Conditions	Joint Orientations	Correlation Eq.	r ²
Very dry (10)	Very Favorable (0)	$GSI = 1.512(RMR) - 40.55$	0.775
	Favorable (-2)	$GSI = 1.512(RMR) - 37.53$	0.775
	Fair (-7)	$GSI = 1.512(RMR) - 29.97$	0.775
	Unfavorable (-15)	$GSI = 1.512(RMR) - 17.87$	0.775
	Very Unfavorable (-25)	$GSI = 1.512(RMR) - 2.747$	0.775
Moist (7)	Very Favorable (0)	$GSI = 1.512(RMR) - 36.02$	0.775
	Favorable (-2)	$GSI = 1.512(RMR) - 32.99$	0.775
	Fair (-7)	$GSI = 1.512(RMR) - 25.43$	0.775
	Unfavorable (-15)	$GSI = 1.512(RMR) - 13.33$	0.775
	Very Unfavorable (-25)	$GSI = 1.512(RMR) + 1.789$	0.775
Water under moderate pressure (4)	Very Favorable (0)	$GSI = 1.512(RMR) - 31.48$	0.775
	Favorable (-2)	$GSI = 1.512(RMR) - 28.45$	0.775
	Fair (-7)	$GSI = 1.512(RMR) - 20.89$	0.775
	Unfavorable (-15)	$GSI = 1.512(RMR) - 8.797$	0.775
	Very Unfavorable (-25)	$GSI = 1.512(RMR) + 6.326$	0.775
Severe Water Problems (0)	Very Favorable (0)	$GSI = 1.512(RMR) - 25.43$	0.775
	Favorable (-2)	$GSI = 1.512(RMR) - 22.40$	0.775
	Fair (-7)	$GSI = 1.512(RMR) - 14.84$	0.775
	Unfavorable (-15)	$GSI = 1.512(RMR) - 2.747$	0.775
	Very Unfavorable (-25)	$GSI = 1.512(RMR) + 12.37$	0.775

[Note] GSI value must be positive and rounded off to the nearest integer.

Table 4.51: RMR-GSI Correlations for Unweathered Shale in Ohio

Groundwater Conditions	Joint Orientations	Correlation Eq.	r ²
Very dry (10)	Very Favorable (0)	$GSI = 1.127(RMR) - 13.50$	0.840
	Favorable (-2)	$GSI = 1.127(RMR) - 11.24$	0.840
	Fair (-7)	$GSI = 1.127(RMR) - 5.608$	0.840
	Unfavorable (-15)	$GSI = 1.127(RMR) + 3.410$	0.840
	Very Unfavorable (-25)	$GSI = 1.127(RMR) + 14.68$	0.840
Moist (7)	Very Favorable (0)	$GSI = 1.127(RMR) - 10.11$	0.840
	Favorable (-2)	$GSI = 1.127(RMR) - 7.863$	0.840
	Fair (-7)	$GSI = 1.127(RMR) - 2.226$	0.840
	Unfavorable (-15)	$GSI = 1.127(RMR) + 6.793$	0.840
	Very Unfavorable (-25)	$GSI = 1.127(RMR) + 18.06$	0.840
Water under moderate pressure (4)	Very Favorable (0)	$GSI = 1.127(RMR) - 6.736$	0.840
	Favorable (-2)	$GSI = 1.127(RMR) - 4.481$	0.840
	Fair (-7)	$GSI = 1.127(RMR) + 1.155$	0.840
	Unfavorable (-15)	$GSI = 1.127(RMR) + 10.17$	0.840
	Very Unfavorable (-25)	$GSI = 1.127(RMR) + 21.45$	0.840
Severe Water Problems (0)	Very Favorable (0)	$GSI = 1.127(RMR) - 2.226$	0.840
	Favorable (-2)	$GSI = 1.127(RMR) + 0.028$	0.840
	Fair (-7)	$GSI = 1.127(RMR) + 5.665$	0.840
	Unfavorable (-15)	$GSI = 1.127(RMR) + 14.68$	0.840
	Very Unfavorable (-25)	$GSI = 1.127(RMR) + 25.96$	0.840

[Note] GSI value must be positive and rounded off to the nearest integer.

Table 4.52: RMR-GSI Correlations for Weathered Shale in Ohio

Groundwater Conditions	Joint Orientations	Correlation Eq.	r ²
Very dry (10)	Very Favorable (0)	$GSI = 0.550(RMR) + 19.58$	0.726
	Favorable (-2)	$GSI = 0.550(RMR) + 20.68$	0.726
	Fair (-7)	$GSI = 0.550(RMR) + 23.43$	0.726
	Unfavorable (-15)	$GSI = 0.550(RMR) + 27.83$	0.726
	Very Unfavorable (-25)	$GSI = 0.550(RMR) + 33.34$	0.726
Moist (7)	Very Favorable (0)	$GSI = 0.550(RMR) + 21.23$	0.726
	Favorable (-2)	$GSI = 0.550(RMR) + 22.33$	0.726
	Fair (-7)	$GSI = 0.550(RMR) + 25.08$	0.726
	Unfavorable (-15)	$GSI = 0.550(RMR) + 29.49$	0.726
	Very Unfavorable (-25)	$GSI = 0.550(RMR) + 34.99$	0.726
Water under moderate pressure (4)	Very Favorable (0)	$GSI = 0.550(RMR) + 22.88$	0.726
	Favorable (-2)	$GSI = 0.550(RMR) + 23.98$	0.726
	Fair (-7)	$GSI = 0.550(RMR) + 26.73$	0.726
	Unfavorable (-15)	$GSI = 0.550(RMR) + 31.14$	0.726
	Very Unfavorable (-25)	$GSI = 0.550(RMR) + 36.64$	0.726
Severe Water Problems (0)	Very Favorable (0)	$GSI = 0.550(RMR) + 25.08$	0.726
	Favorable (-2)	$GSI = 0.550(RMR) + 26.18$	0.726
	Fair (-7)	$GSI = 0.550(RMR) + 28.93$	0.726
	Unfavorable (-15)	$GSI = 0.550(RMR) + 33.34$	0.726
	Very Unfavorable (-25)	$GSI = 0.550(RMR) + 38.84$	0.726

[Note] GSI value must be positive and rounded off to the nearest integer.

4.6 Critical Design Parameter Calculations

Shear strength and elastic modulus of rock masses are critical for designing highway bridge foundations that are going to rest directly on rock. And, the RMR system has a simple method, proposed by Carter and Kulhawy (1988), to estimate the lower bound bearing capacity for shallow foundations resting on rock. The GSI system does not appear to have a step that directly addresses the foundation's bearing capacity.

$$E_m = \left(\frac{E_m}{E_i}\right) E_i = 0.80 \times 39.3 = 31.44 \text{ GPa} = 4560 \text{ ksi}$$

According to the ASSHTO diagrams, the instantaneous friction angle (ϕ'_i) is:

$$m = 1.85, \quad s = 0.058$$

$$h = 1 + \frac{16(m\sigma'_n + sq_u)}{3m^2q_u} = 1.11$$

$$\phi'_i = \tan^{-1}\{4h \cos^2[30 + 0.33 \sin^{-1}(h^{-1.5})] - 1\}^{-0.5} = 47.1^\circ$$

The shear strength (τ) is calculated by:

$$\tau = \frac{1}{8}(\cot \phi'_i - \cos \phi'_i)mq_u = 82.8 \text{ ksf}$$

So, the instantaneous cohesion (c) is:

$$\sigma'_n = \gamma H = 167 \times 50 = 8350 \text{ psf} = 8.35 \text{ ksf}$$

$$c = \tau - \sigma'_n \tan \phi'_i = 73.8 \text{ ksf}$$

The lower limit of the bearing capacity can be estimated as:

$$q_{ult} = \left(\sqrt{s} + \sqrt{m\sqrt{s} + s}\right)q_u = 1368.6 \text{ ksf}$$

(2) Calculations Based on the GSI System

The GSI value is estimated using the linear correlation equation as:

$$GSI = 1.323(RMR) - 24.43 = 80.08 \approx 80$$

The material constants in the GSI system are calculated as below, assuming D

(disturbance factor) = 1.0:

$$m_b = m_i \cdot \exp\left(\frac{GSI - 100}{28 - 14D}\right) = 2.64$$

$$s = \exp\left(\frac{GSI - 100}{9 - 3D}\right) = 0.04$$

$$a = \frac{1}{2} + \frac{1}{6}\left(e^{-\frac{GSI}{15}} - e^{-\frac{20}{3}}\right) = 0.50$$

Based on the Poisson's ratio (ν) and uniaxial compression strength (σ_{ci}) values, the minor effective principle stress (σ'_3) and major effective principle stress (σ'_1) are determined as:

$$\sigma'_3 = \gamma H \cdot \frac{\nu}{1 - \nu} = 2.49 \text{ ksf}, \quad \sigma_{ci} = 11406 \text{ psi}$$

$$\sigma'_1 = \sigma'_3 + \sigma_{ci} \left(m_b \frac{\sigma'_3}{\sigma_{ci}} + s \right)^a = 329.0 \text{ ksf}$$

The normal stress (σ'_n) and shear stress (τ) are calculated through:

$$d\sigma'_1/d\sigma'_3 = 1 + am_b \left(m_b \cdot \frac{\sigma'_1}{\sigma'_3} + s \right)^{a-1} = 7.61$$

$$\sigma'_n = \frac{\sigma'_1 + \sigma'_3}{2} - \frac{\sigma'_1 - \sigma'_3}{2} \cdot \frac{(d\sigma'_1/d\sigma'_3 - 1)}{(d\sigma'_1/d\sigma'_3 + 1)} = 40.41 \text{ ksf}$$

$$\tau = (\sigma'_1 - \sigma'_3) \frac{\sqrt{d\sigma'_1/d\sigma'_3}}{d\sigma'_1/d\sigma'_3 + 1} = 104.6 \text{ ksf}$$

After transforming the unconfined compression strength (σ_{ci}) from psi to MPa, the elastic modulus of the rock mass (E_m) is determined by:

$$E_m = \left(1 - \frac{D}{2}\right) \sqrt{\frac{\sigma_{ci}}{100}} \cdot 10^{\frac{GSI-10}{40}} = 24.93 \text{ GPa} = 3616.4 \text{ ksi}$$

The tensile strength (σ_t) of the rock mass is:

$$\sigma_t = -\frac{s\sigma_{ci}}{m_b} = -22.2 \text{ ksf}$$

If $\sigma_t < \sigma'_3 < \frac{\sigma_{ci}}{4}$, the rock mass strength (σ'_{cm}) can be calculated as:

$$\sigma'_{cm} = \sigma_{ci} \cdot \frac{[m_b + 4s - a(m_b - 8s)](0.25m_b + s)^{a-1}}{2(1+a)(2+a)} = 420.6 \text{ ksf}$$

Joint Orientations = Very Favorable,

Rating = 0

$$RMR = 7 + 13 + 20 + 20 + 10 = 70,$$

Class No. II = Good

The elastic modulus of the rock mass (E_m) is:

$$E_m = 10^{\frac{RMR-10}{40}} = 31.62 \text{ GPa} = 4586.1 \text{ ksi}$$

The elastic modulus of the rock mass (E_m) can be also estimated from the elastic modulus of intact rock (E_i) as:

$$E_m = \left(\frac{E_m}{E_i}\right) E_i = 0.70 \times 14.7 = 10.29 \text{ GPa} = 1492.4 \text{ ksi}$$

According to the ASSHTO diagrams, the instantaneous friction angle (ϕ'_i) is:

$$m = 2.208, \quad s = 0.00293$$

$$h = 1 + \frac{16(m\sigma'_n + sq_u)}{3m^2q_u} = 1.02$$

$$\phi'_i = \tan^{-1}\{4h \cos^2[30 + 0.33 \sin^{-1}(h^{-1.5})] - 1\}^{-0.5} = 60.0^\circ$$

The shear strength (τ) is calculated by:

$$\tau = \frac{1}{8} (\cot \phi'_i - \cos \phi'_i) m q_u = 24.6 \text{ ksf}$$

So, the instantaneous cohesion (c) is:

$$\sigma'_n = \gamma H = 142 \times 50 = 7100 \text{ psf} = 7.10 \text{ ksf}$$

$$c = \tau - \sigma'_n \tan \phi'_i = 12.3 \text{ ksf}$$

The lower limit of the bearing capacity can be estimated as:

$$q_{ult} = \left(\sqrt{s} + \sqrt{m\sqrt{s} + s} \right) q_u = 465.5 \text{ ksf}$$

(2) Calculations Based on the GSI System

The GSI value is estimated using the linear correlation equation as:

$$GSI = 1.572(RMR) - 46.70 = 63.34 \approx 63$$

The material constants in GSI system are calculated as below, assuming $D = 0.8$:

$$m_b = m_i \cdot \exp\left(\frac{GSI - 100}{28 - 14D}\right) = 2.10$$

$$s = \exp\left(\frac{GSI - 100}{9 - 3D}\right) = 0.003$$

$$a = \frac{1}{2} + \frac{1}{6} \left(e^{-\frac{GSI}{15}} - e^{-\frac{20}{3}} \right) = 0.50$$

Based on the Poisson's ratio (ν) and uniaxial compression strength (σ_{ci}), the minor effective principle stress (σ'_3) and major effective principle stress (σ'_1) are determined as:

$$\sigma'_3 = \gamma H \cdot \frac{\nu}{1 - \nu} = 1.78 \text{ ksf}, \quad \sigma_{ci} = 7597 \text{ psi}$$

$$\sigma'_1 = \sigma'_3 + \sigma_{ci} \left(m_b \frac{\sigma'_3}{\sigma_{ci}} + s \right)^a = 92.81 \text{ ksf}$$

The normal stress (σ'_n) and shear stress (τ) are calculated through:

$$d\sigma'_1/d\sigma'_3 = 1 + am_b \left(m_b \cdot \frac{\sigma'_1}{\sigma'_3} + s \right)^{a-1} = 13.39$$

$$\sigma'_n = \frac{\sigma'_1 + \sigma'_3}{2} - \frac{\sigma'_1 - \sigma'_3}{2} \cdot \frac{(d\sigma'_1/d\sigma'_3 - 1)}{(d\sigma'_1/d\sigma'_3 + 1)} = 8.10 \text{ ksf}$$

$$\tau = (\sigma'_1 - \sigma'_3) \frac{\sqrt{d\sigma'_1/d\sigma'_3}}{d\sigma'_1/d\sigma'_3 + 1} = 23.2 \text{ ksf}$$

After converting the unconfined compression strength (σ_{ci}) from psi to MPa, the elastic modulus of the rock mass (E_m) is estimated as:

$$E_m = \left(1 - \frac{D}{2}\right) \sqrt{\frac{\sigma_{ci}}{100}} \cdot 10^{\frac{GSI-10}{40}} = 9.18 \text{ GPa} = 1331.1 \text{ ksi}$$

The tensile strength (σ_t) of the rock mass is determined to be:

$$\sigma_t = -\frac{s\sigma_{ci}}{m_b} = -1.91 \text{ ksf}$$

If $\sigma_t < \sigma'_3 < \frac{\sigma_{ci}}{4}$, the rock mass strength (σ'_{cm}) can be calculated as:

$$\sigma'_{cm} = \sigma_{ci} \cdot \frac{[m_b + 4s - a(m_b - 8s)](0.25m_b + s)^{a-1}}{2(1+a)(2+a)} = 214.8 \text{ ksf}$$

Then, the upper limit of the confining stress (σ'_{3max}) on the rock mass may be set at:

$$\sigma'_{3max} = \sigma'_{cm} \cdot 0.72 \left(\frac{\sigma'_{cm}}{\gamma H}\right)^{-0.91} = 6.95 \text{ ksf}$$

Finally, the effective friction angle (ϕ') and effective cohesion (c') can be computed through:

$$\sigma'_{3n} = \frac{\sigma'_{3max}}{\sigma_{ci}} = 0.01$$

$$\phi' = \sin^{-1} \left[\frac{2(1+a)(2+a)}{6am_b(s + m_b\sigma'_{3n})^{a-1}} + 1 \right]^{-1} = 59.9^\circ$$

$$c' = \frac{\sigma_{ci}[(1+2a)s + (1-a)m_b\sigma'_{3n}](s + m_b\sigma'_{3n})^{a-1}}{\sqrt{[1 + 6am_b(s + m_b\sigma'_{3n})^{a-1}](1+a)(2+a)}} = 8.6 \text{ ksf}$$

4.6.3 Example 3 – Unweathered Shale in Southeast Region

For the third example, this unweathered shale mass in the northeast region is assumed to possess average limestone properties of the region. That is:

Unit Weight = 165pcf, Unconfined Compression Strength (q_u) = 3 ksi

Depth = 50 ft, $m_i = 19$, Poisson's Ratio = 0.09

(1) Calculations Based on the RMR System

Unconfined Compression Strength = 3000 psi = 432ksf,	Rating = 2
RQD = 65%,	Rating = 13
Joint Spacing = 1 to 3ft,	Rating = 20
Joint Conditions = Slightly Rough,	Rating = 20
Groundwater Condition = Dry,	Rating = 10
Joint Orientations = Very Favorable,	Rating = 0
RMR = 2 + 13 + 20 + 20 + 10 = 65,	Class No. II = Good

The elastic modulus of the rock mass (E_m) is estimated as:

$$E_m = 10^{\frac{RMR-10}{40}} = 23.71 \text{ GPa} = 3439.4 \text{ ksi}$$

The elastic modulus of the rock mass (E_m) can be also determined from the elastic modulus of intact rock (E_i) as:

$$E_m = \left(\frac{E_m}{E_i}\right) E_i = 0.56 \times 9.79 = 5.48 \text{ GPa} = 794.8 \text{ ksi}$$

According to the ASSHTO diagrams, the instantaneous friction angle (ϕ'_i) is:

$$m = 0.821, \quad s = 0.00293$$

$$h = 1 + \frac{16(m\sigma'_n + sq_u)}{3m^2q_u} = 1.15$$

$$\phi'_i = \tan^{-1}\{4h \cos^2[30 + 0.33 \sin^{-1}(h^{-1.5})] - 1\}^{-0.5} = 44.2^\circ$$

The shear strength (τ) is calculated as:

$$\tau = \frac{1}{8}(\cot \phi'_i - \cos \phi'_i)mq_u = 13.8 \text{ ksf}$$

So, the instantaneous cohesion (c) is:

$$\sigma'_n = \gamma H = 165 \times 50 = 8250 \text{ psf} = 8.25 \text{ ksf}$$

$$c = \tau - \sigma'_n \tan \phi'_i = 5.8 \text{ ksf}$$

The lower limit of the bearing capacity can be estimated as:

$$q_{ult} = \left(\sqrt{s} + \sqrt{m\sqrt{s} + s} \right) q_u = 117.4 \text{ ksi}$$

(2) Calculations Based on the GSI System

The GSI value is estimated using the linear correlation equation as:

$$GSI = 1.128(RMR) - 13.5 = 59.79 \approx 60$$

The material constants in GSI system are calculated as below, assuming $D = 0$:

$$m_b = m_i \cdot \exp\left(\frac{GSI - 100}{28 - 14D}\right) = 4.55$$

$$s = \exp\left(\frac{GSI - 100}{9 - 3D}\right) = 0.01$$

$$a = \frac{1}{2} + \frac{1}{6} \left(e^{-\frac{GSI}{15}} - e^{-\frac{20}{3}} \right) = 0.50$$

Based on the Poisson's ratio (ν) and uniaxial compression strength (σ_{ci}), the minor effective principle stress (σ'_3) and major effective principle stress (σ'_1) are determined as:

$$\sigma'_3 = \gamma H \cdot \frac{\nu}{1 - \nu} = 0.82 \text{ ksf}, \quad \sigma_{ci} = 1508 \text{ psi}$$

$$\sigma'_1 = \sigma'_3 + \sigma_{ci} \left(m_b \frac{\sigma'_3}{\sigma_{ci}} + s \right)^a = 37.3 \text{ ksf}$$

The normal stress (σ'_n) and shear stress (τ) are calculated through:

$$d\sigma'_1/d\sigma'_3 = 1 + am_b \left(m_b \cdot \frac{\sigma'_1}{\sigma'_3} + s \right)^{a-1} = 14.45$$

$$\sigma'_n = \frac{\sigma'_1 + \sigma'_3}{2} - \frac{\sigma'_1 - \sigma'_3}{2} \cdot \frac{(d\sigma'_1/d\sigma'_3 - 1)}{(d\sigma'_1/d\sigma'_3 + 1)} = 3.20 \text{ ksf}$$

$$\tau = (\sigma'_1 - \sigma'_3) \frac{\sqrt{d\sigma'_1/d\sigma'_3}}{d\sigma'_1/d\sigma'_3 + 1} = 9.0 \text{ ksf}$$

After transforming the unconfined compression strength (σ_{ci}) from psi to MPa, the elastic modulus of the rock mass (E_m) is estimated as:

$$E_m = \left(1 - \frac{D}{2}\right) \sqrt{\frac{\sigma_{ci}}{100}} \cdot 10^{\frac{GSI-10}{40}} = 5.73 \text{ GPa} = 831.7 \text{ ksi}$$

The tensile strength (σ_t) of the rock mass is determined to be:

$$\sigma_t = -\frac{s\sigma_{ci}}{m_b} = -0.56 \text{ ksf}$$

If $\sigma_t < \sigma'_3 < \frac{\sigma_{ci}}{4}$, the rock mass strength (σ'_{cm}) can be calculated as:

$$\sigma'_{cm} = \sigma_{ci} \cdot \frac{[m_b + 4s - a(m_b - 8s)](0.25m_b + s)^{a-1}}{2(1+a)(2+a)} = 63.5 \text{ ksf}$$

Then, the upper limit of confining stress (σ'_{3max}) on the rock mass may be set at:

$$\sigma'_{3max} = \sigma'_{cm} \cdot 0.72 \left(\frac{\sigma'_{cm}}{\gamma H}\right)^{-0.91} = 7.10 \text{ ksf}$$

Finally, the effective friction angle (ϕ') and effective cohesion (c') can be computed through:

$$\sigma'_{3n} = \frac{\sigma'_{3max}}{\sigma_{ci}} = 0.03$$

$$\phi' = \sin^{-1} \left[\frac{2(1+a)(2+a)}{6am_b(s + m_b\sigma'_{3n})^{a-1}} + 1 \right]^{-1} = 55.0^\circ$$

$$c' = \frac{\sigma_{ci}[(1+2a)s + (1-a)m_b\sigma'_{3n}](s + m_b\sigma'_{3n})^{a-1}}{\sqrt{[1 + 6am_b(s + m_b\sigma'_{3n})^{a-1}](1+a)(2+a)}} = 4.6 \text{ ksf}$$

4.6.4 Comments on Computation Examples

Table 4.53 on the next page summarizes the three RMR/GSI computational examples.

Based on these outcomes, the following statements can be made:

- With the ranges of m_i and σ_{ci} identified and the RMR-GSI correlation established, the GSI method can be applied to Ohio rocks to estimate their key engineering properties and use them in bridge foundation design work.
- Both RMR and GSI have a tendency to overestimate the value of the friction angle ϕ' . Any unrealistic value ϕ' of may have to be lowered to a reasonable value for the rock type considered.
- It appears that the GSI method may be somewhat less conservative for strong and good-quality (high RQD) rock masses, compared to RMR.
- As the rock gets weaker and more fractured, engineering properties determined by GSI appear to approach those by RMR method. This statement is only applicable for cases where core specimens can be recovered for compressive strength testing.

Table 4.53: Summary of RMR-GSI Computation Examples

Example	Description	RMR Method	GSI Method
1	Limestone in Southwest UW = 167 pcf UCS = 1440 ksf RQD = 80% D = 1.0	RMR = 79 $E_m = 7,700$ or $4,560$ ksi $\phi'_i = 47.1^\circ \rightarrow 40^\circ$ $c_i = 73.8$ ksf $\tau = 82.8$ ksf $q_{ult} = 1,369$ ksf	GSI = 80 $E_m = 3,616$ ksi $\phi'_i = 55.7^\circ \rightarrow 40^\circ$ $c_i = 49.3$ ksf $\tau = 104.6$ ksf $\sigma_{cm} = 421$ ksf $\sigma_{ci} = 1,642$ ksf
2	Sandstone in Northeast UW = 142 pcf UCS = 1152 ksf RQD = 70% D = 0.8	RMR = 70 $E_m = 4,586$ or $1,492$ ksi $\phi'_i = 60.0^\circ \rightarrow 34^\circ$ $c_i = 12.3$ ksf $\tau = 24.6$ ksf $q_{ult} = 466$ ksf	GSI = 63 $E_m = 1,331$ ksi $\phi'_i = 59.9^\circ \rightarrow 34^\circ$ $c_i = 8.6$ ksf $\tau = 23.2$ ksf $\sigma_{cm} = 215$ ksf $\sigma_{ci} = 1,094$ ksf
3	Shale (unweathered) in Southeast UW = 165 pcf UCS = 432 ksf RQD = 65% D = 0	RMR = 65 $E_m = 3,439$ or 795 ksi $\phi'_i = 44.2^\circ \rightarrow 27^\circ$ $c_i = 5.8$ ksf $\tau = 13.8$ ksf $q_{ult} = 117$ ksf	GSI = 60 $E_m = 832$ ksi $\phi'_i = 55.0^\circ \rightarrow 27^\circ$ $c_i = 4.6$ ksf $\tau = 9.0$ ksf $\sigma_{cm} = 64$ ksf $\sigma_{ci} = 217$ ksf

CHAPTER 5 : SUMMARY AND CONCLUSIONS

5.1 Summary

Section 10 of the AASHTO LRFD Bridge Design Specifications is expected to transition in the near future from the Rock Mass Rating (RMR) system to the Geological Strength Index (GSI) system for estimating rock mass properties that are needed for highway bridge foundation design work. GSI has been evolving in the past two decades due to difficulties experienced with RMR in some case studies. The main problem with RMR arises from the fact that rock masses are often badly damaged due to blasting and natural activities and/or at many sites it is difficult to obtain high-quality rock core specimens for measuring compressive strength required for the RMR system. GSI does not require compressive strength and is believed to be more convenient and applicable to a wider range of rock mass situations. Also, RMR demands the knowledge of the rock mass's joint orientations. This information is generally unavailable at most highway bridge project sites, as the rock mass's vertical facing must be largely exposed to attain the joint orientation information.

The current project was carried out to meet the following objectives:

- 1) To conduct an extensive literature review to gather information on the geology of Ohio rock, the Rock Mass Rating (RMR) system, the Geological Strength Index (GSI) system, the AASHTO LRFD highway bridge foundation design specifications, and basic/strength properties of Ohio rock samples;
- 2) To evaluate the values of the parameters included in the Geological Strength Index (GSI) classification using the rock sample strength data gathered in Ohio;
- 3) To address regional characteristics in the Ohio rock's properties;
- 4) To refine the design parameter charts to be used by Design Engineers based on regional differences; and

5) To develop the correlation between RMR and GSI systems and present it through a set of easy-to-understand charts and/or tables.

For the first objective, the Ohio University team conducted an online literature search using popular search engines and databases tied to geotechnical engineering/geological science journals and professional organizations. The team contacted the ODOT for any rock property data they have and also names of private testing companies, university research groups, and government agencies which may have additional data in hand. These entities included Advanced Terra Testing Inc. (Lakewood CO), Colorado School of Mines (Golden, CO), Golder Associates (Atlanta GA), and US Army Corps of Engineers (Huntington WV, Louisville KY, Pittsburgh PA).

For the second objective, the team ended up performing strength tests on many rock core samples in the lab. For each of these specimens tested, GSI was first visually estimated and subsequently adjusted/verified through a back-calculation procedure. Once GSI values were secured, the team employed computational tools to calculate the ranges of GSI parameters m_i and σ_{ci} for Ohio rock materials. There are two methods to calculate the m_i value. The first method is described by Hoek and Brown in their 1997 paper titled “Practical Estimates of Rock Mass Strength.” The second method is the LMA (Levenberg–Marquardt Algorithm) method used in the software “RocLab 1.0”, which is created by Rocscience Inc. in 2003. The LMA method is an iterative method based on the Gauss-Newton algorithm, which is supposed to be stable and can converge fast.

For the third objective, the data compiled in the study were entered into the statistical computer software package SPSS (Statistical Product and Service Solutions) to determine a 95% confidence interval of each rock property. SPSS was also utilized to perform t-tests to detect any regional differences that may exist in the data set.

For the fourth objective, the ranges of parameters for GSI system have been determined for each geological region in Ohio. Engineers can refer to these ranges during foundation design work.

For the fifth objective, the RMR-GSI correlation was explored numerically using the GSI determined, unconfined compression strength, and RQD. To somewhat generalize the correlation, a few variations in groundwater and joint orientation conditions were considered. To further illustrate the RMR and GSI, the team developed a few computation examples to show how some engineering properties of rock masses can be estimated using both RMR and GSI systems. While going through the GSI calculation steps, results (RMR-GSI correlation, a range of m_i , a range of σ_{ci}) of the current study were fully incorporated.

5.2 Findings and Conclusions

This section summarizes all the key findings made and conclusions reached in the current project.

5.2.1 Literature Review

- Section 10.4.6.4 of the AASHTO LRFD Bridge Design Specifications (2010) provides all essential details of the RMR system.
- A technical paper by Hoek et al. (2002) describes the latest version of the GSI system. Additional information on the GSI system can be found in his earlier publications (Hoek 1995, 1997).
- NCHRP Report 651 (2010) outlines changes that have been recommended to Section 10 (foundations) of the AASHTO LRFD Specifications, which include descriptions of GSI and failure mechanisms/bearing capacity issues for shallow

foundations on rock.

5.2.2 Gathering of Ohio Rock Property Data

- Ohio rock property data assembled in the project came from ODOT's Material Testing Laboratory, ODOT database FALCON GDMS (Geotechnical Document Management System), and Ohio University team's laboratory testing.
- Contrary to the initial hope, no useful compressive strengths on Ohio regional rocks were available from the US Army Corps of Engineers, private firms (ex. Advanced Terra Testing, Golder Associates), and the Colorado School of Mines.
- ODOT's Material Testing Laboratory provided 109 unit weights and 109 unconfined compression strength values. During the exploration of the database FALCON GDMS, 61 unit weights and 203 unconfined compression strength values were located. The Ohio University team contributed 127 unit weights, 47 unconfined compression tests, and 80 triaxial tests.
- The data compiled during the current project covered five major rock types (limestone, sandstone, unweathered shale, weathered shale, and claystone) and many of the geological regions of Ohio.
- Hoek cell provides a simple and quick procedure for obtaining a triaxial compression strength of rock core specimens whose strength is 1 ksi or higher. Weaker rock specimens can be best tested using a standard soil triaxial cell system.

5.2.3 Ranges of Basic Ohio Rock Properties

- For each major Ohio rock type, the range of unit weight is generally narrower than the range listed in ODOT Rock Slope Design Guide (2011).

- Limestone and sandstone are both heavier than what ODOT 2011 report indicated.
- Shale (unweathered; weathered) is lighter than what ODOT 2011 report indicated.
- Claystone is much lighter than what ODOT 2011 report indicated.
- The ranges of unconfined compression strength are also much narrower than those provided in the 2011 ODOT report for limestone and sandstone.
- Unconfined compression strength of shale (unweathered) is slightly higher than what ODOT 2011 report indicated.
- Shale (weathered) and claystone are each much weaker than what ODOT 2011 report indicated.

5.2.4 Regional Variations of Basic Ohio Rock Properties

- Unit Weight of Limestone – Similar among the northwest, northeast, southwest, and southeast regions; The central region stands out alone.
- Unconfined Compression Strength of Limestone –Similar among the northwest, central, and southwest regions; It is different in the northeast and southeast regions.
- Unit Weight of Sandstone -- Similar between the northeast and east regions; It is different in the southeast region.
- Unconfined Compression Strength of Sandstone –All different among the northeast, east, and southeast regions.
- Unit Weight of Shale (unweathered) – Similar among the northeast, east, and central regions; It differs in the southwest and southeast regions.
- Unconfined Compression Strength of Shale (unweathered) –Similar among the

northeast, east, southwest, and southeast regions; The central region stands out alone.

- Unit Weight of Shale (weathered) – Similar among the east, central, and southwest regions; It is different in the northeast and southeast regions.
- Unconfined Compression Strength of Shale (weathered) – Similar among the northeast, southwest, and southeast regions; It is different in the east and central regions.
- For each major rock type, the regional differences detected among its unconfined compression strength values did not agree with those observed among its unit weights.
- For any given rock type, equality of the unit weights in two different geological regions may not imply that the unconfined compression strengths are also the same between the regions. Thus, caution is to be exercised when estimating the basic rock properties.

5.2.5 Ranges of GSI Parameter m_i

- The m_i values determined by the Hoek's linear regression method had a tendency to be extreme and very different from the values he provided himself. Sometimes, these m_i values were higher than 100 or lower than 0. This situation frequently occurred due to the fact that low confining pressure levels were used. Hoek stated that ideally confining pressure needs to be half of the uniaxial compressive strength.
- The LMA (Levenberg–Marquardt Algorithm) method converges efficiently, and its m_i values are always within the range provided by Hoek. According to Hoek's research, the typical m_i value of weak ductile rock is 5 and that of very strong

brittle rock is 35, RocLab sets the m_i value from 1 to 50 to cover this range.

- The range of m_i value seen for each rock type generally agrees with the range provided by Hoek, except for limestone and unweathered shale. Since unweathered shale in the SW region is embedded with limestone, the range of m_i value tends to be higher than that specified by Hoek for shale.

5.2.6 RMR-GSI Correlation

- The visually determined and back-calculated GSI values agreed well in most cases. Thus, the back-calculation technique can serve as an effective way to verify the visual value.
- For generalizing the RMR-GSI relationship somewhat, the team considered three different groundwater conditions (very dry, moist, under moderate pressure) and four types of joint orientations (very favorable, favorable, fair, unfavorable). Variations in RQD are embedded within RMR.
- In most cases, a simple linear function ($y = mx + c$) was sufficient to describe the relationship between RMR and GSI for Ohio rocks with a reasonably strong correlation ($r^2 = 0.7$ to 0.85).
- The slope (m) of the linear correlation is independent of the groundwater and joint orientation conditions. In contrast, the intercept (c) varies according to the groundwater and joint orientation conditions.
- The slope of the linear correlation between RMR and GSI differed among rock types. It appears that the slope becomes steeper for stronger rock material.
- With the ranges of m_i and σ_{ci} identified and the RMR-GSI correlations established, the GSI method can be applied to Ohio rocks to estimate their key engineering properties and use them in bridge foundation design work.

- It appears that the GSI method may be somewhat less conservative for strong and good-quality (high RQD) rock masses, compared to RMR.
- As the rock gets weaker and more fractured, engineering properties determined by the GSI system appear to approach those by the RMR system. This statement is only applicable for cases where core specimens can be recovered for compressive strength testing.
- The RMR system has a simple method to estimate the lower bound bearing capacity for shallow foundations resting on rock. The GSI system does not appear to have a way to address the foundation's bearing capacity.

5.3 Recommendations

Based on the findings and results obtained in the current project, the following recommendations are warranted:

- Additional unit weight and unconfined compression values will be needed to check the regional differences that were detected in the basic rock properties.
- Additional unconfined compression strength values will be needed for limestone in the east region and sandstone in the central region.
- Additional limestone specimens will be necessary for conducting triaxial tests and setting up a range of m_i value in the east and northeast regions.
- Additional sandstone specimens will be needed for performing triaxial tests and setting up a range of m_i value in the central region.
- Some of the m_i value ranges should be verified by running the Hoek test at much higher confining pressure levels.
- The σ_{ci} ranges determined in the study should be checked/improved for each

major Ohio rock type.

- Additional test data are desired for verifying the RMR-GSI correlations determined in this study.
- Additional test data are needed to develop regional RMR-GSI relationships for each major Ohio rock type.
- It appears that results (τ , E_m) coming out of GSI are sensitive to the value of Disturbance Factor (D). Guidelines are needed to correlate RQD and D.

CHAPTER 6 : IMPLEMENTATIONS

Based on the findings and conclusions made in the current project, the following implementation plans are highly recommended to ODOT:

- The ranges of unit weight and unconfined compression strength values listed in ODOT's Rock Slope Design Guide (2011) need to be revised based on the 95% confidence intervals determined in the current project.
- The ranges of m_i value published by Hoek can be applied to Ohio rocks.
- The linear correlations between RMR and GSI summarized in Tables 4.49 through 4.52 are ready to be adapted by ODOT.
- For strong rock materials such as relatively intact limestone, sandstone, and unweathered shale, consulting firms and test labs can continue performing just the unconfined compression strength tests. If the unconfined strength falls within the range reported by the Ohio University team, the m_i value found in the current study can be applied.
- For weak soil-like rock materials such as weathered shale and claystone (unconfined compression strength < 1 ksi), they are advised to perform both unconfined compression and triaxial compression tests. The latter can be conducted using the soil triaxial test system. Confining pressure levels should be set to cover the maximum depth of foundation in the design. Once the tests are done, their data can be analyzed using RocLab computer software.
- The ODOT Office of Geotechnical Engineering (OGE) should continue compiling additional rock property data and analyze larger data set using RocLab and SPSS to either verify or improve the results of the current study so that in the near future they can develop regional bridge design guidelines in Ohio.

REFERENCES

- American Association of State Highway and Transportation Officials (2010). AASHTO LRFD Bridge Design Specifications – Section 10 (Foundations), 5th Edition, Transportation Research Board, Washington, D. C.
- American Society of Testing and Materials or ASTM D 2664 (1995). “Standard Test Method for Triaxial Compressive Strength of Undrained Rock Core Specimens Without Pore Pressure Measurements.” West Conshohocken, PA, 3 pp.
- American Society of Testing and Materials or ASTM D 2850 (1993). “Standard Test Method for Unconsolidated – Undrained Triaxial Compression Test on Cohesive Soils.” West Conshohocken, PA, 6 pp.
- American Society of Testing and Materials or ASTM D 2938 (1995). “Standard Test Method for Unconfined Compressive Strength of Intact Rock Core Specimens.” West Conshohocken, PA, 3 pp.
- American Society of Testing and Materials or ASTM D 4543 (2004). “Standard Practices for Preparing Rock Core Specimens and Determining Dimensional and Shape Tolerances.” West Conshohocken, PA, 5 pp.
- American Society of Testing and Materials or ASTM D 7012 (2004). “Standard Test Method for Compressive Strength and Elastic Moduli of Intact Rock Core Specimens under Varying States of Stress and Temperatures.” West Conshohocken, PA, 8 pp.
- Bieniawski, Z. T. (1974). “Geomechanics Classification of Rock Masses and Its Application in Tunneling.” Academy of Sciences, Washington, D. C., pp. 27-32.
- Bieniawski, Z. T. (1976). “Rock Mass Classification in Rock Engineering.” Proceedings of the Symposium on Exploration for Rock Engineering, Volume 1, Cape Town, Balkema, pp. 97-106.

Bieniawski, Z. T. (1989). *Engineering Rock Mass Classifications*, John Wiley & Sons, New York.

Bishoni, B. L. (1968). "Bearing Capacity of a Closely Jointed Rock." Doctoral Dissertation, Civil Engineering Dept., Georgia Institute of Technology, 120 pp.

Canadian Geotechnical Society (2006). *Canadian Foundation Engineering Manual*, 4th Edition, Richmond, BC, 488 pp.

Carter, J. P., and Kulhawy, F. H. (1988). "Analysis and Design of Foundations Socketed into Rock." Report No. EL-5918, Empire State Electric Engineering Research Corp. & Electric Power Research Institute, New York, 158 pp.

Failmezger, R. A., White, D. J., and Handy, R. L. (2008). "Measurement of Effective Stress Shear Strength of Rock." Proceedings of Geotechnical and Geophysical Site Characterization, London, GB, pp. 335-339.

Goodman, R. E. (1980). *Introduction to Rock Mechanics*, A Book Published by Wiley, New York, 478 pp.

Hoek, E., and Franklin, J. A. (1968). "A Simple Triaxial Cell for Field and Laboratory Testing of Rock." Transactions of Institution of Mining & Metallurgy, Issue 77, pp. 22-26.

Hoek, E., Kaiser, P. K., and Bawden, W. F. (1995). *Support of Underground Excavations in Strong rock*. A Book Published by Taylor & Francis Group, 300 pp.

Hoek, E., and Brown, E. T. (1997). "Practical Estimates of Rock Mass Strength." International Journal of Rock Mechanics and Mining Sciences, Volume 34, Number 8, pp. 1165-1186.

Hoek, E., Carranza-Torres, C., and Corkum, B. (2002). "Hoek-Brown Failure Criterion – 2002 Edition." Proceedings of the 5th North American Rock Mechanics Symposium, Volume 1, pp. 267–273.

Masada, T. (1986). "Characterization of Engineering Behavior of Ohio Nondurable Shale." A MS Thesis, Civil Engineering Department, Ohio University, Athens, OH, 146 pp.

Masada, T., and Han, X. (2012a). "Rock Mass Classification System: Transition from RMR to GSI." A Student Study Proposal, Submitted to ODOT, Civil Engineering Department, Ohio University, Athens, OH, 35 pp.

Masada, T., and Han, X. (2012b). "Rock Mass Classification System: Transition from RMR to GSI." A Power-Point Presentation for Project Start-up Meeting, Submitted to ODOT, Civil Engineering Department, Ohio University, Athens, OH, 35 pp.

Masada, T., and Han, X. (2013). "Rock Mass Classification System: Transition from RMR to GSI." A Power-Point Presentation for Project Annual Review Session, Submitted to ODOT, Civil Engineering Department, Ohio University, Athens, OH, 35 pp.

National Co-operative Highway Research Report 651 or NCHRP 651 (2010). LRFD Design and Construction of Shallow Foundations for Highway Bridge Structures, Transportation Research Board, Washington, D. C., 139 pp.

Nusairat, J., Engel, R., Liang, R. Y., and Young, K. (2006). "Vertical and Lateral Load Testing of Drilled Shafts Socketed into Rock at the Pomeroy-Mason Bridge over the Ohio River." A Technical Paper Presented at the 2006 Annual TRB Meeting, Transportation Research Board, Washington, D. C., 23 pp.

Ohio Department of Transportation or ODOT (2011). Rock Slope Design Guide, Columbus, OH, 58 pp.

Osgoui, R. and Ünal, E. (2005). "Rock Reinforcement Design for Unstable Tunnels Originally Excavated in Very Poor Rock Mass." Proceedings of International Conference – Underground Space Use: Analysis of the Past and Lessons for the Future, London, Taylor & Francis Group, pp. 291-296.

RocScience (2012). User's Manual for Free Software RocLab 1.0.

Rusnak, J., and Mark, C. (2000). "Using the Point Load Test to Determine the Uniaxial Compressive Strength of Coal Measure Rock." Proceedings of the 19th International Conference on Ground Control in Mining, Morgantown, WV, pp. 362-371.



ORITE • 141 StockerCenter•Athens, Ohio 45701-2979 • 740-593-2476
Fax: 740-593-0625 • orite@bobcat.ent.ohiou.edu • <http://webce.ent.ohiou.edu//orite/>